**Pompei, Ercolano, Oplonti** Stefano Lugli


NO WARNING.
NO ESCAPE.
POMPEII IN 3D
TRISTAR PICTURES AND FILMDISTRICT PRESENT A CONSTANTIN FILM INTERNATIONAL/IMPACT PICTURES (POMPEII) PRODUCTION A FILM BY PAUL W.S. ANDERSON "POMPEII" KIT HARINGTON CARRIE-ANNE MOSS
EMILY BROWNING ADEWALE AKINNUOYE-AGBAJE JESSICA LUCAS WITH JARED HARRIS AND KIEFER SUTHERLAND CASTING BY RONNA KRESS C.S.A. DEIRDRE BOWEN MUSIC BY CLINTON SHORTER DIGITAL VISUAL EFFECTS BY MR. X INC. VISUAL EFFECTS SUPERVISOR DENNIS BERARDI
COSTUME DESIGNER WENDY PARTRIDGE EXECUTIVE IN CHARGE OF PRODUCTION CHRISTINE ROTHE EDITED BY MICHELE CONROY PRODUCTION DESIGNER PAUL DENHAM AUSTERBERRY DIRECTOR OF PHOTOGRAPHY GLEN MacPHERSON ASC, CSC EXECUTIVE PRODUCERS MARTIN MOSZKOWICZ PETER SCHLESSEL JON BROWN
Soundtrack on Milan Music and Koenigskinder Music
PRODUCED BY JEREMY BOLT PAUL W.S. ANDERSON ROBERT KULZER DON CARMODY WRITTEN BY JANET SCOTT BATCHLER & LEE BATCHLER AND MICHAEL ROBERT JOHNSON DIRECTED BY PAUL W.S. ANDERSON
Constantin Film
IMPACT PICTURES
FILMDISTRICT
PG-13
IN THEATERS FEBRUARY 2014
PompeiiMovie.tumblr.com
Sony Entertainment Network
SONY
TRI STAR

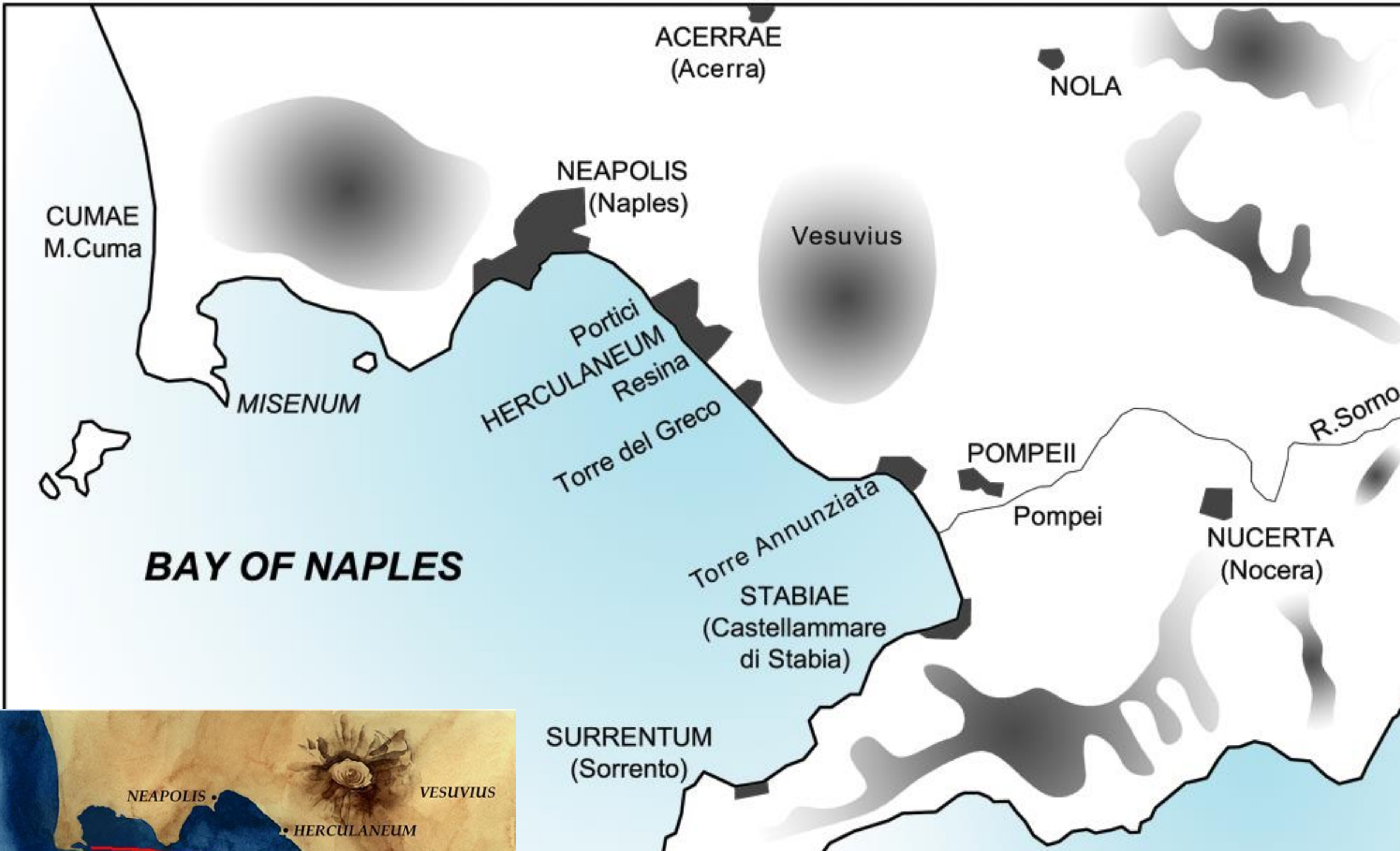
ACERRAE
(Acerra)
NOLA
NEAPOLIS
(Naples)
CUMAE
M.Cuma
Vesuvius
Portici
HERCULANEUM
Resina
Torre del Greco
MISENUM
R.Sorno
POMPEII
Pompei
Torre Annunziata
NUCERTA
(Nocera)
BAY OF NAPLES
STABIAE
(Castellammare
di Stabia)
SURRENTUM
(Sorrento)


NEAPOLIS
VESUVIUS
HERCULANEUM
MISENUM
POMPEII
BAY OF NAPLES
STABIAE
route of Pliny the Elder

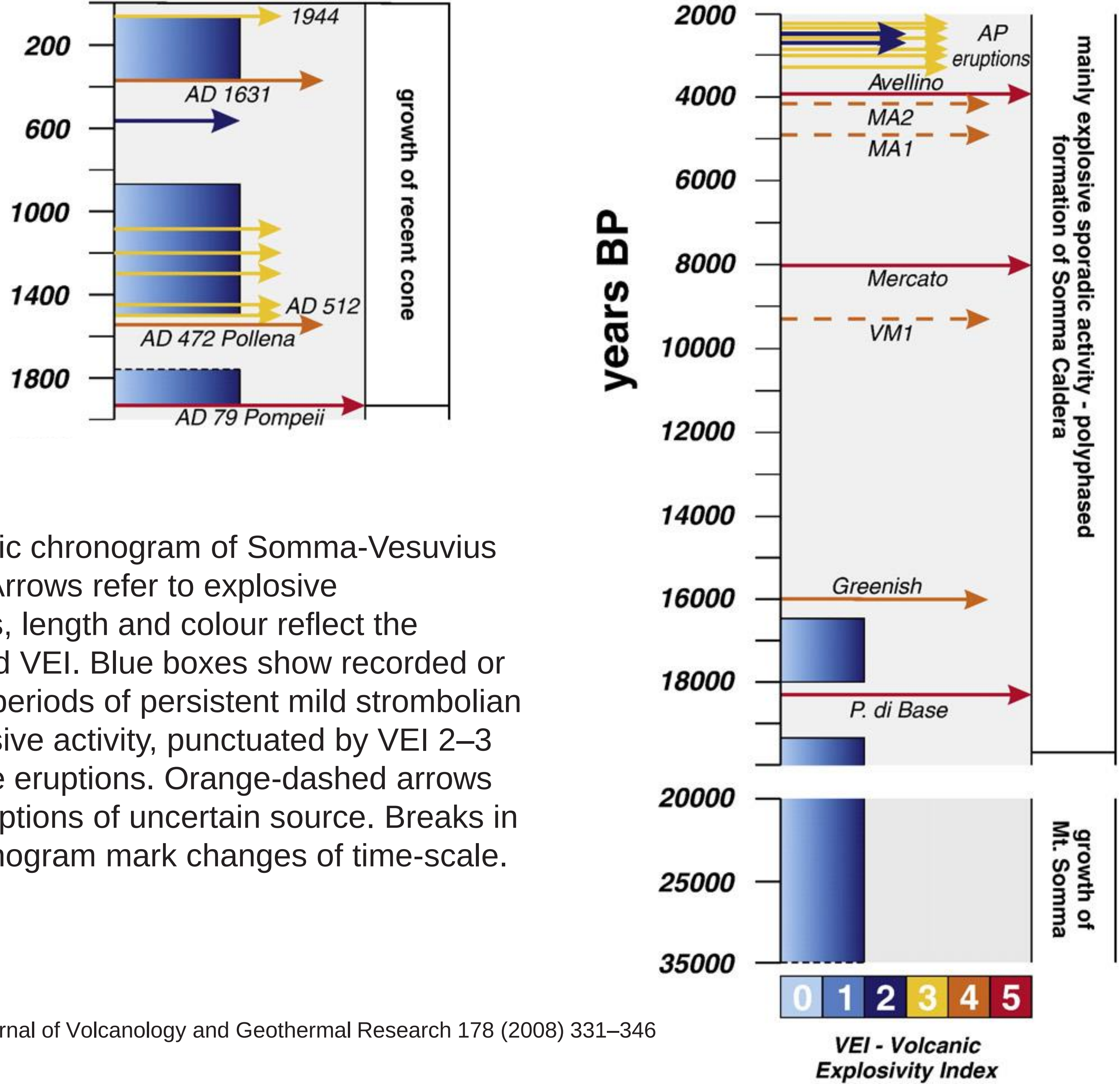


Schematic chronogram of Somma-Vesuvius activity. Arrows refer to explosive eruptions, length and colour reflect the estimated VEI. Blue boxes show recorded or inferred periods of persistent mild strombolian and effusive activity, punctuated by VEI 2–3 explosive eruptions. Orange-dashed arrows mark eruptions of uncertain source. Breaks in the chronogram mark changes of time-scale.

Cioni et al, Journal of Volcanology and Geothermal Research 178 (2008) 331–346

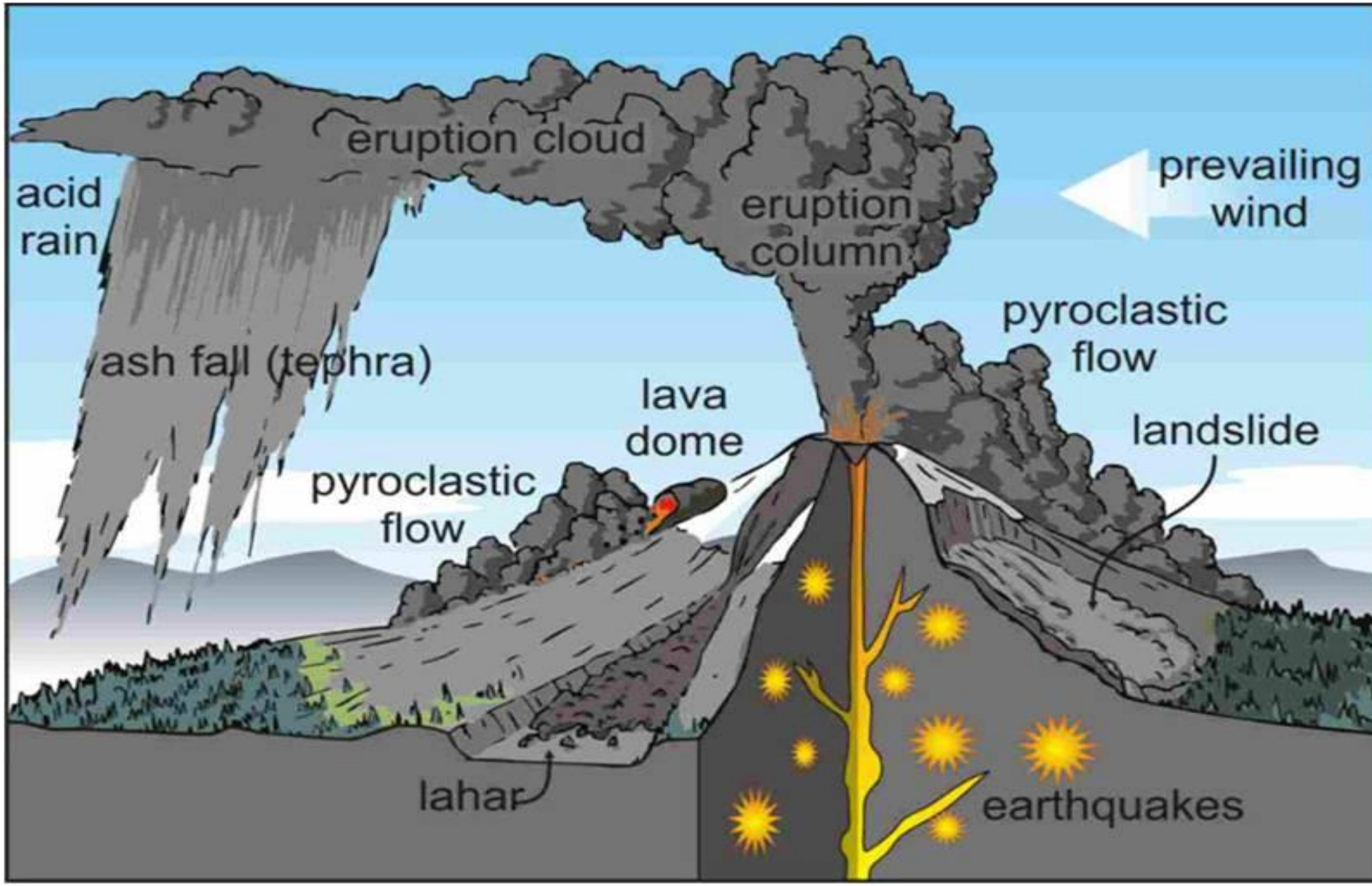
eruption cloud
acid rain
eruption column
prevailing wind
pyroclastic flow
ash fall (tephra)
lava dome
landslide
pyroclastic flow
lahar
earthquakes

*Table 3.6 Classification of volcaniclastic grains and sediments on grain-size.*

| | **Volcaniclastic grains** | **Size** | **Volcaniclastic sediment terms (tephra)** |
|---|---|---|---|
| | bombs – ejected fluid<br>blocks – ejected solid | coarse<br>– 256 mm –<br>fine | agglomerate<br>volcanic breccia |
| 64 mm | | | |
| | lapilli | coarse<br>– 16 mm –<br>medium<br>– 4 mm –<br>fine | lapillistone |
| 2 mm | | | |
| | ash | very coarse<br>– 1 mm –<br>coarse<br>– 0.5 mm –<br>medium<br>– 0.06 mm –<br>fine | tuff – vitric<br>tuff – lithic<br>tuff – crystal |

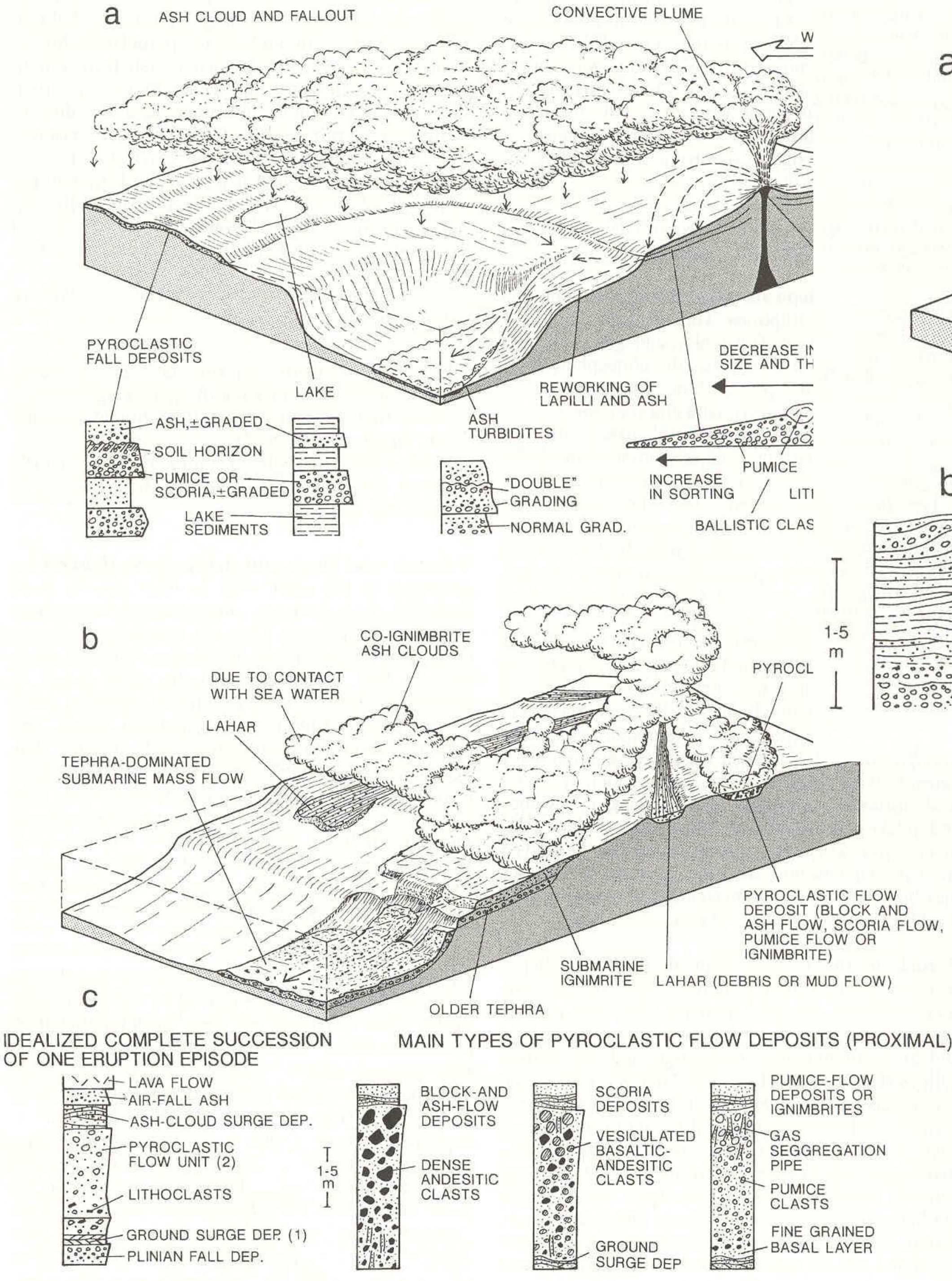
a
ASH CLOUD AND FALLOUT
CONVECTIVE PLUME
PYROCLASTIC FALL DEPOSITS
LAKE
REWORKING OF LAPILLI AND ASH
ASH TURBIDITES
DECREASE IN SIZE AND TH
INCREASE IN SORTING
PUMICE
BALLISTIC CLAS
ASH,±GRADED
SOIL HORIZON
PUMICE OR SCORIA,±GRADED
LAKE SEDIMENTS
"DOUBLE" GRADING
NORMAL GRAD.
b
CO-IGNIMBRITE ASH CLOUDS
DUE TO CONTACT WITH SEA WATER
PYROCL
LAHAR
TEPHRA-DOMINATED SUBMARINE MASS FLOW
PYROCLASTIC FLOW DEPOSIT (BLOCK AND ASH FLOW, SCORIA FLOW, PUMICE FLOW OR IGNIMBRITE)
SUBMARINE IGNIMRITE
LAHAR (DEBRIS OR MUD FLOW)
OLDER TEPHRA
c
IDEALIZED COMPLETE SUCCESSION OF ONE ERUPTION EPISODE
LAVA FLOW
AIR-FALL ASH
ASH-CLOUD SURGE DEP.
PYROCLASTIC FLOW UNIT (2)
LITHOCLASTS
GROUND SURGE DEP. (1)
PLINIAN FALL DEP.
1-5 m
MAIN TYPES OF PYROCLASTIC FLOW DEPOSITS (PROXIMAL)
BLOCK-AND ASH-FLOW DEPOSITS
DENSE ANDESITIC CLASTS
SCORIA DEPOSITS
VESICULATED BASALTIC-ANDESITIC CLASTS
GROUND SURGE DEP
PUMICE-FLOW DEPOSITS OR IGNIMBRITES
GAS SEGGREGATION PIPE
PUMICE CLASTS
FINE GRAINED BASAL LAYER

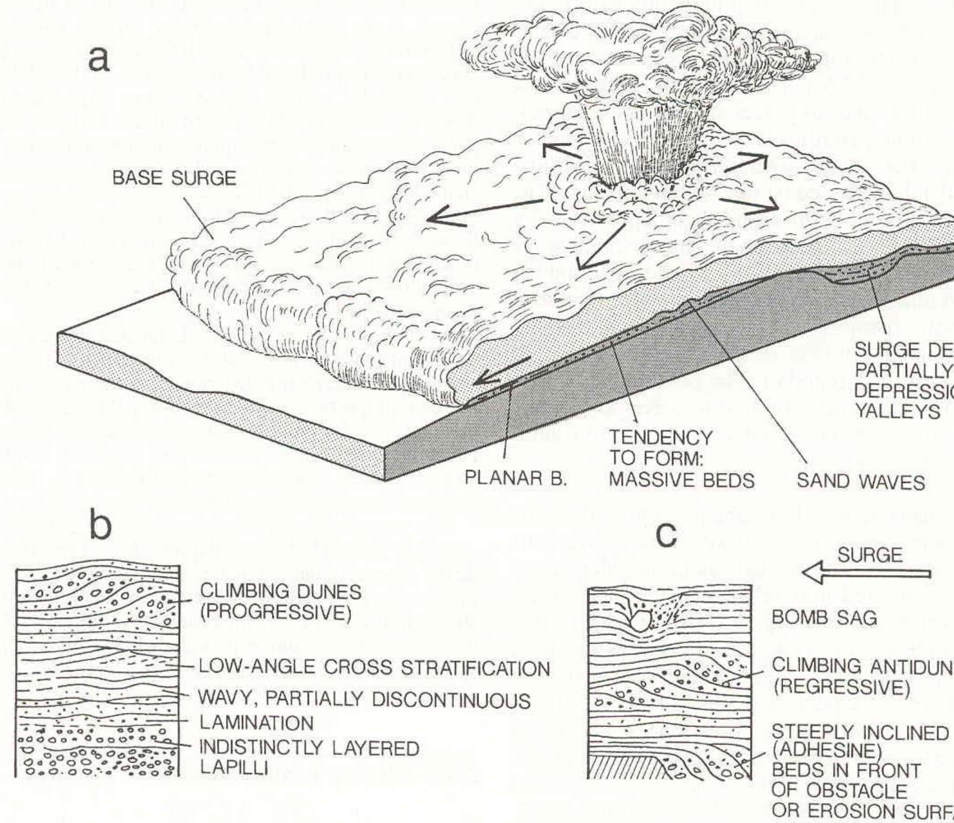
a
BASE SURGE
SURGE DE PARTIALLY DEPRESSIO YALLEYS
TENDENCY TO FORM:
PLANAR B.
MASSIVE BEDS
SAND WAVES
b
CLIMBING DUNES (PROGRESSIVE)
LOW-ANGLE CROSS STRATIFICATION
WAVY, PARTIALLY DISCONTINUOUS
LAMINATION
INDISTINCTLY LAYERED LAPILLI
1-5 m
c
SURGE
BOMB SAG
CLIMBING ANTIDUN (REGRESSIVE)
STEEPLY INCLINED (ADHESINE) BEDS IN FRONT OF OBSTACLE OR EROSION SURF

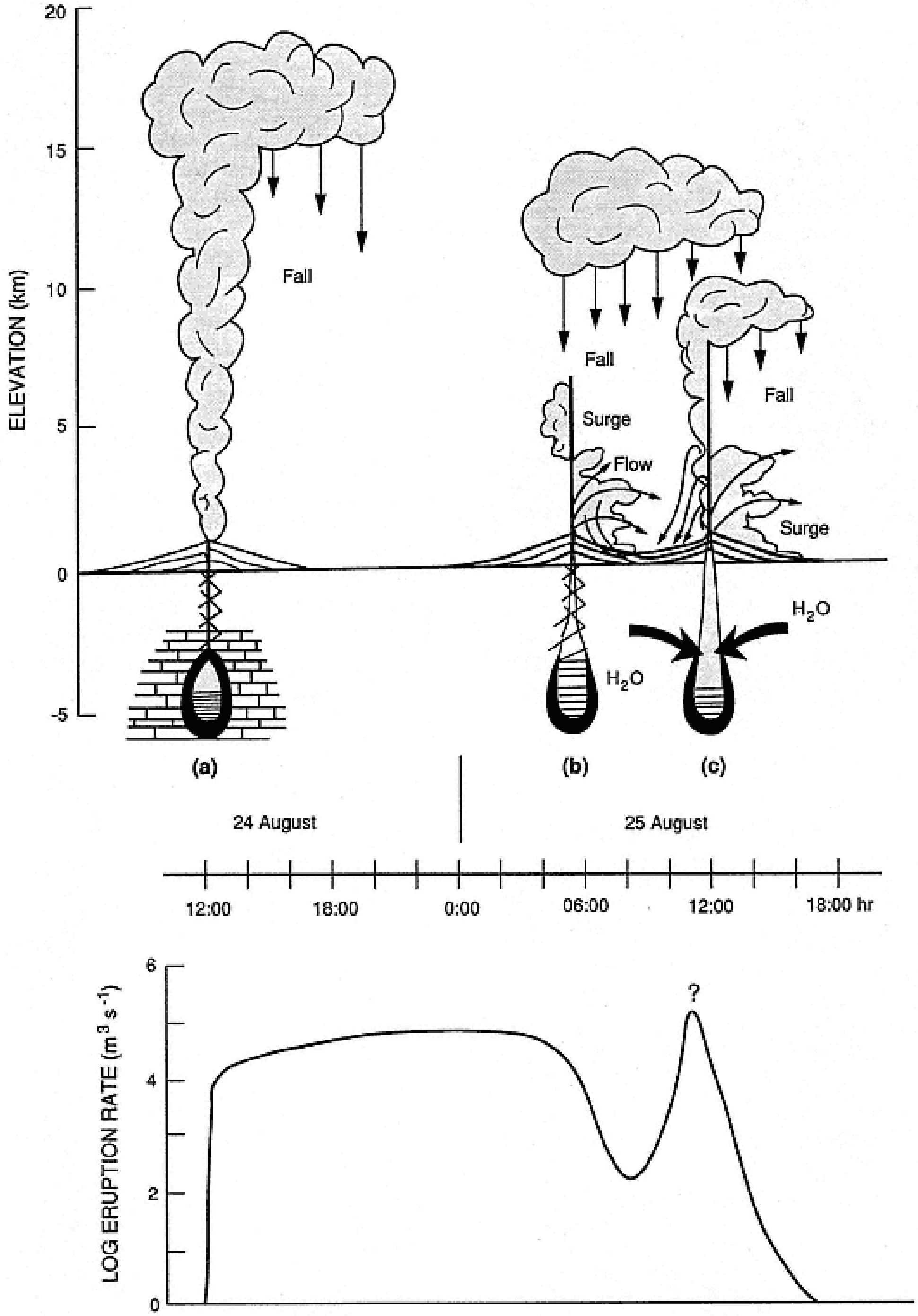

ELEVATION (km)
20
15
10
5
0
-5
Fall
Fall
Surge
Flow
Fall
Surge
$H_2O$
$H_2O$
(a)
(b)
(c)
24 August
25 August
12:00
18:00
0:00
06:00
12:00
18:00 hr
LOG ERUPTION RATE ($m^3 s^{-1}$)
6
4
2
0
?

### *3.11.1.1 Pyroclastic fall deposits*

These include subaerial and subaqueous (submarine or sublacustrine) fallout tephra. They are characterised by a gradual decrease in both bed thickness and grain-size away from the site of eruption. Beds are typically well sorted and normally graded. However, they are frequently reworked by currents and waves if deposited in water, or wind if subaerial, and thus may show cross- or planar lamination (strictly these would then be epiclastic deposits). Larger fragments of pumice may occur on top of the beds if they floated before being deposited. These deposits can be spread over wide areas and are useful for stratigraphic correlation, forming marker beds. Pyroclastic fall deposits mantle the topography, with layers of roughly constant thickness over both hills and valleys (Fig. 3.24).

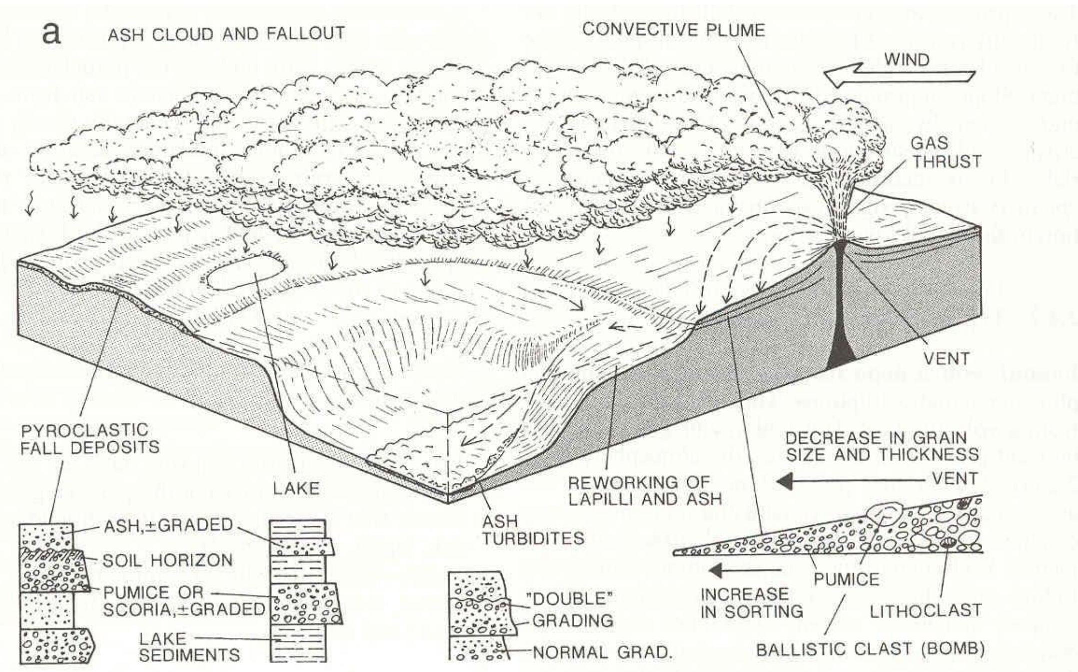

### *3.11.1.2 Pyroclastic flow deposits*

These are the product of hot gas/solid high-concentration density currents, which may travel at velocities of 20–100 m $s^{-1}$. One common pyroclastic flow deposit is an *ignimbrite*, produced by a violent plinian eruption, which generally occurs in subaerial situations, although the flows may continue into the sea or a lake. Ignimbrites are characterised by their homogeneous appearance with little sorting of the finer ash particles, so they lack internal stratification. Coarse lithic clasts in the bed may be normally graded (size decreasing upward) whereas large pumice clasts (which are very light at the time of eruption) may show reverse grading (size increasing upward), or glassy material is deformed around them. Some ignimbrites have a columnar jointing, also indicating that they were still hot on deposition. Typical thicknesses of an ignimbrite deposit are 1 m to 10 m or more. The flows are topographically controlled and so the deposits fill valleys and depressions (Fig. 3.24).

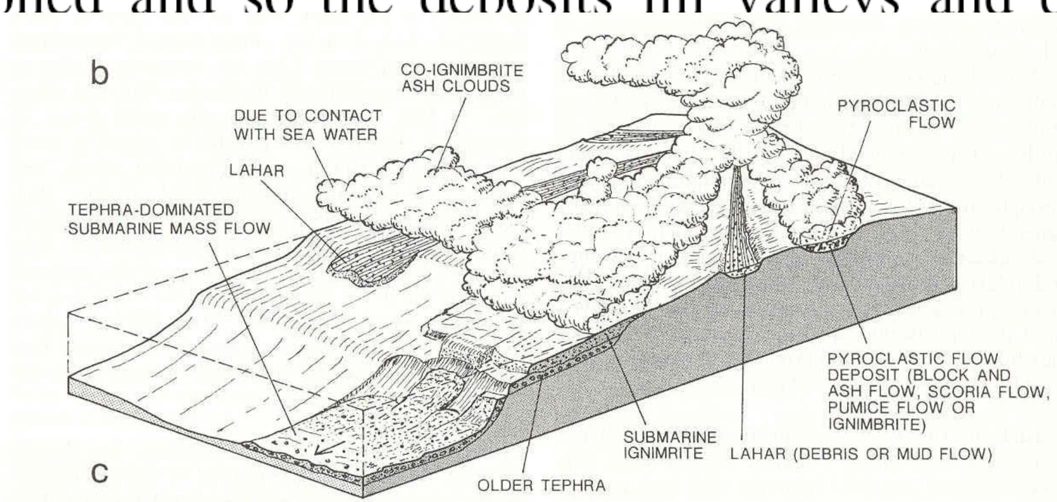

### *3.11.1.3 Pyroclastic surge deposits*

These result from highly expanded turbulent gas–solid density currents with low particle concentrations. Phreatomagmatic and phreatic eruptions involve steam and generate base-surge deposits. They are characterised by well-developed unidirectional sedimentary bedforms (dunes) giving cross-stratification (Fig. 3.26), pinch-and-swell features and antidune cross-bedding (Section 5.3.3.15), since they are deposited by very fast-flowing ash-laden steam flows. Individual laminae are generally well sorted. These deposits tend to blanket the topography, although they do thicken into the depressions (Fig. 3.24). There is a complete gradation between high-particle concentration pyroclastic flows and low-particle concentration pyroclastic surges.

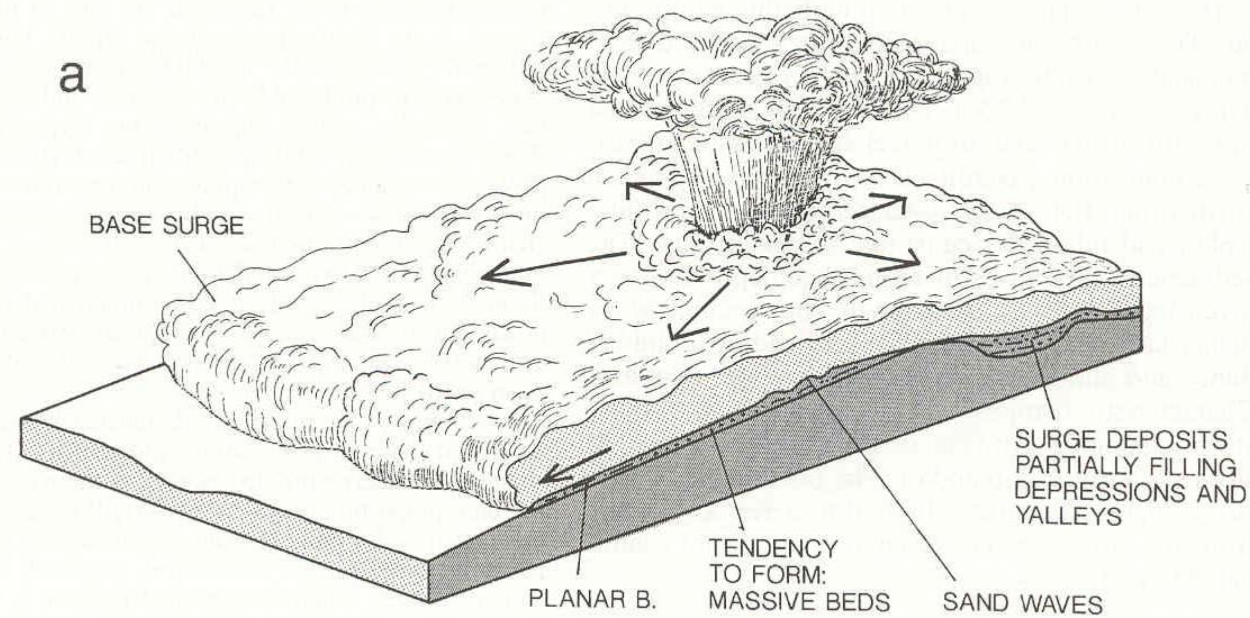

Pyroclastic flows are high-density mixtures of hot, dry rock fragments and hot gases that move away from the vent that erupted them at high speeds. They may result from the explosive eruption of molten or solid rock fragments, or both. They may also result from the nonexplosive eruption of lava when parts of dome or a thick lava flow collapses down a steep slope. Most pyroclastic flows consist of two parts: a basal flow of coarse fragments that moves along the ground, and a turbulent cloud of ash that rises above the basal flow. Ash may fall from this cloud over a wide area downwind from the pyroclastic flow.

A pyroclastic flow will destroy nearly everything in its path. With rock fragments ranging in size from ash to boulders traveling across the ground at speeds typically greater than 80 km per hour, pyroclastic flows knock down, shatter, bury or carry away nearly all objects and structures in their way. The extreme temperatures of rocks and gas inside pyroclastic flows, generally between 200°C and 700°C, can cause combustible material to burn, especially petroleum products, wood, vegetation, and houses.

Pyroclastic flows vary considerably in size and speed, but even relatively small flows that move less than 5 km from a volcano can destroy buildings, forests, and farmland. And on the margins of pyroclastic flows, death and serious injury to people and animals may result from burns and inhalation of hot ash and gases.

Pyroclastic flows generally follow valleys or other low-lying areas and, depending on the volume of rock debris carried by the flow, they can deposit layers of loose rock fragments to depths ranging from less than one meter to more than 200 m.

USGS

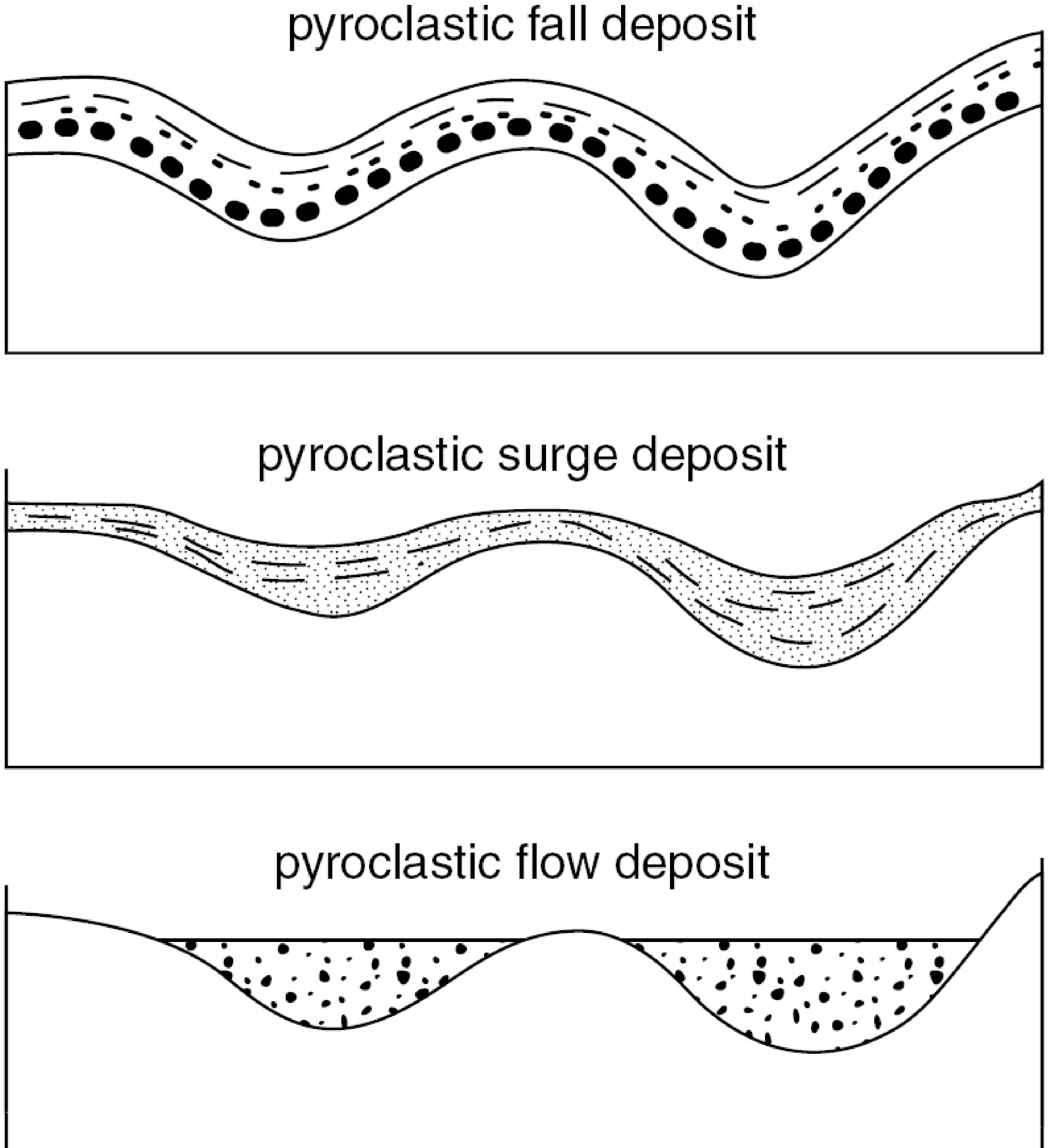
pyroclastic fall deposit
pyroclastic surge deposit
pyroclastic flow deposit

*Haraldur Sigurdsson and Steven Carey*

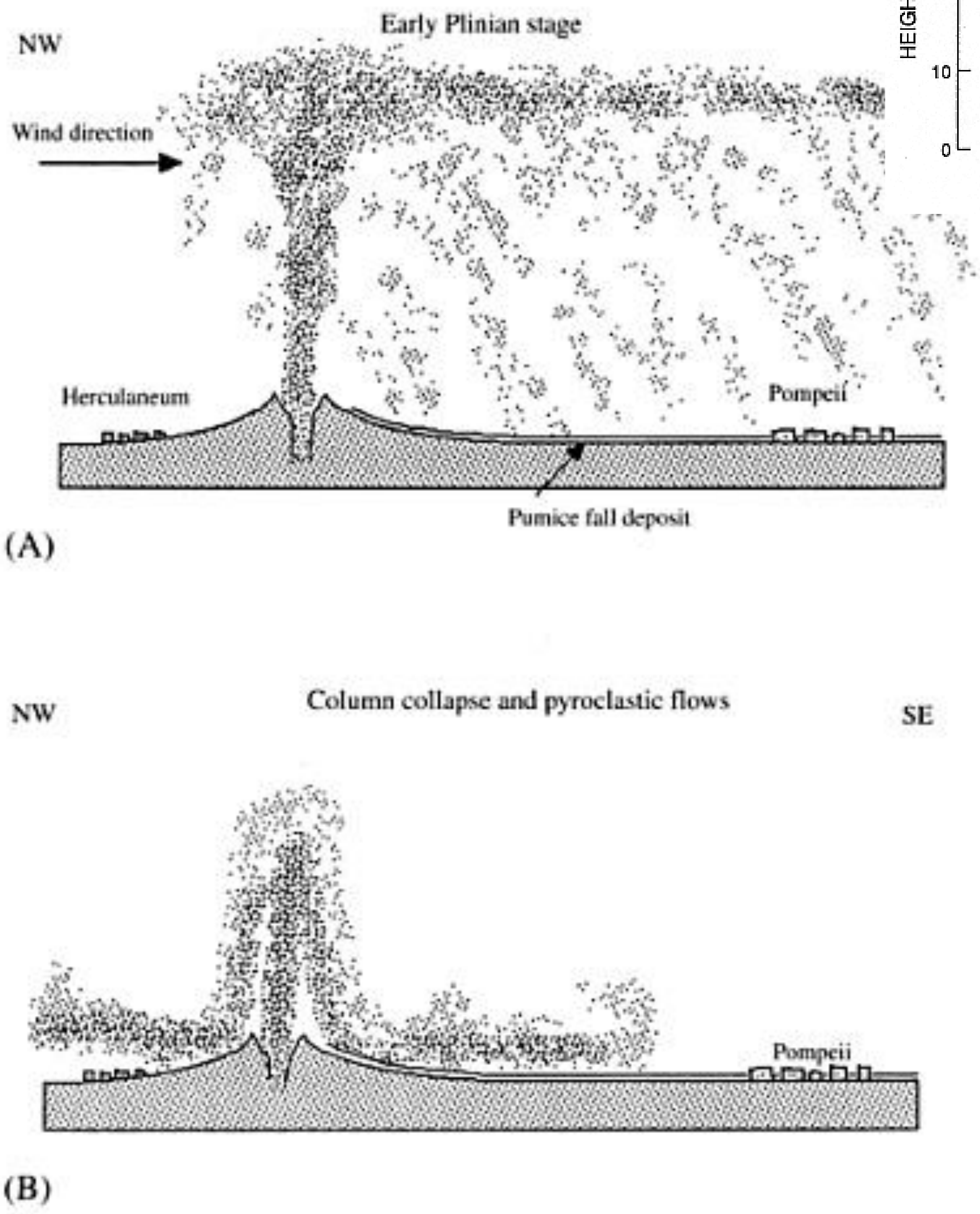


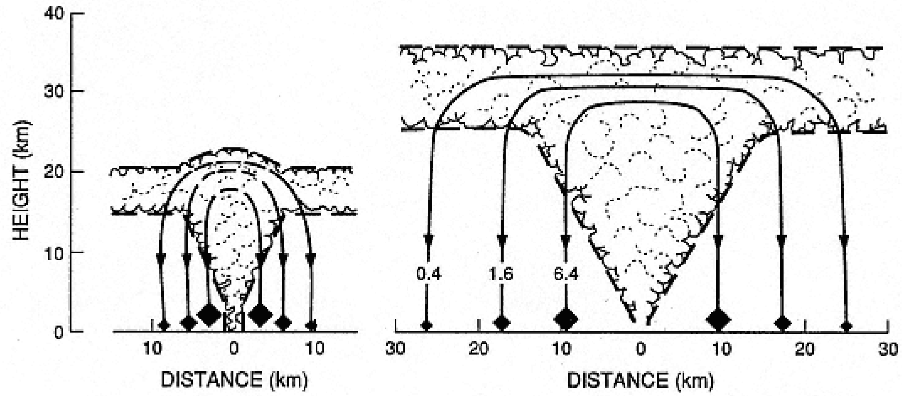


Clast trajectories from the umbrella region of a Plinian eruption column; clast sizes are given in centimeters. Note that the dispersal is greater for the 35-km-high column than for the 21-km-high column. (Adapted from Carey and Sparks, 1986.)

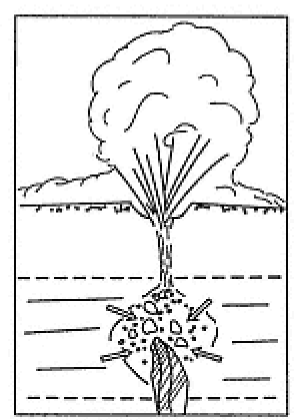

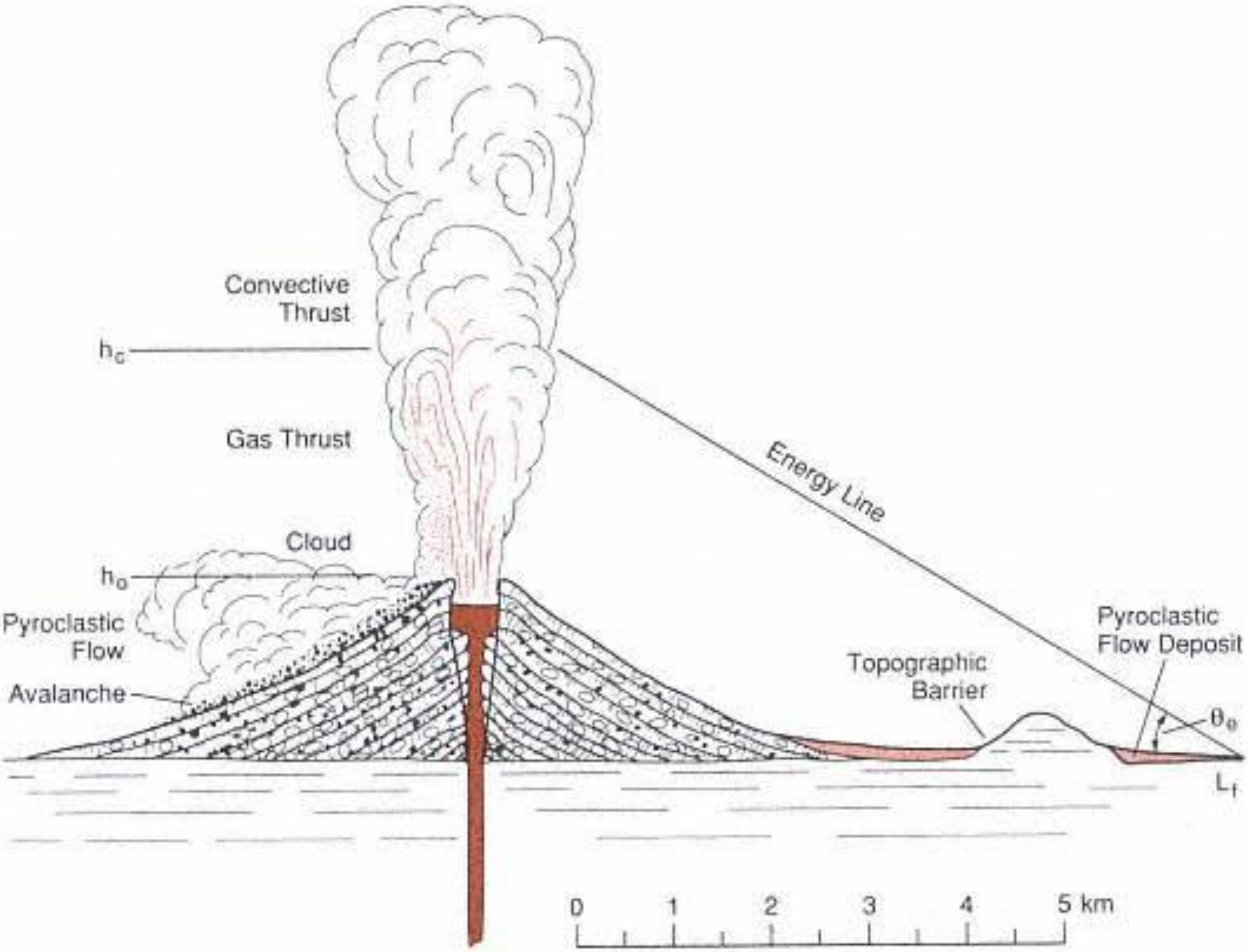
Convective Thrust
$h_c$
Gas Thrust
Energy Line
Cloud
$h_o$
Pyroclastic Flow
Avalanche
Pyroclastic Flow Deposit
Topographic Barrier
$\theta_e$
$L_f$
0
1
2
3
4
5 km

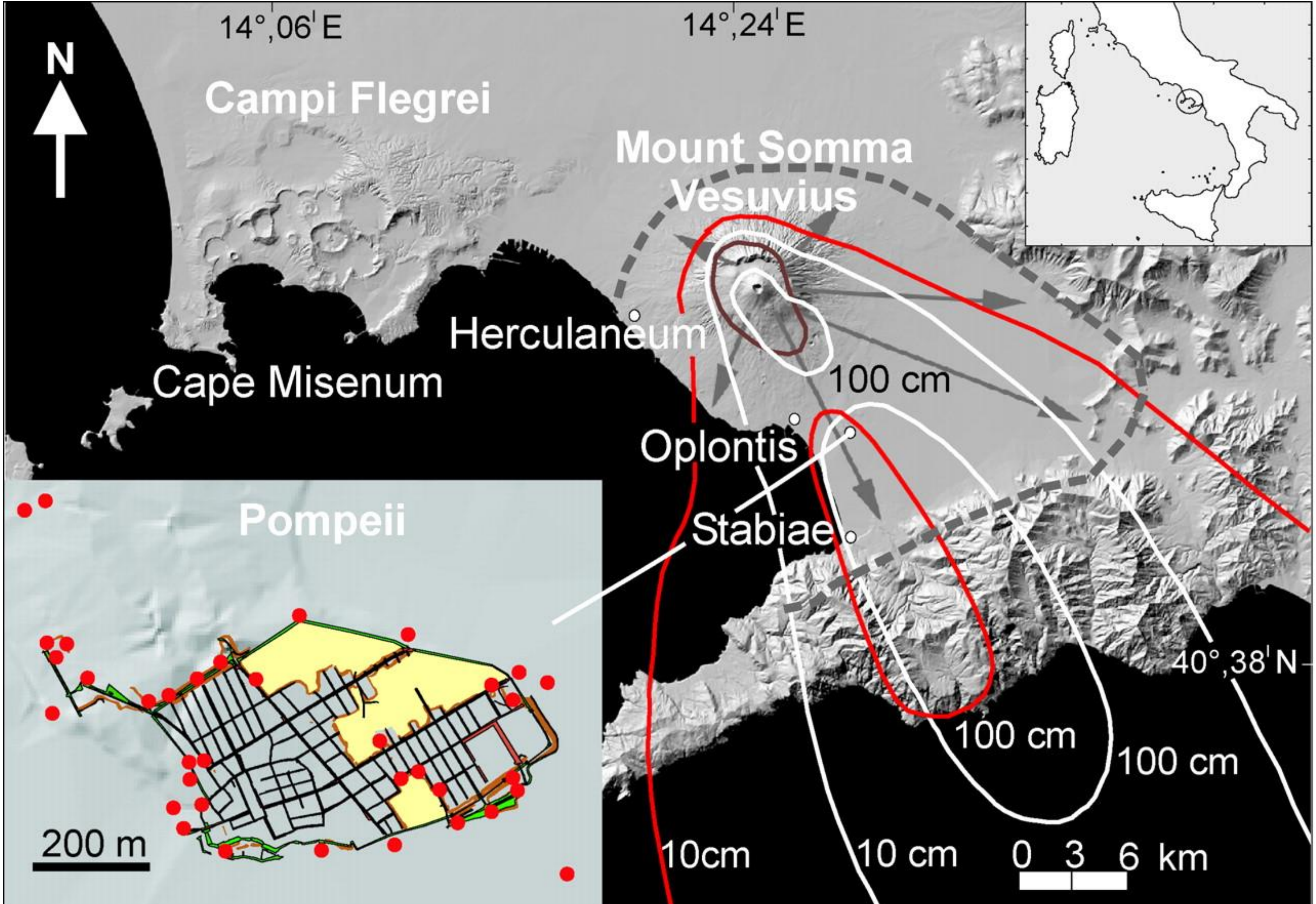

14°,06' E
14°,24' E
N
Campi Flegrei
Mount Somma
Vesuvius
Herculaneum
Cape Misenum
100 cm
Oplontis
Pompeii
Stabiae
40°,38' N
100 cm
100 cm
200 m
10cm
10 cm
0 3 6 km

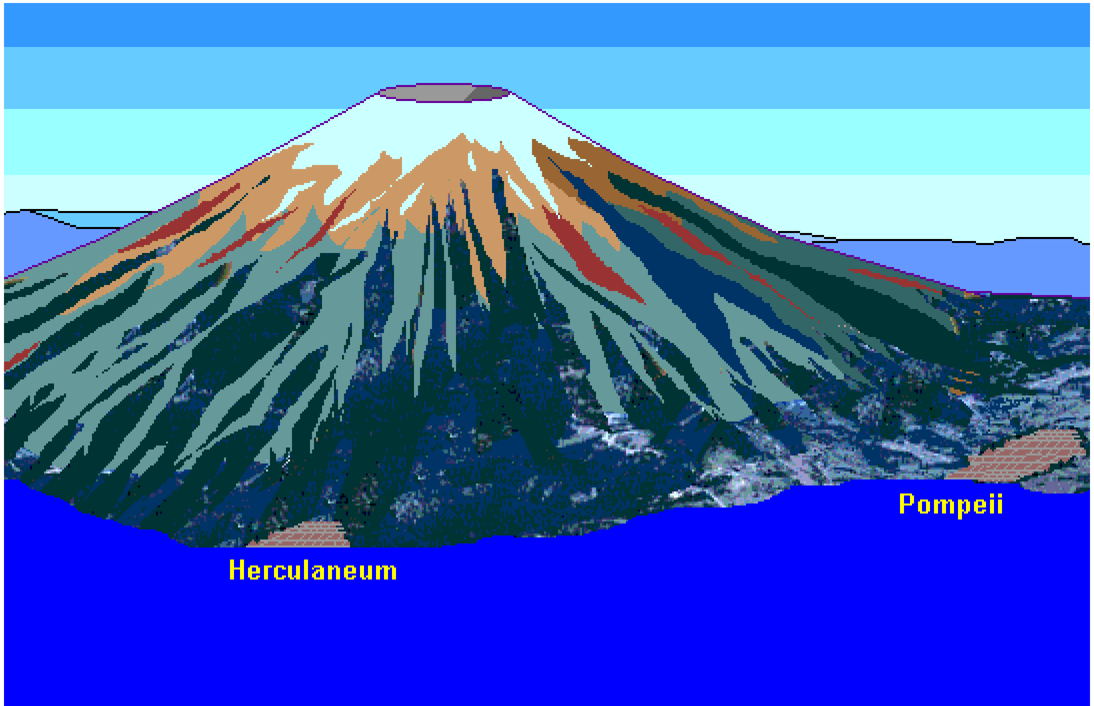
Pompeii
Herculaneum

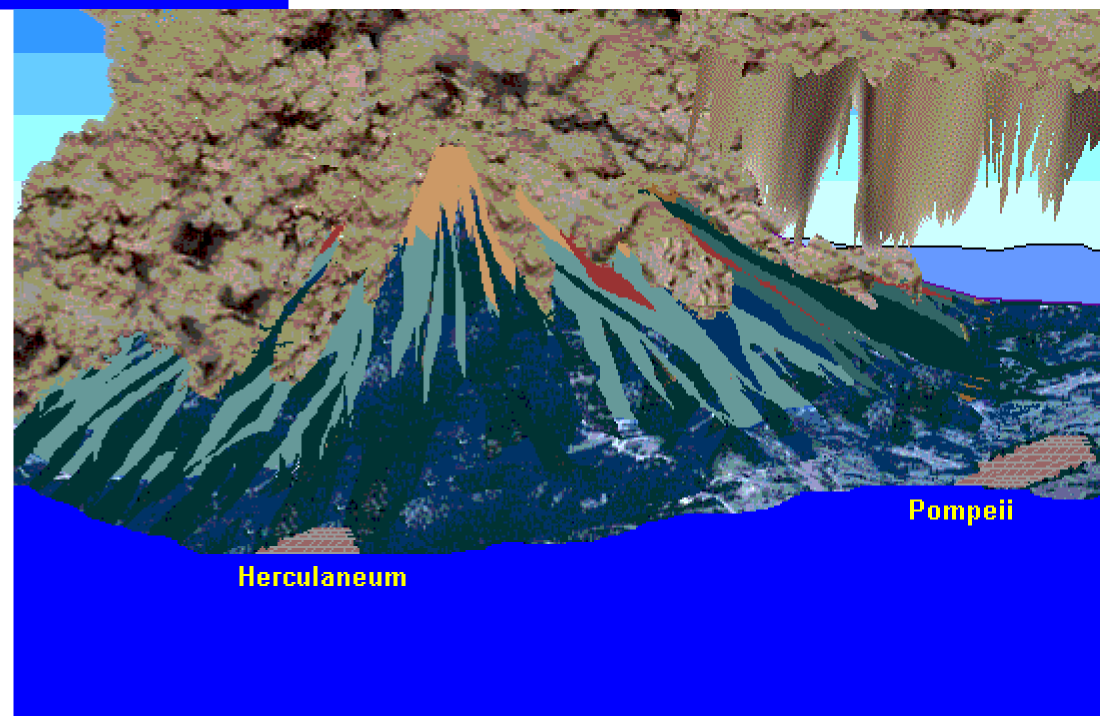
Pompeii
Herculaneum


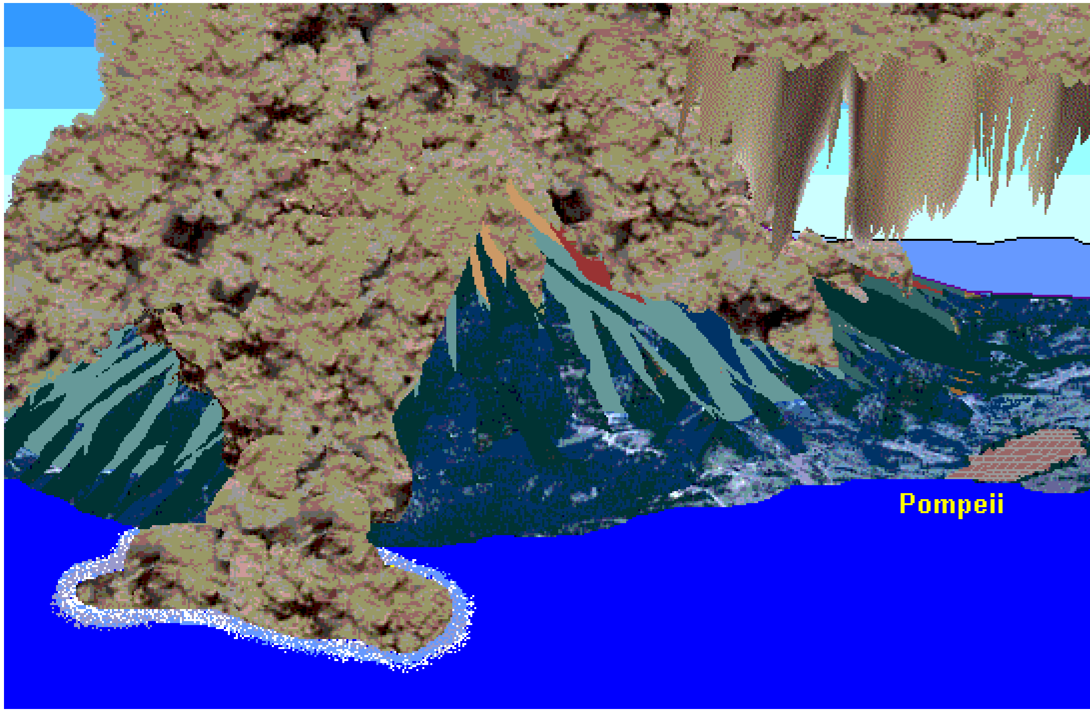


S. Dutch

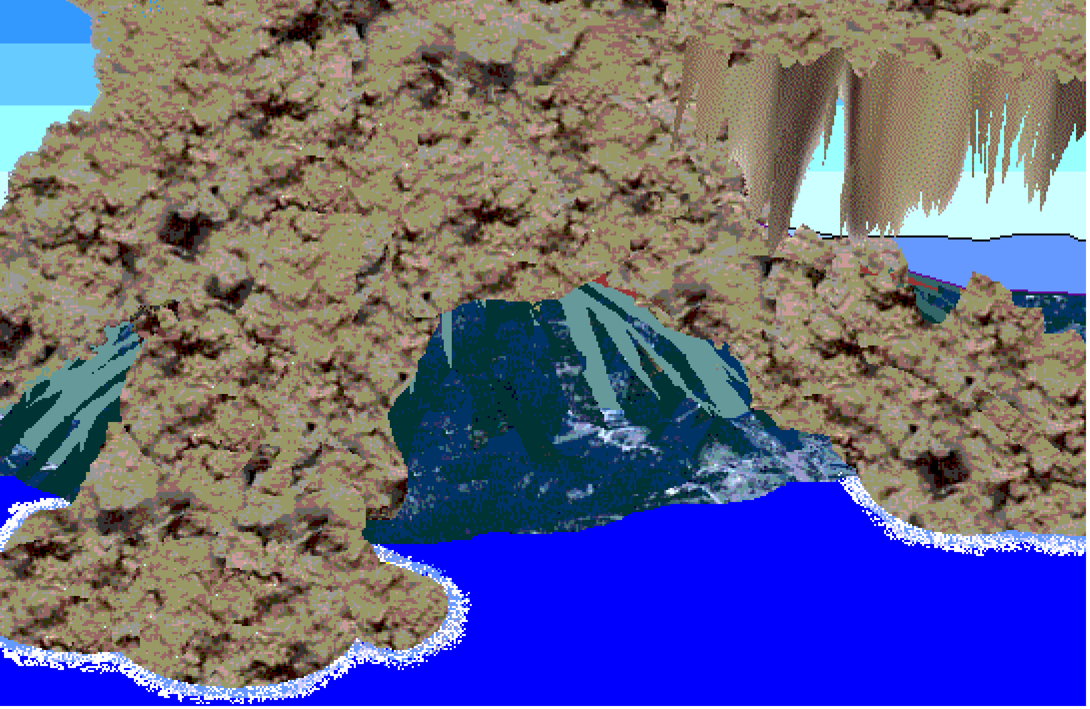

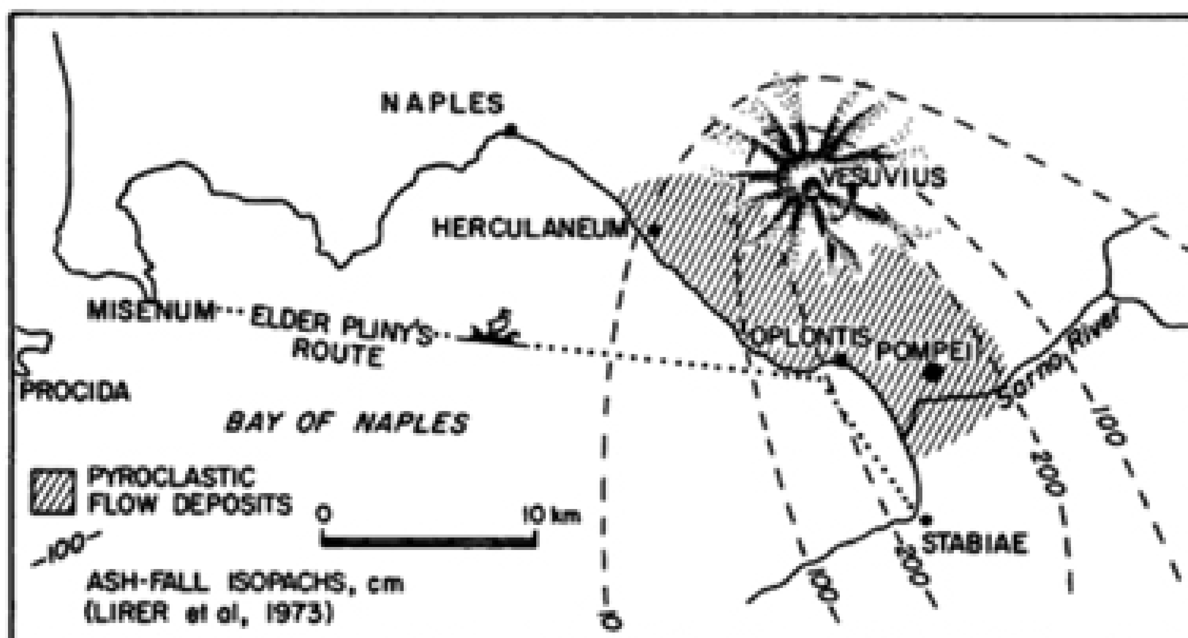

NAPLES
VESUVIUS
HERCULANEUM
MISENUM
ELDER PLINY'S ROUTE
PROCIDA
OPLONTIS
POMPEII
Sarno River
BAY OF NAPLES
PYROCLASTIC FLOW DEPOSITS
0
10 km
100
ASH-FALL ISOPACHS, cm
(LIRER et al, 1973)
STABIAE
200
100
0


S. Dutch

# VESUVIUS


## *Areas of ash-fall and pyroclastic flow in Naples bay area.*

*Wind direction determined the ash-fall pattern.*

*The direction of the pyroclastic flows supports the "two peak" theory of how Vesuvius looked before the 79 AD eruption.*

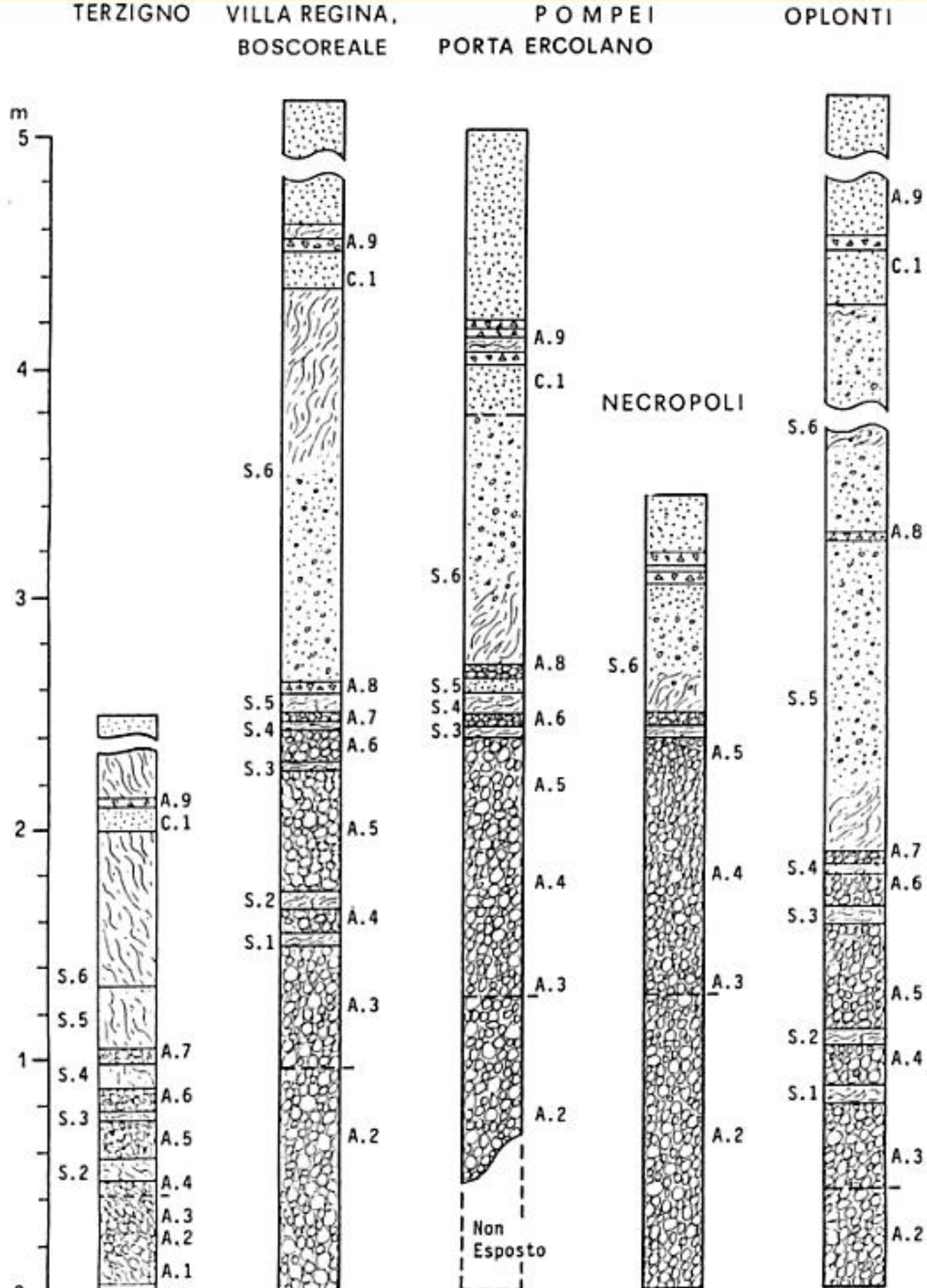
TERZIGNO
VILLA REGINA, BOSCOREALE
POMPEI PORTA ERCOLANO
NECROPOLI
OPLONTI
m
5
4
3
2
1
0
A.9
C.1
S.6
S.5
A.7
S.4
A.6
S.3
A.5
S.2
A.4
A.3
A.2
A.1
A.8
S.1
Non Esposto

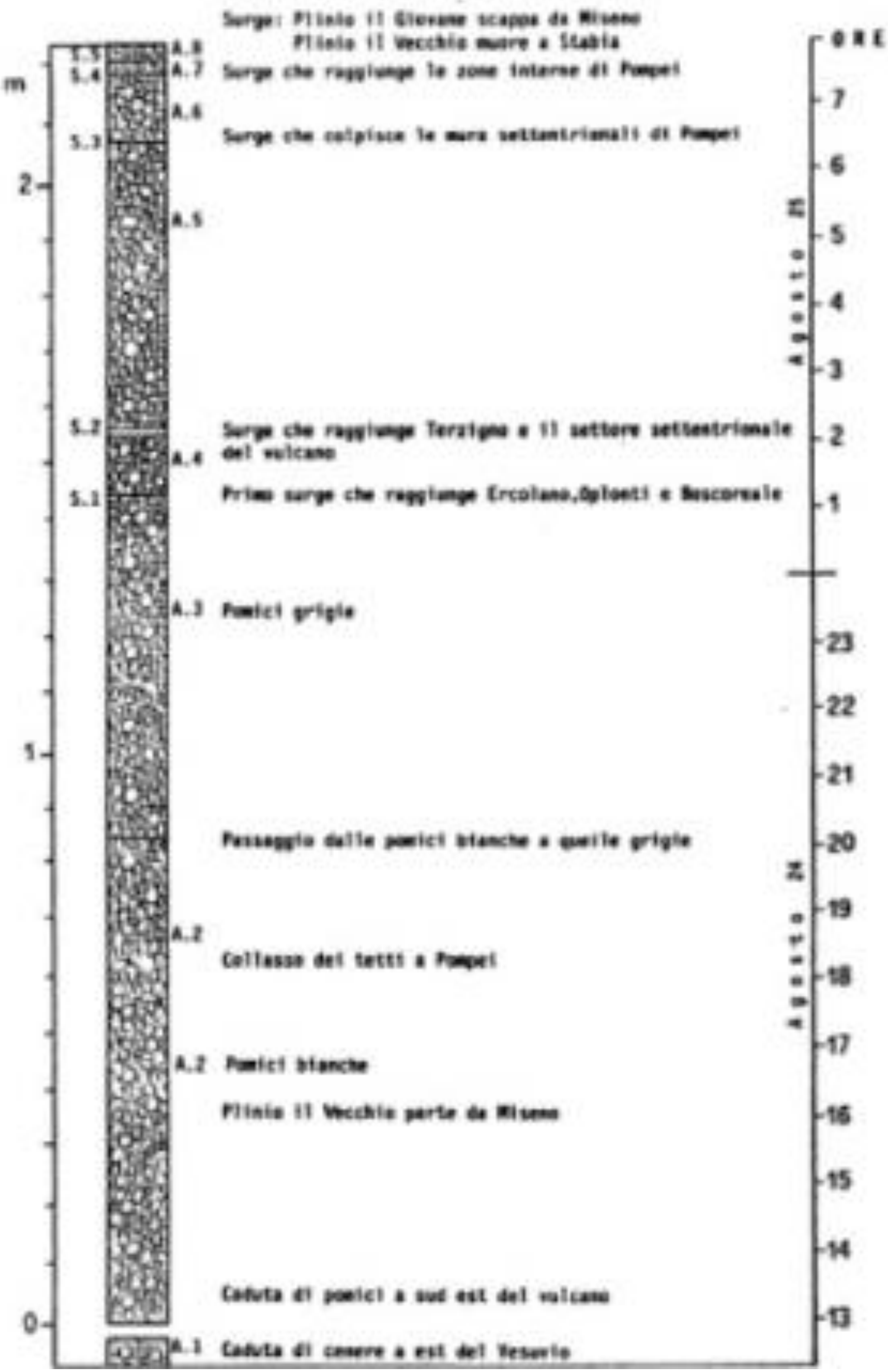


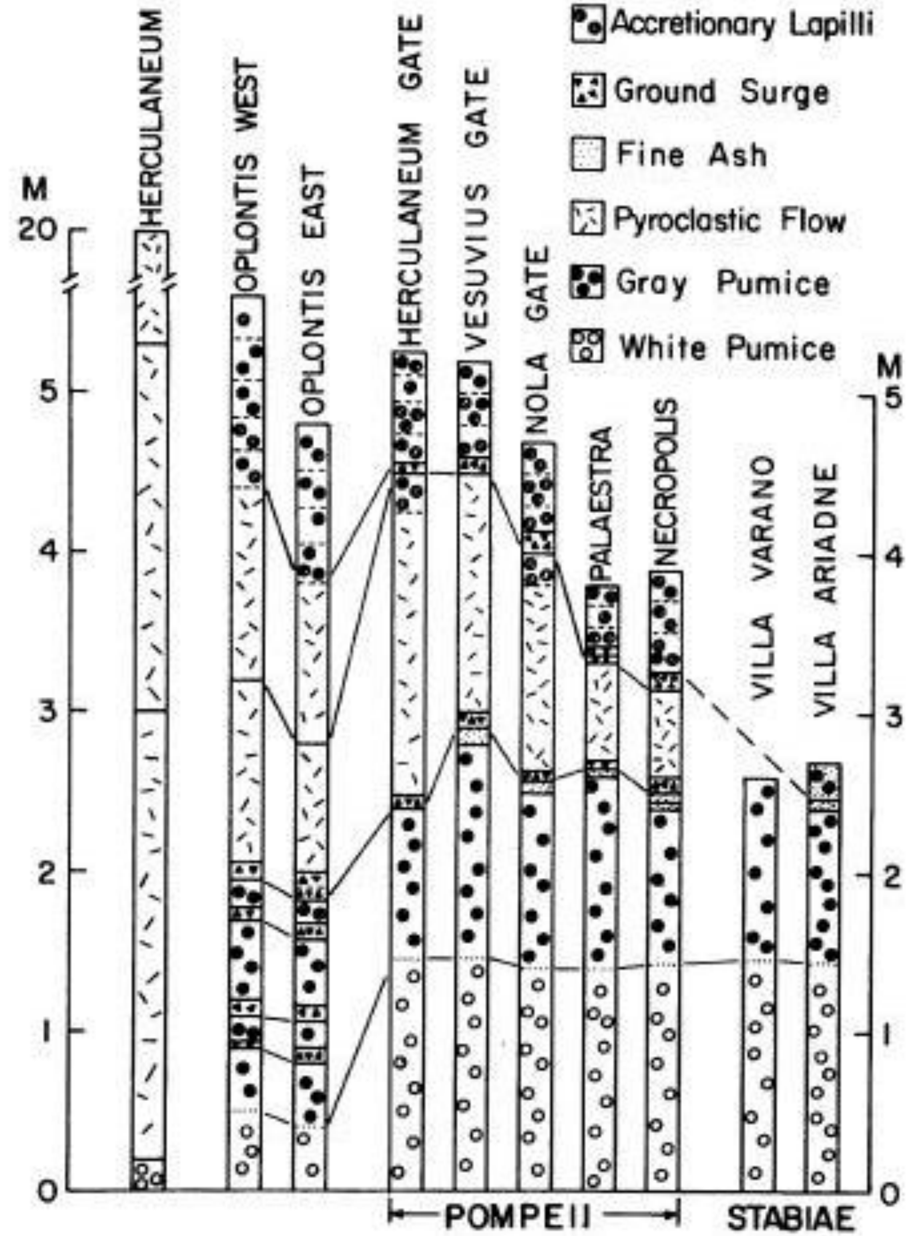


Ill. 2. Stratigraphy of the deposits of A.D. 79 in excavations west and south of Vesuvius

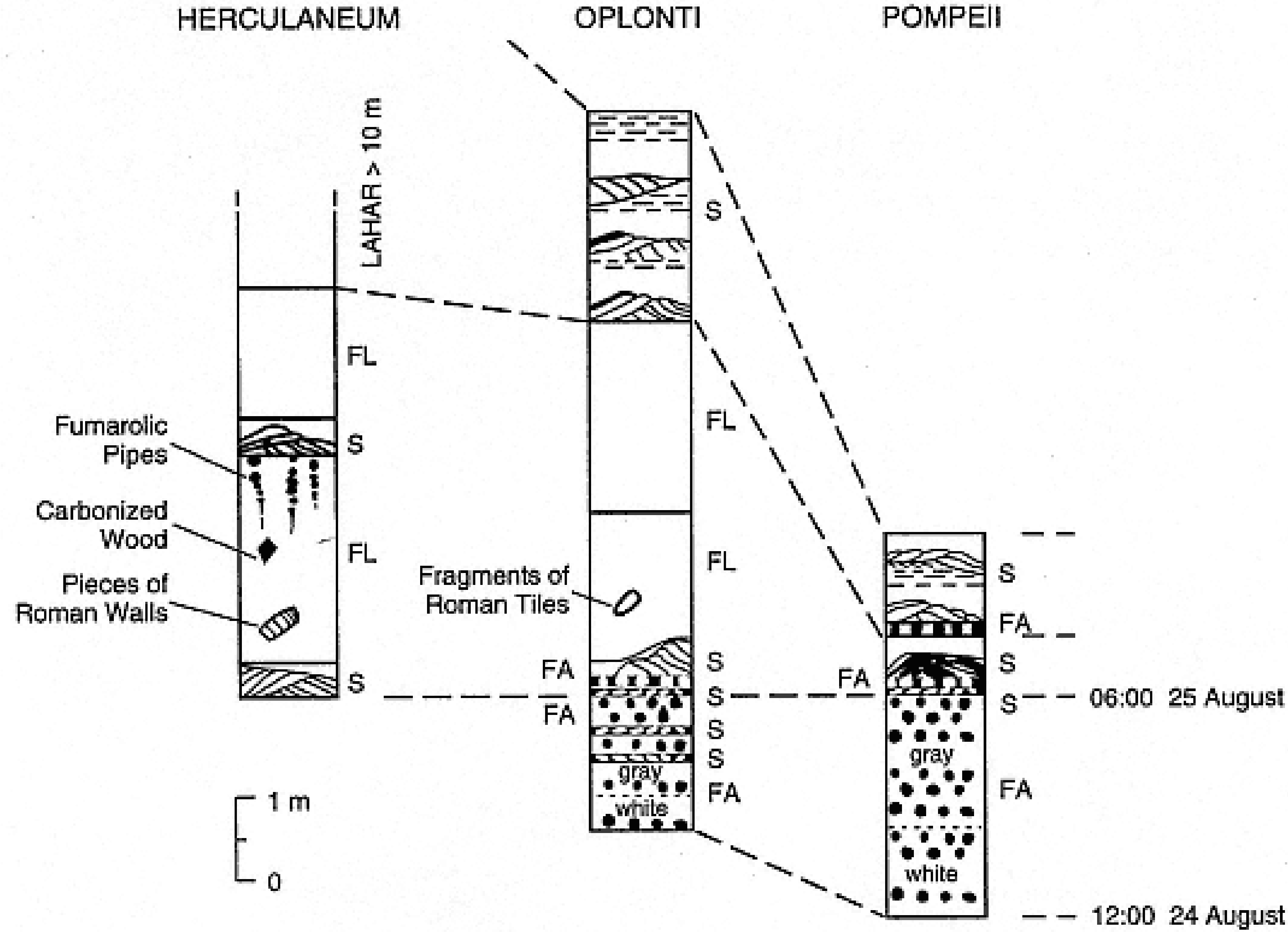


Fig. 2.18 Representative stratigraphy of AD 79 pyroclastic deposits exposed in archaeological excavations along the coastal side of Vesuvius; FA = pumice fallout, FL = pyroclastic flows, and S = surges. The basal white and gray pumice fallout was from early

Villa Regina (Boscoreale)

The tree was partially buried by the fall of pumice and then was bent by the pyroclastic flow

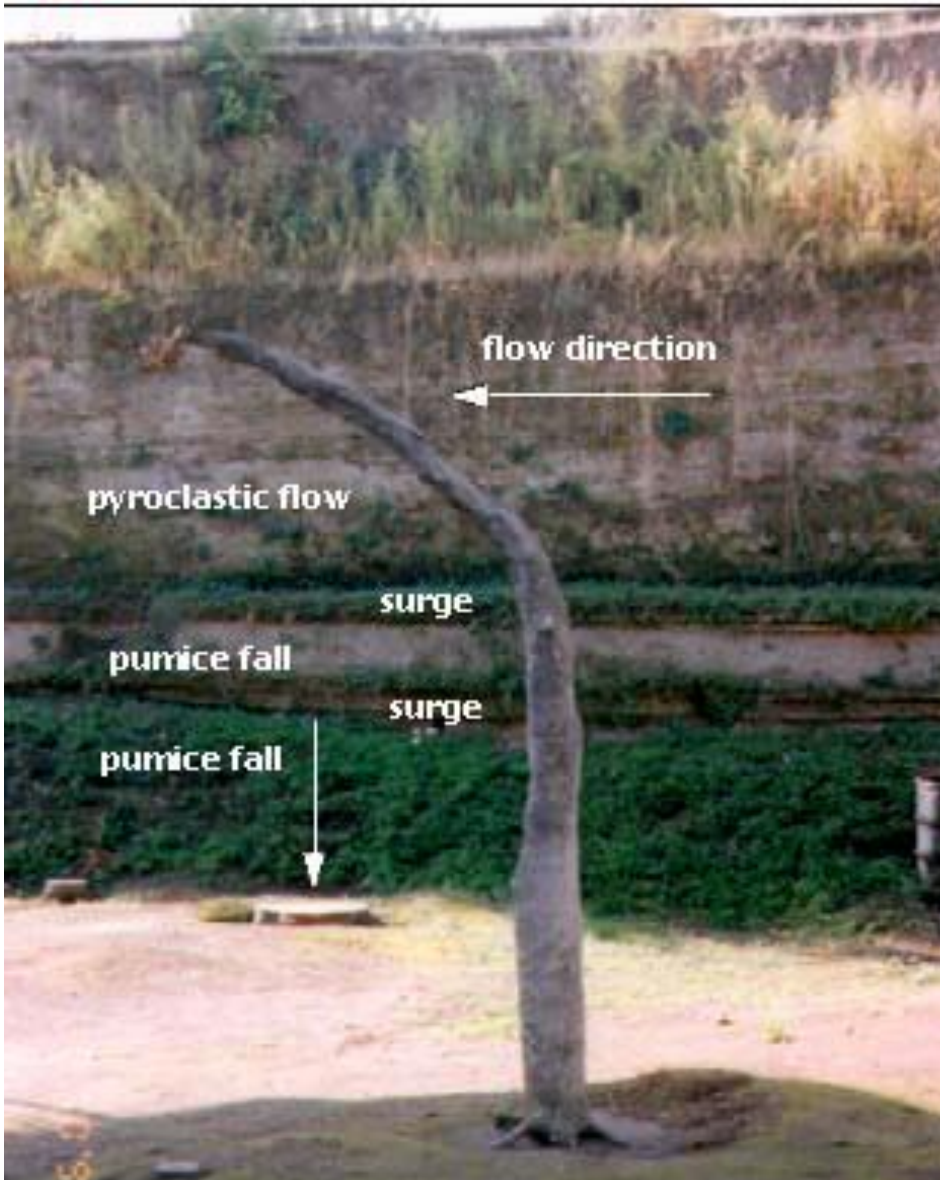


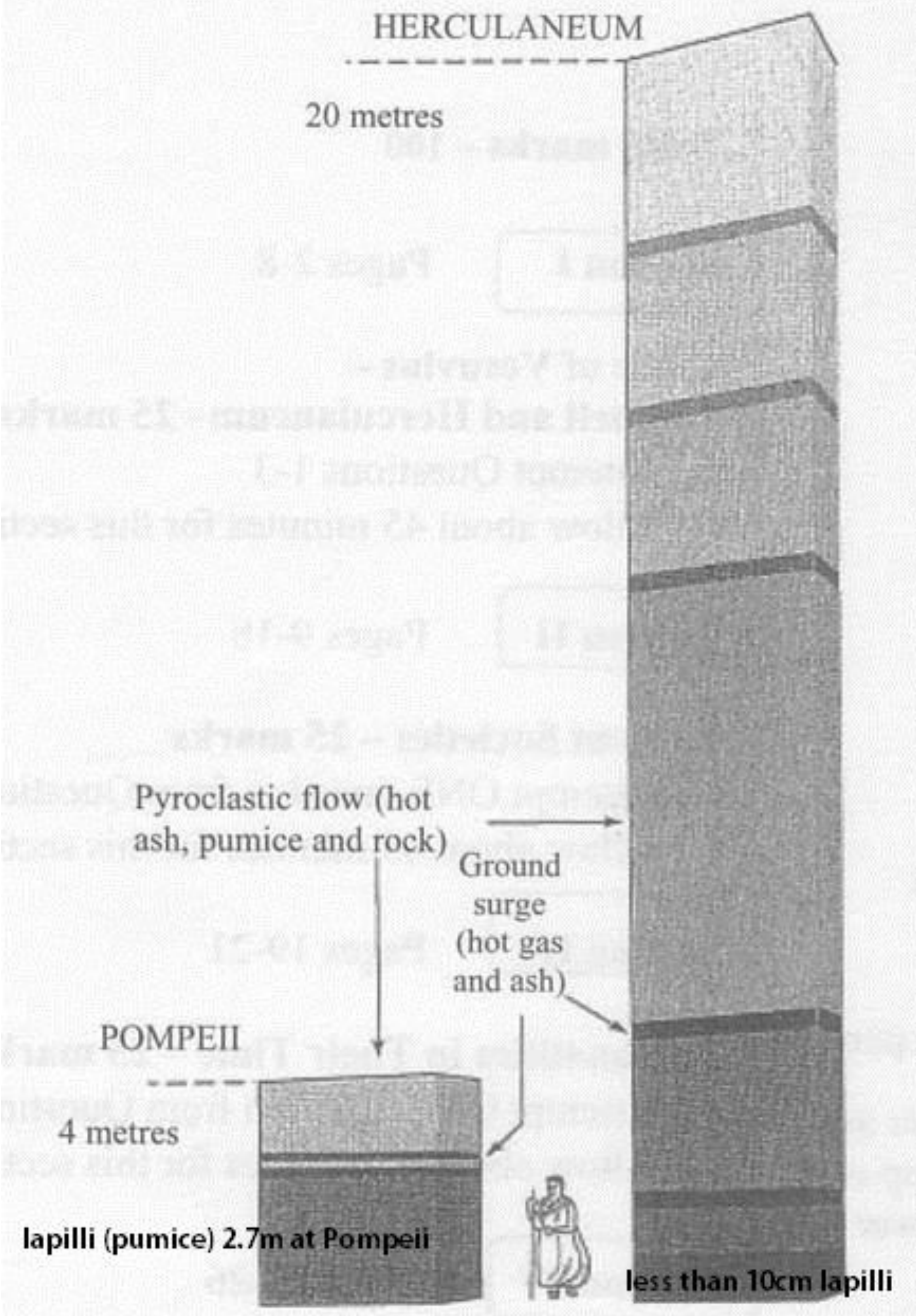

HERCULANEUM
20 metres
Pyroclastic flow (hot ash, pumice and rock)
Ground surge (hot gas and ash)
POMPEII
4 metres
lapilli (pumice) 2.7m at Pompeii
less than 10cm lapilli

Oplonti (Torre Annunziata)

12000 abitanti
1047 vittime
103 calchi

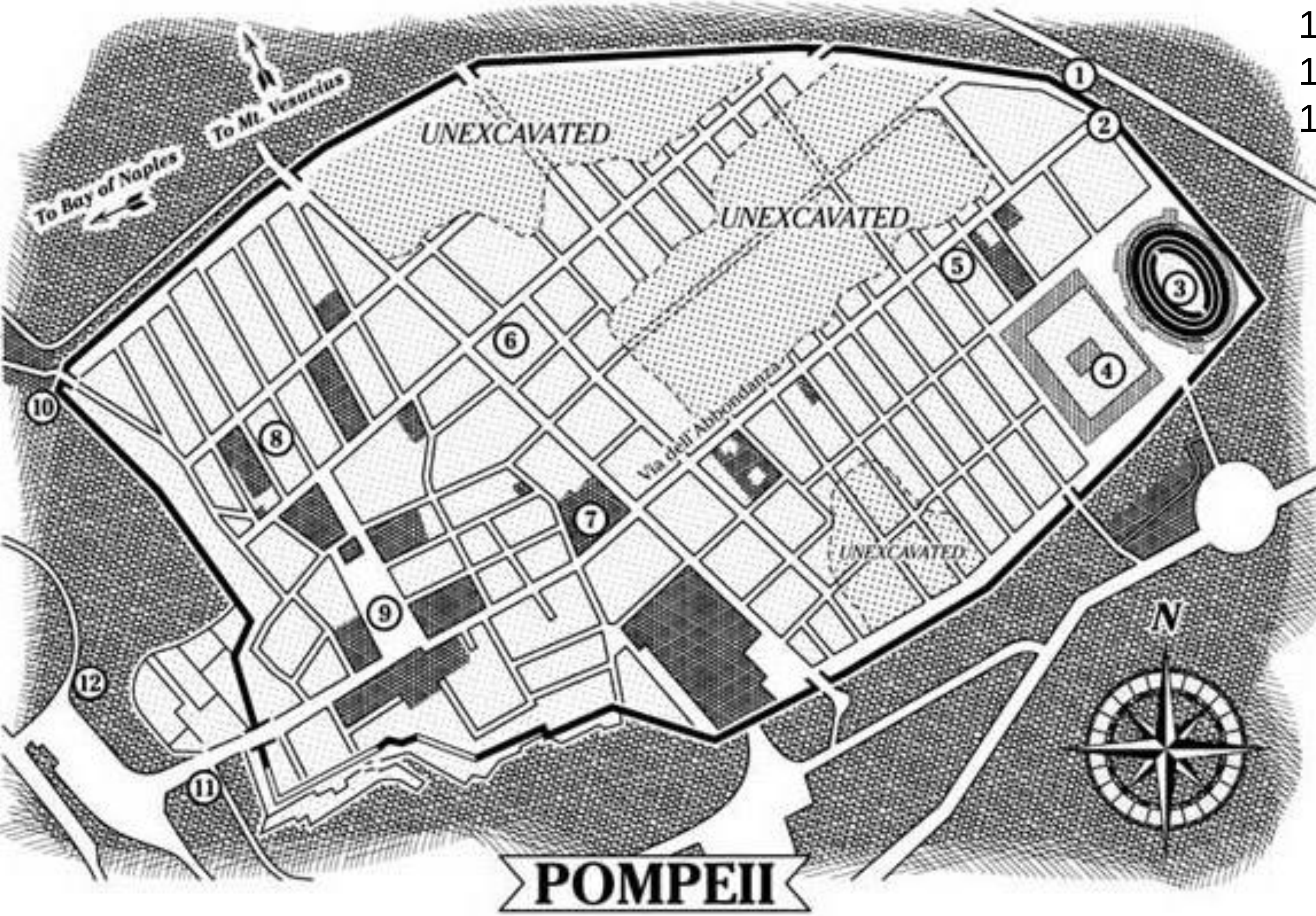


| | | | | | |
|---|---|---|---|---|---|
| 1 | VILLA DEIDAMIA | 5 | HOUSE OF OCTAVIUS QUARTUS | 9 | FORUM |
| 2 | PORTA DI SARNO | 6 | HOUSE OF JULIA FELIX | 10 | PORTA ERCOLANO |
| 3 | AMPHITHEATRE | 7 | STABIAN BATHS | 11 | PORTA MARINA |
| 4 | GRAND PALAESTRA | 8 | HOUSE OF THE TRAGIC POET - Cave Canem | 12 | UMBERTO'S CAFE |

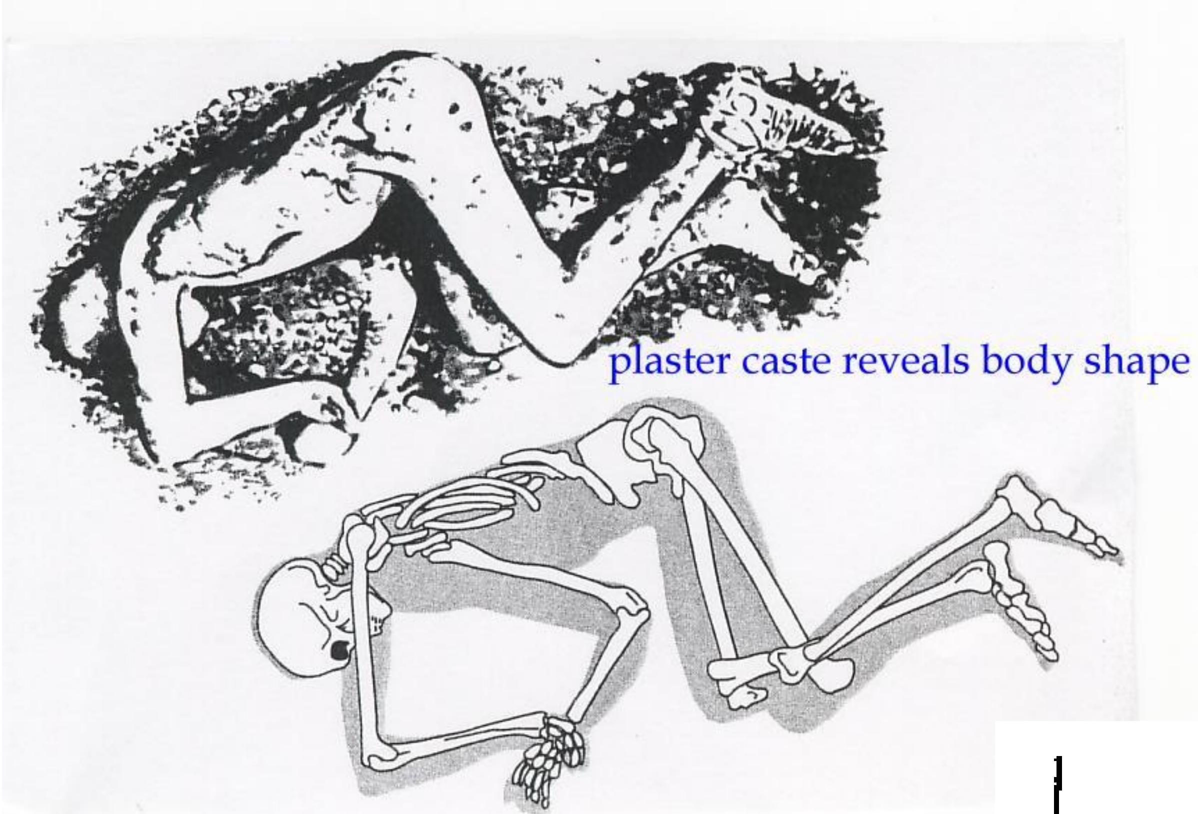
plaster caste reveals body shape

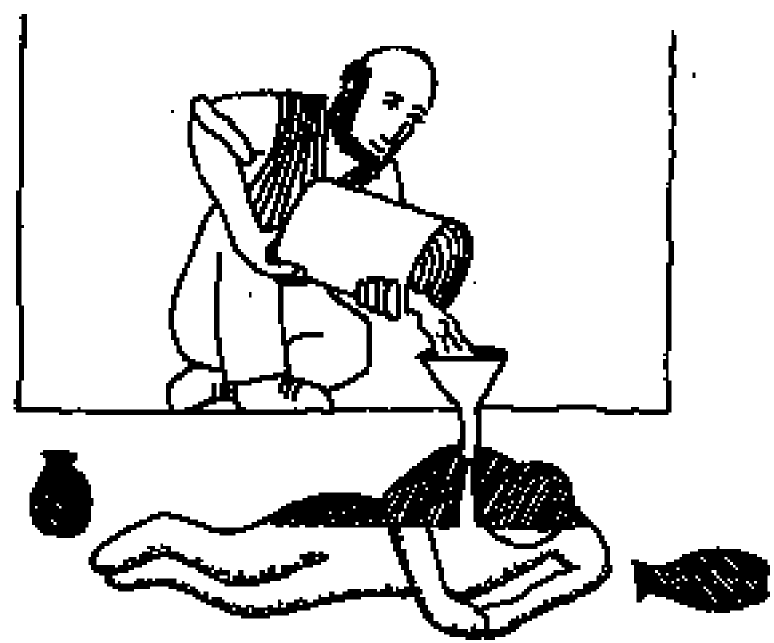




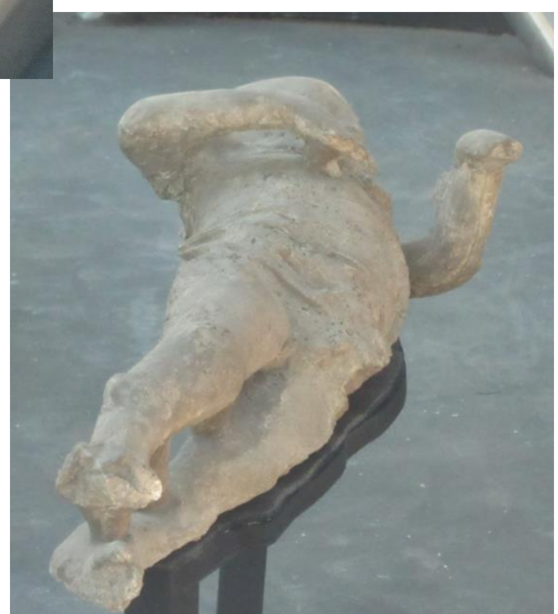



Group of corpses (casts and skeletons) near the Casa del Criptoportico 1914. They were encountered in the ash and pumice PDCs deposit above a thick, white^grey, lapilli pumice fall deposit. Below the human cast on the right side the stratigraphic sequence from unit B to E1 is well exposed. (Soprintendenza Archeologica di Pompei) Luongo et al., 2003

Casa del Criptoportico

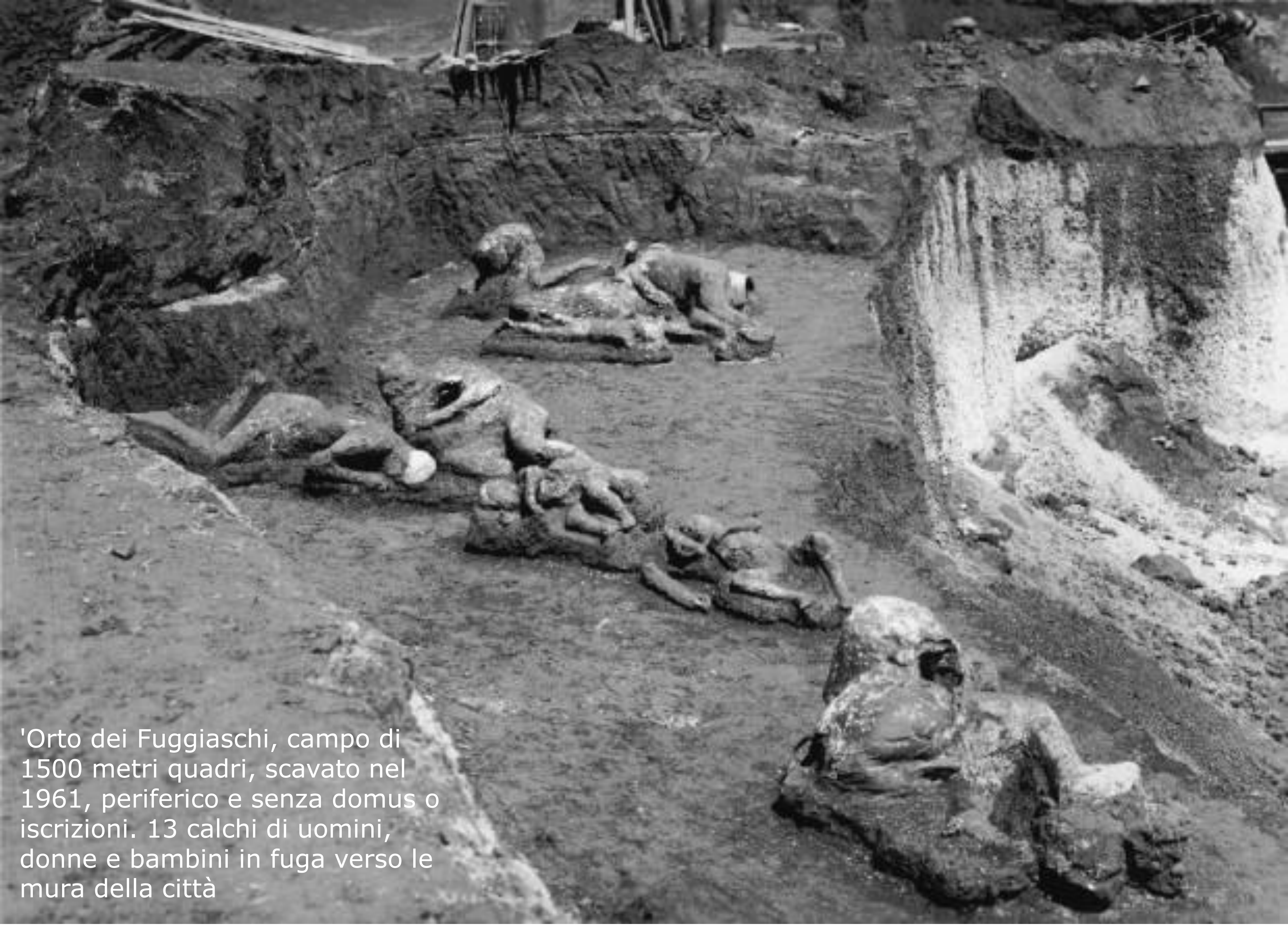

'Orto dei Fuggiaschi, campo di 1500 metri quadri, scavato nel 1961, periferico e senza domus o iscrizioni. 13 calchi di uomini, donne e bambini in fuga verso le mura della città

## Variations in EU4pf flow direction (anisotropy of magnetic susceptibility [AMS] data) and temperature (thermal remanent magnetization [TRM] data).

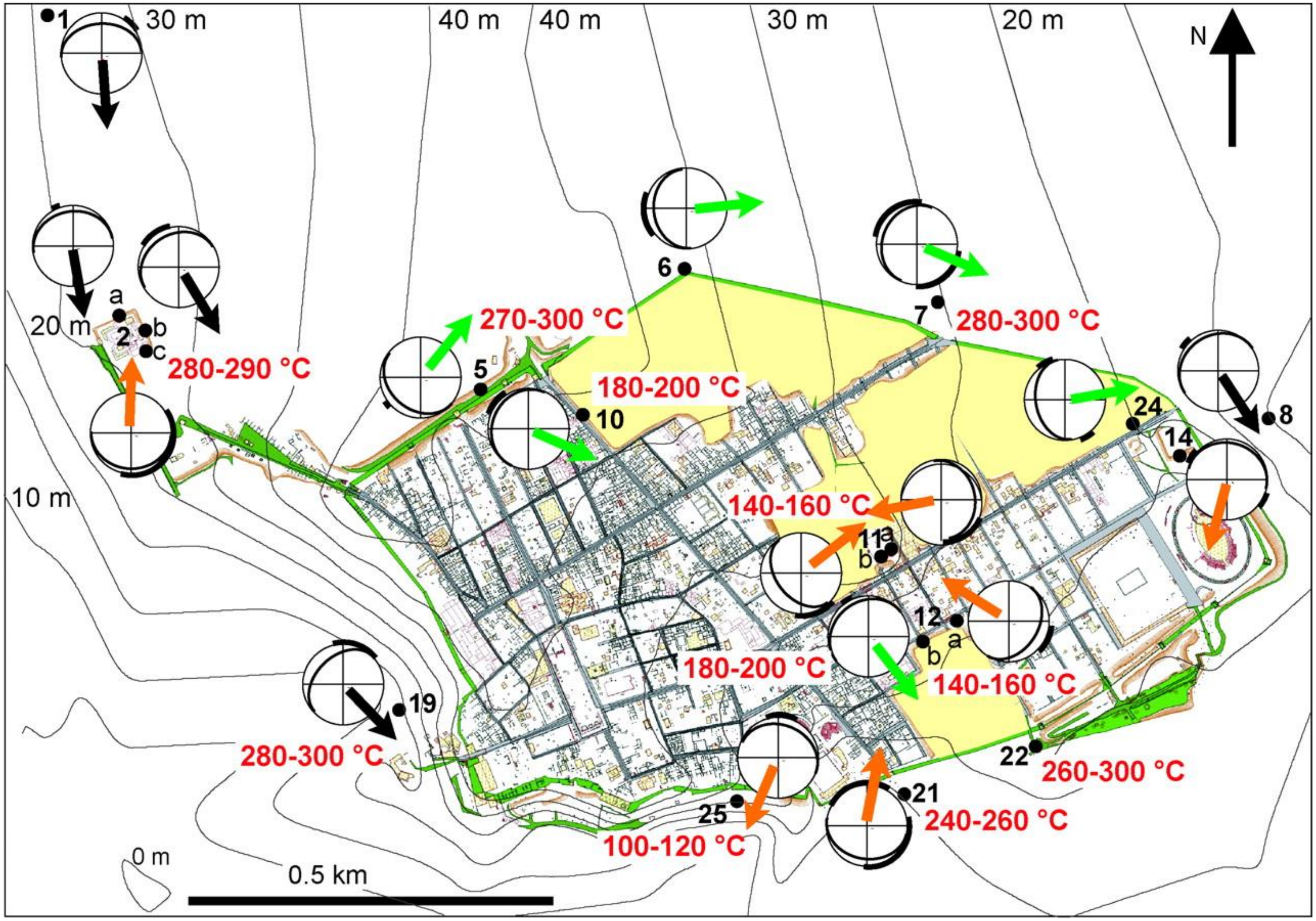


**Lucia Gurioli et al. Geology 2005;33:441-444**

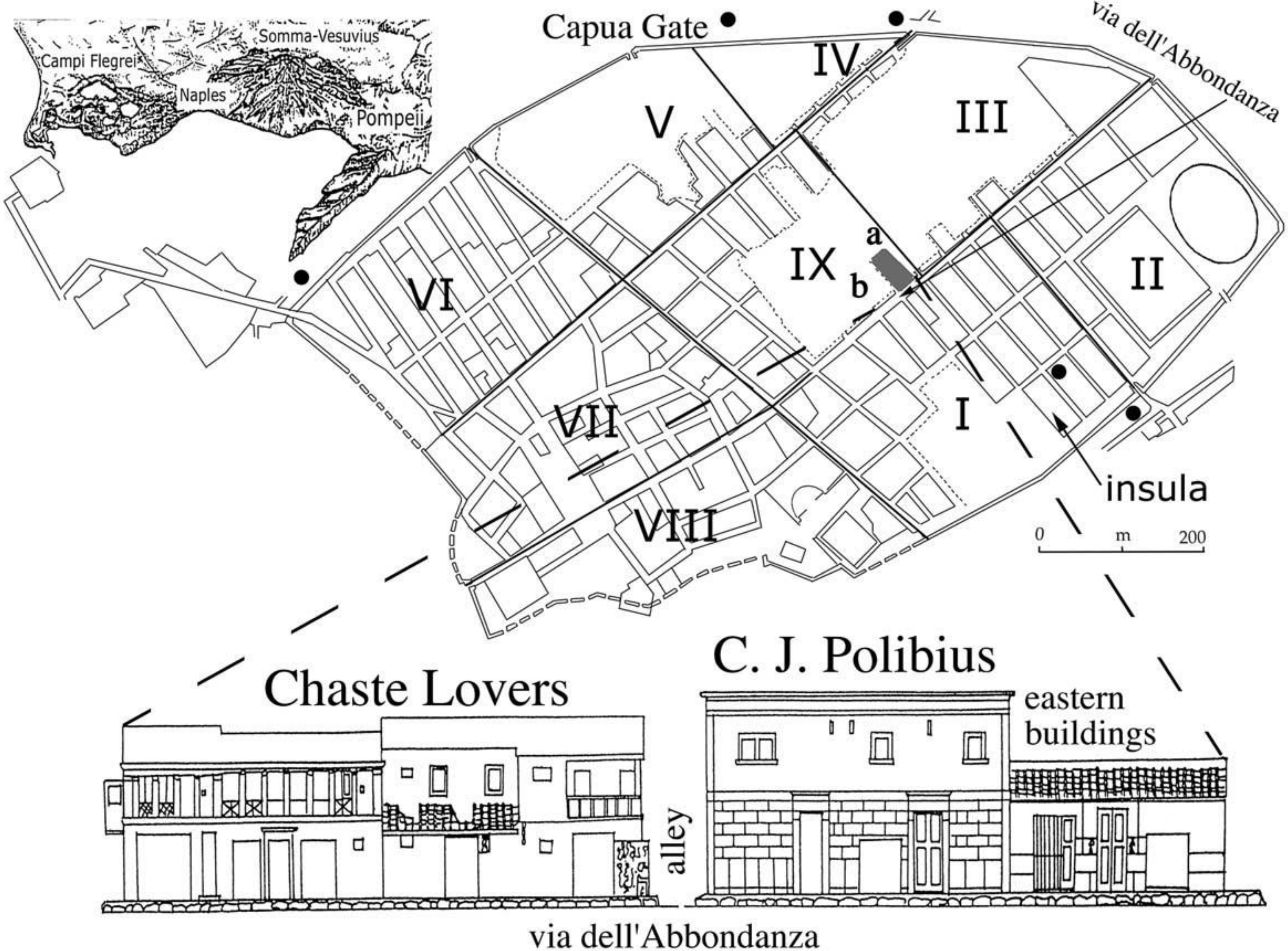


Luongo et al. / Journal of Volcanology and Geothermal Research 126 (2003) 201-223

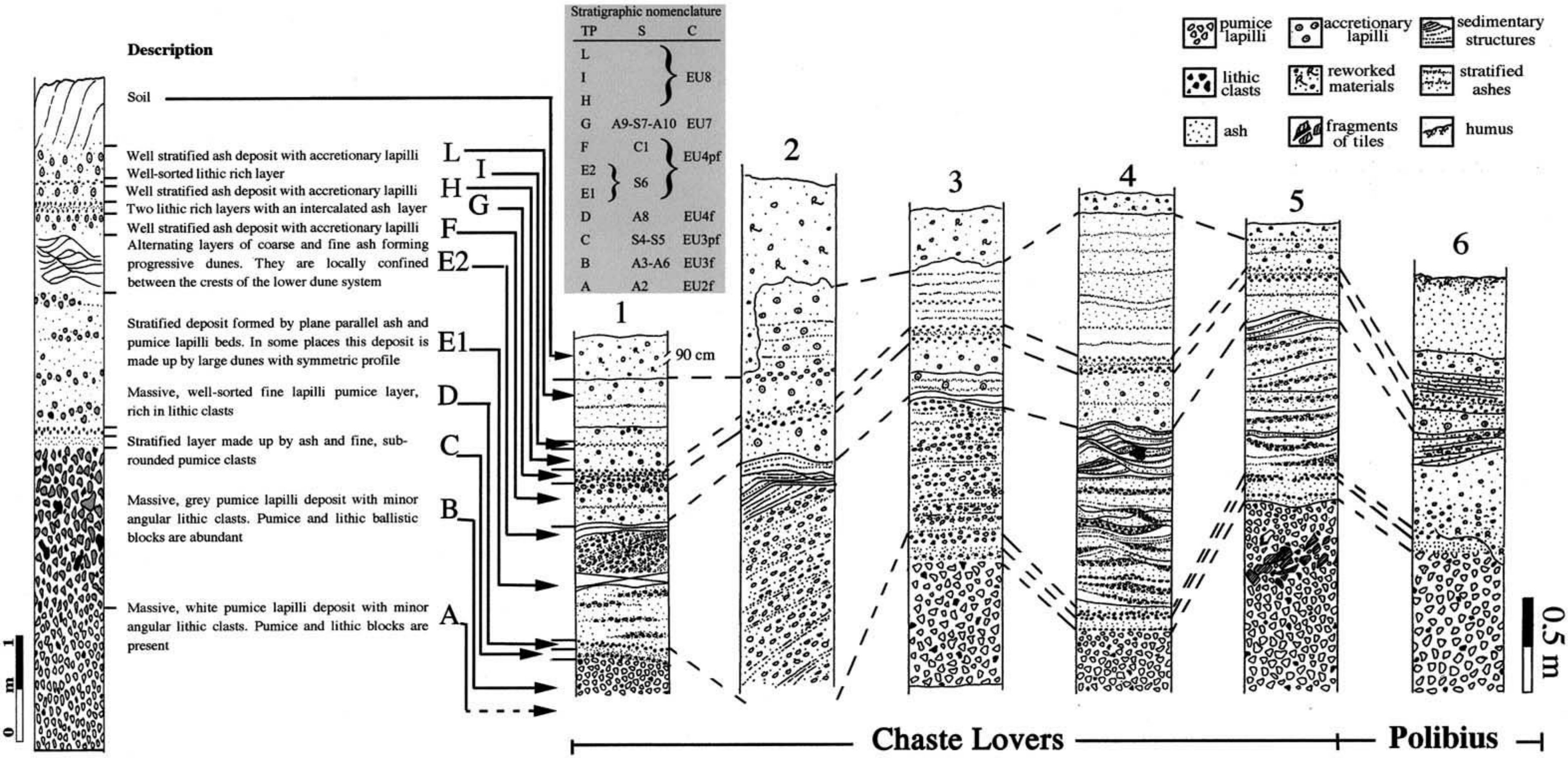


Fig. 2. Left: composite stratigraphic section showing the maximum thickness of the units of the AD 79 deposit at Pompeii. A lithofacies description is also illustrated.
Right: detailed stratigraphic columns along the western side of the house of the Chaste Lovers and in a hole dug a few metres from the eastern perimeter wall of the Polibius' house. For location of the sections, see Figs. 1 and 4. Inset: relationship between the stratigraphy presented in this paper (TP) and those published by Sigurdsson et al., 1985 (S) and Cioni et al., 1996 (C).

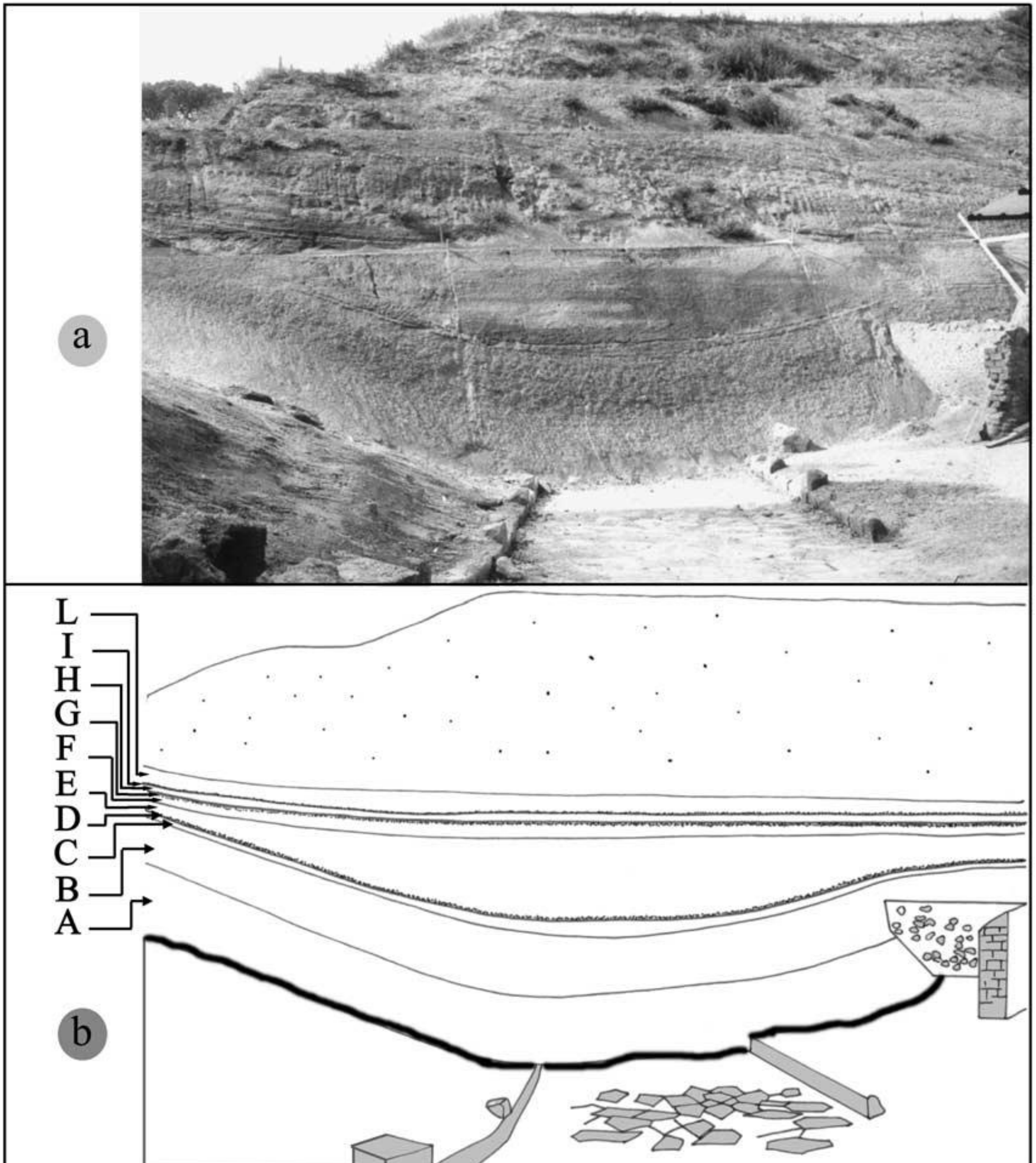


(a) The complete sequence of the AD 79 pyroclastic deposit at Nola Gate (for location, see Fig. 1). The pyroclastic deposit thickens in correspondence of a Roman road enclosed between an embankment that rests on the city walls and an enclosure wall. (b) geometry of the di!erent units distinguished throughout the AD 79 deposit. Note the mantling nature of the fall units (A, B, D, G, and I) while the PDC units show different geometric relationships with respect to the palaeo-topography. Unit C mantles the topography and thickens in the depression; unit E is valley-ponding, filling the topographic depression. The upper part of the sequence (dotted layer) is made of reworked material accumulated during past excavations (removed).

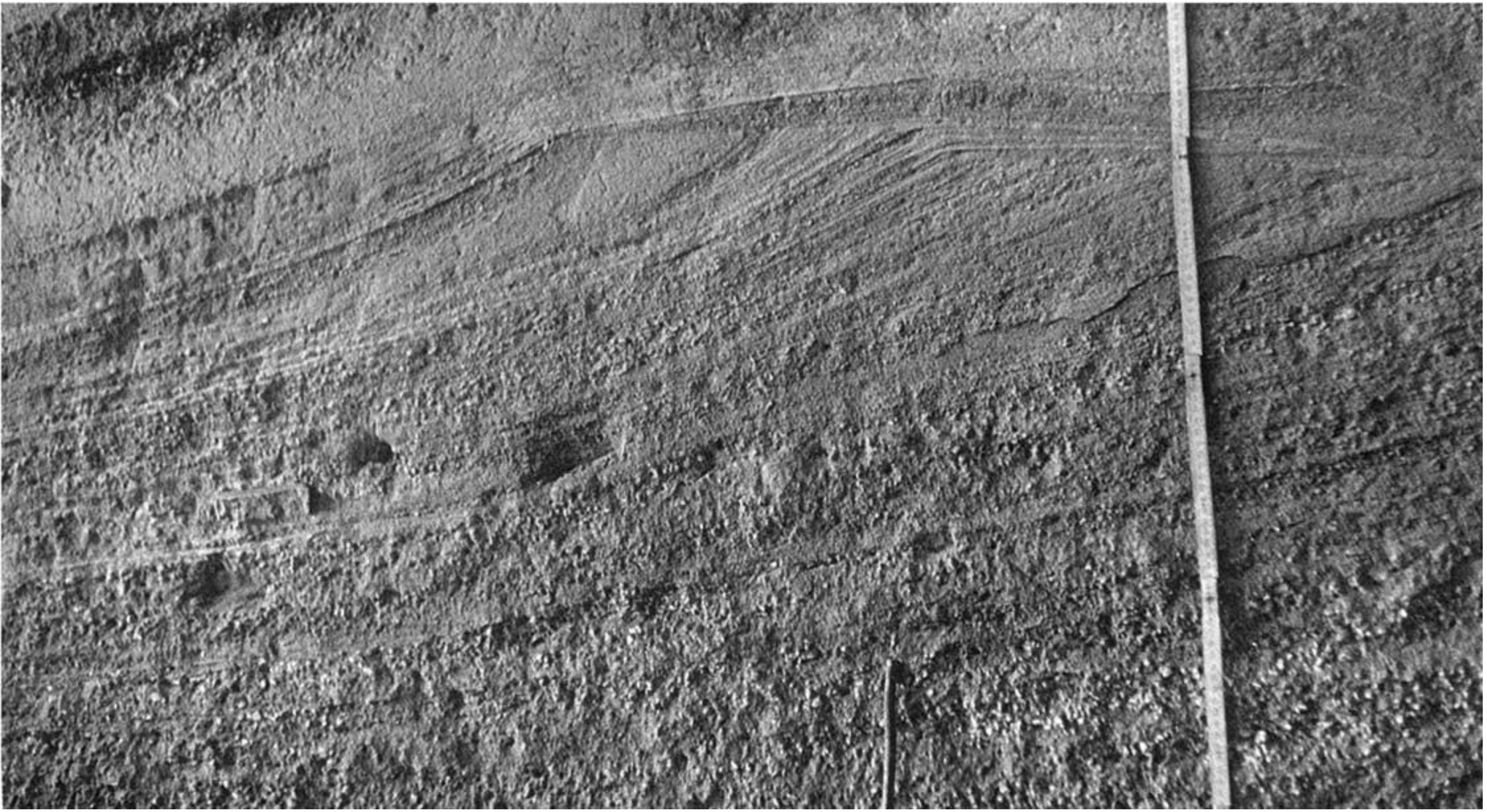

Fig. 5. Unit E2 forming progressive dunes in the central part of the pyroclastic current deposits at the house of the Chaste Lovers. Flow direction is from right to left. Scale is in 20-cm intervals

Fig. 9. Some of the skeletons in room [GG]. Skeletons (III) and (IV) are above an ash layer, 20-40 cm thick, lying directly on the floor. The skull of skeleton (I) is close to the feet of skeleton (IV).

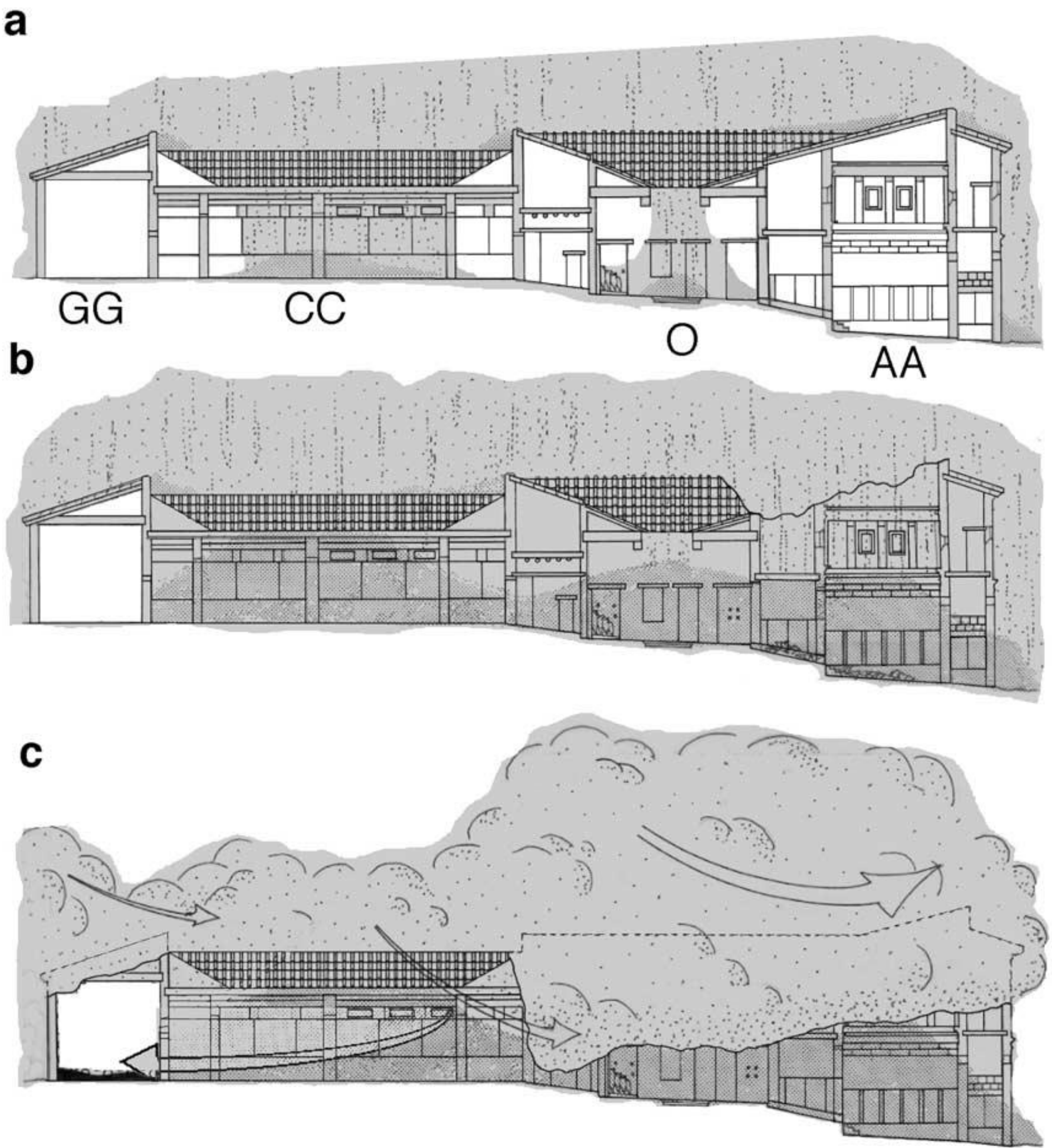


Fig. 14. The destructive effects of the different eruptive phases on the Polibius' house. The section is drawn according to trace I in Fig. 6; Mount Vesuviu is to the left of the building. (a) Fall product accumulate in the alleys on the roofs, in the peristyle and the rooms with impluvium during the ea hours of the eruption. (b) Roofs and attics of some front rooms collapse under the pumice lapilli load. (c Pyroclastic currents by-pass the rear rooms and destroy the east-west trending walls in the fron part of the house; a reflected flow invades th rooms where the inhabitants had taken

# Ercolano

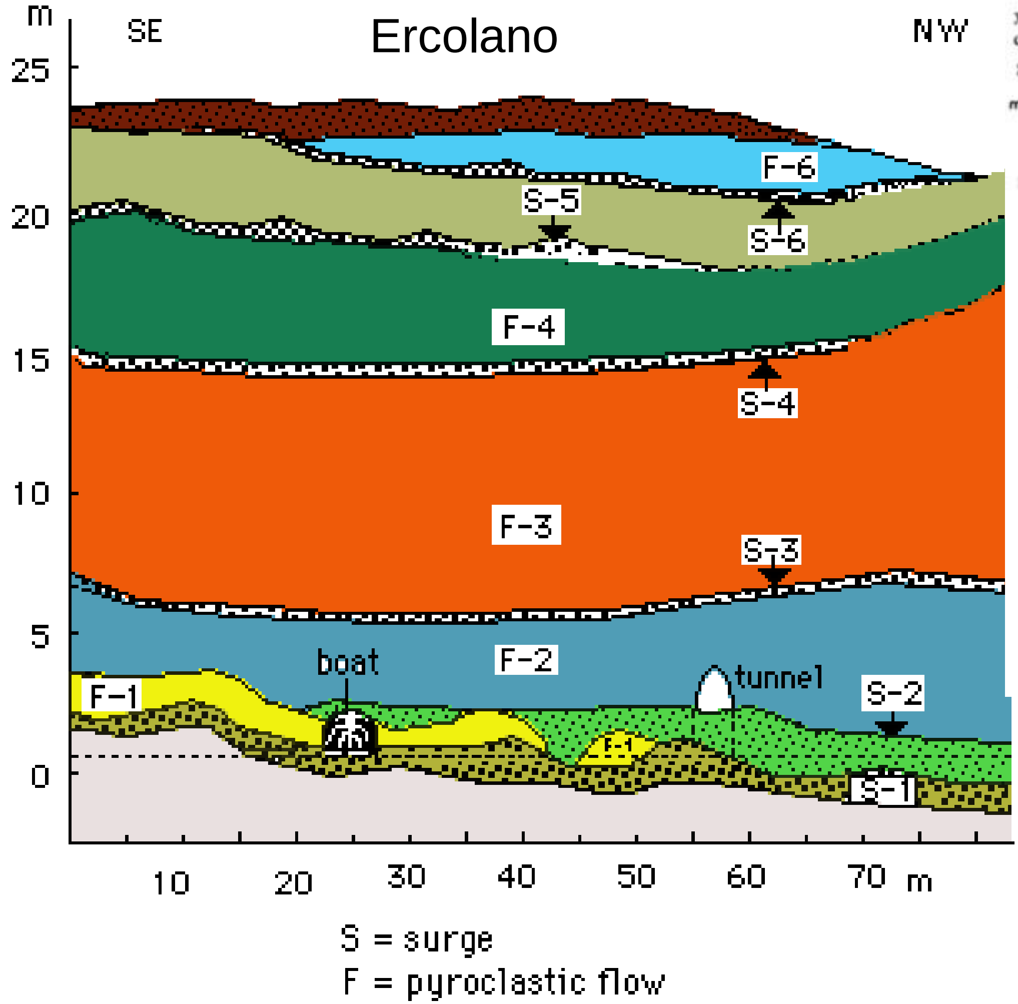


XCV, 2. Stratigrafia dei depositi vulcanici del 79 d.C. a Ercolano. La scala verticale inizia a 5 m al di sotto dell'attuale livello del mare (da Sigurdsson et al., 1985).

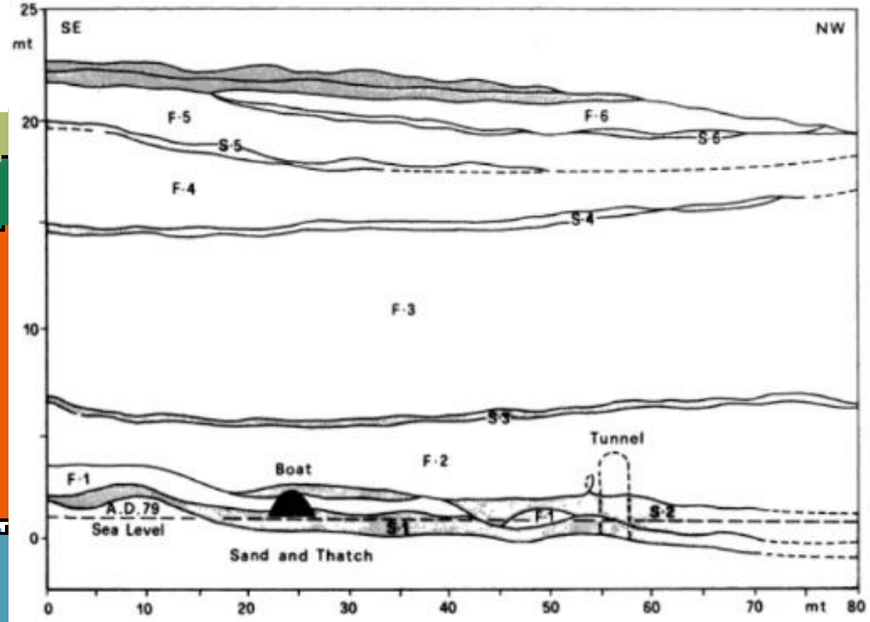


Pyroclastic Flow: A hot, chaotic avalanche of pumice, ash, and gasses. Pyroclastic flows can move at high speeds along the ground and pass over substantial objects. Their distribution is strongly controlled by topography.

Pyroclastic Surge: A turbulent cloud of volcanic ash and hot gasses, which hugs the ground and travels at speeds often exceeding 100 km per hour. Surge deposits are more widely distributed than pyroclastic flow deposits though not as widespread as air fall pumice layers.

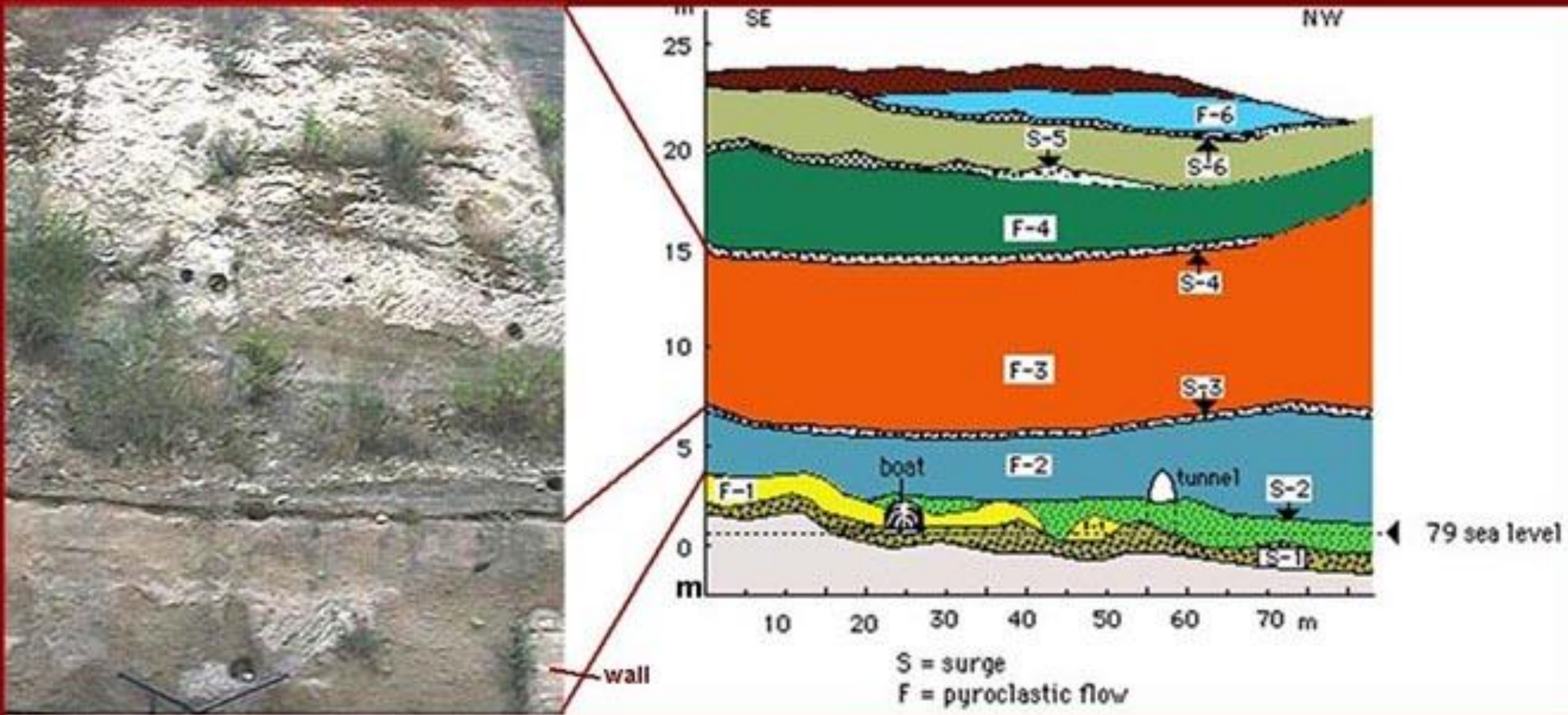


***At Herculaneum, there were six surge/flow pairs, and, although they may have contained moisture, none of them could be characterized as "mud flows" (lahars). Because Herculaneum was so close to the crater, the flow deposits were much hotter than those at Pompeii -- hot enough to fuse together into the much harder overlay than the deposits at Pompeii. The flows did act as a liquid, however: Solid particles were suspended in a gas (mostly just hot air) and fluid mechanics determined how the flows spread.***

**Stratigraphy of the AD 79 Eruption Deposits seen at Herculaneum**

The diagram (by Roberto Scandone )above shows the stratigraphy at Herculaneum, as identified by Haraldur Sigurdsson in 1985. (The **upper flow units** F4 etc can also be identified in Pompeii). There is a very thin base lapilli layer of a few centimetres. The first broad deposit shown immediately above the ancient coast is an ashy layer interpreted as a surge. It is 20-40 cm thick and is a result of a surge of gaseous material. The majority of the skeletons found in this area lie within this deposit. Above this layer is a deposit of a pyroclastic flow containing carbonized wood and fragments of tiles. The thickness of this deposit is less than 1.5 m. Above this layer are several alternating surge and pyroclastic flow layers resulting in a 20 to 23 metre thick cover. Flow 3 is particularly strong. According to some authors (Mike Sheridan, for example) the topmost layers are related to mudflows.

In many houses there is abundant evidence of processes of carbonization of wood due to the high temperature of the first surge and flow. On this profile, the extension of the coastline is identifiable. Also notice the location of the boatshed.

Surge 3 reached the walls of Pompeii. The next three surges covered Pompeii, S-4, S-5 and S-6. The first of these surges would have been most damaging to people, whereas the last surge would have been most damaging to buildings. S-4 may have had temperatures around 400°C upon its arrival at Pompeii. (Martini *et al. 1995* )

The key basis for distinction is the amount and nature of the pyroclastic material included in the mixture of volcanic solids and gas. Denser mixtures which include larger fragments at higher solid concentrations are typically categorized as pyroclastic flow, while less dense mixtures where the pyroclasts are primarily fine dust and ash are categorized as pyroclastic surge. The term "glowing avalanche" is sometimes used to describe pyroclastic flow, while the terms "glowing cloud" and "ground surge", are sometimes used to describe pyroclastic surge. The French term "nuée ardente" is often used to describe a common phenomenon where an avalanche of coarse material, a pyroclastic flow, is accompanied by an overriding ash cloud of fine material, a pyroclastic surge. The diagram below shows how the ash cloud (surge) layer of a nuée ardente separates from the ash-and-block (flow) layer. The surge layer may separate from the flow layer climbing hills and travelling greater distances
Fisher 1995

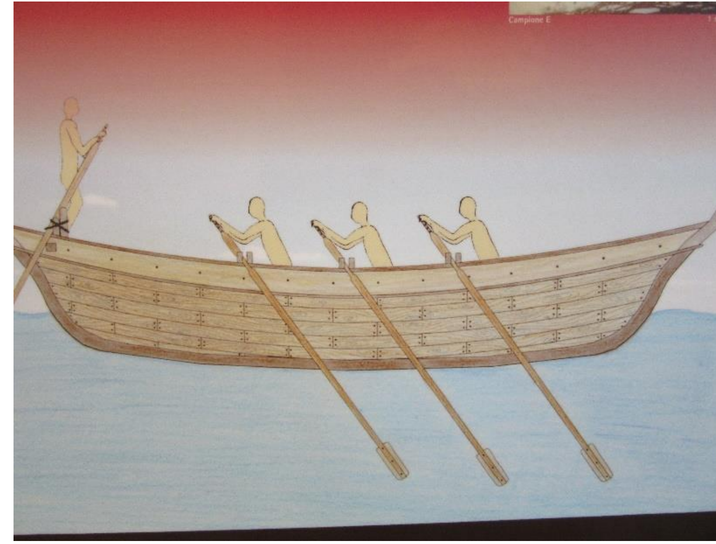

Ercolano

Scoperta 1738
Spoliata attrraverso cunicoli fino al 1828
Pochi resti umani
Città evacuata?
1981 scavo dei fornici sulla spiaggia
160 scheletri di cui 12 bambini
Popolazione stimata: 5000

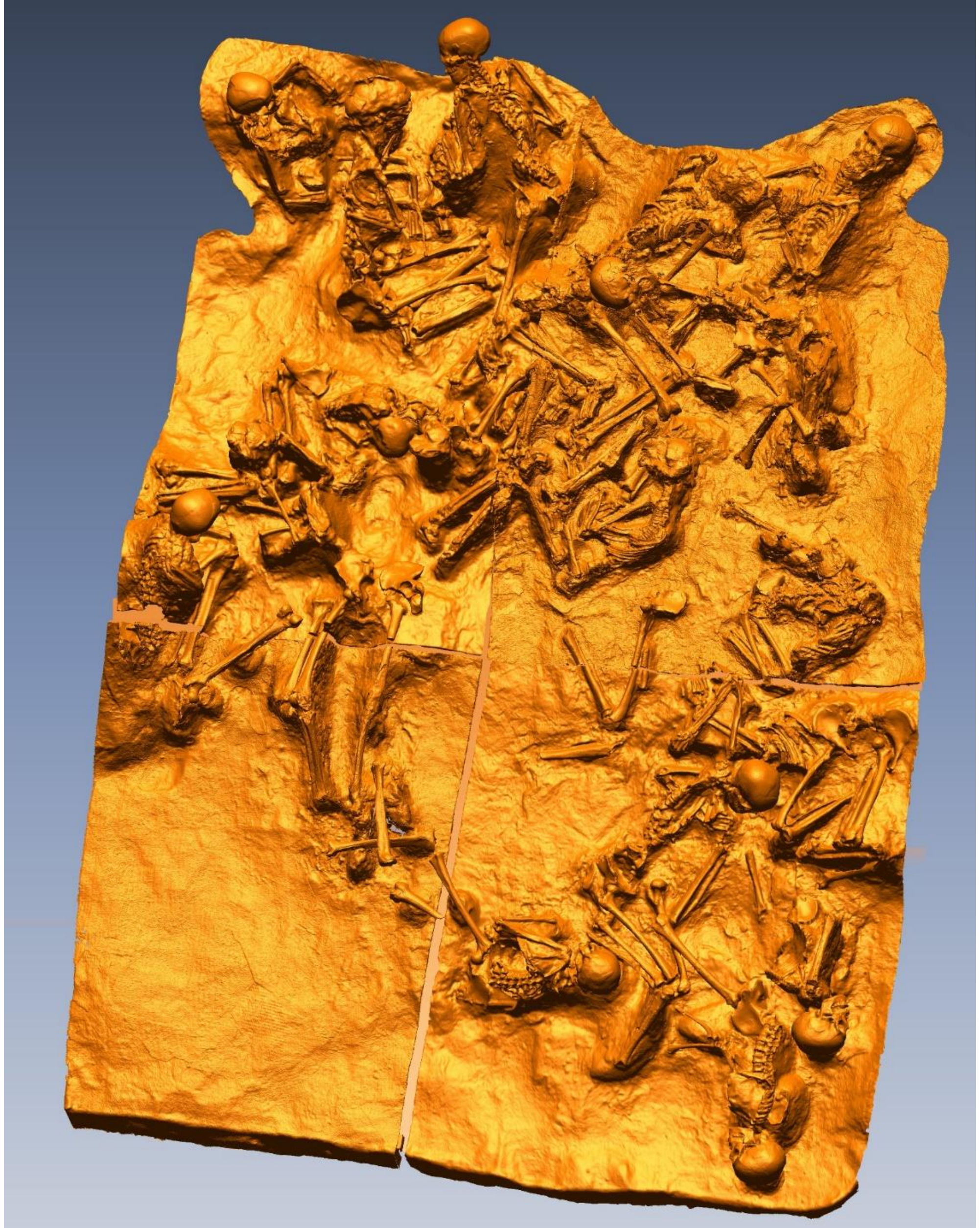

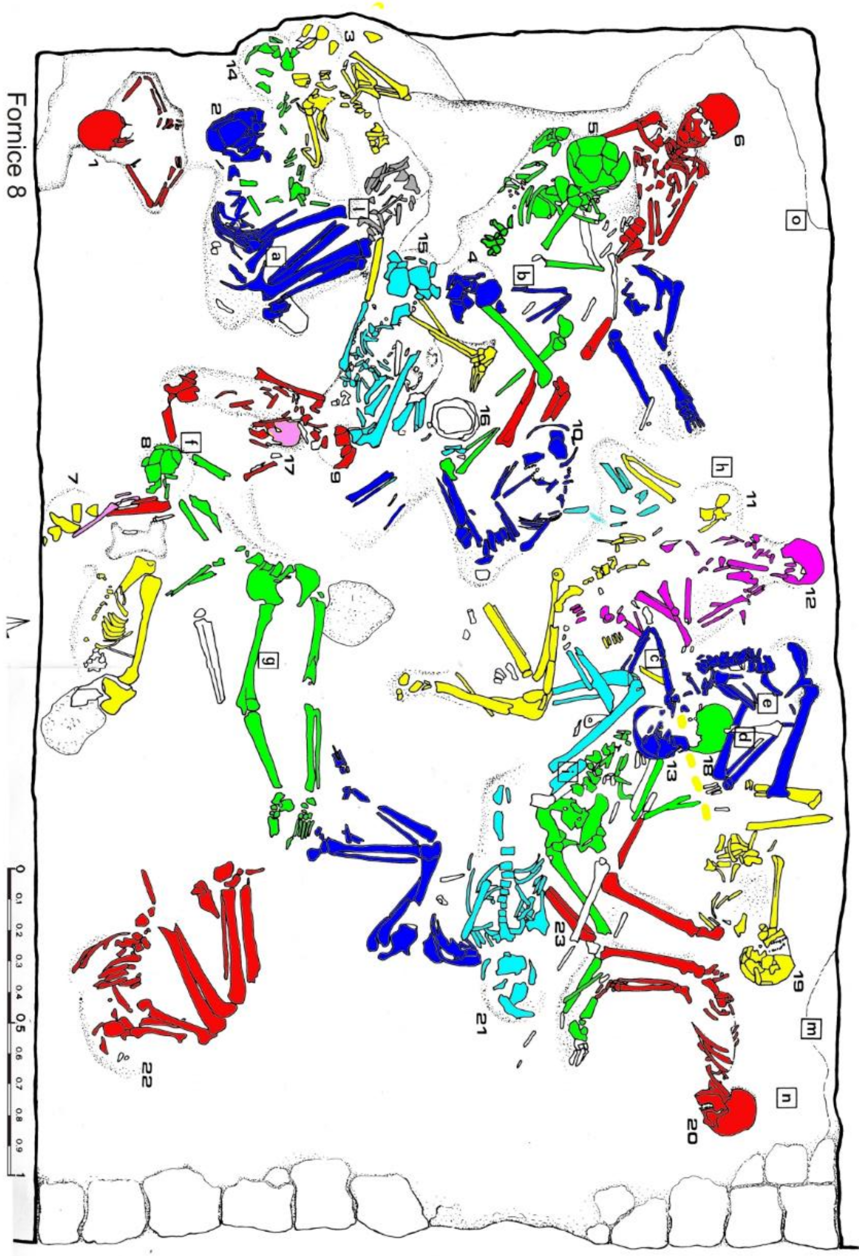
Fornice 8

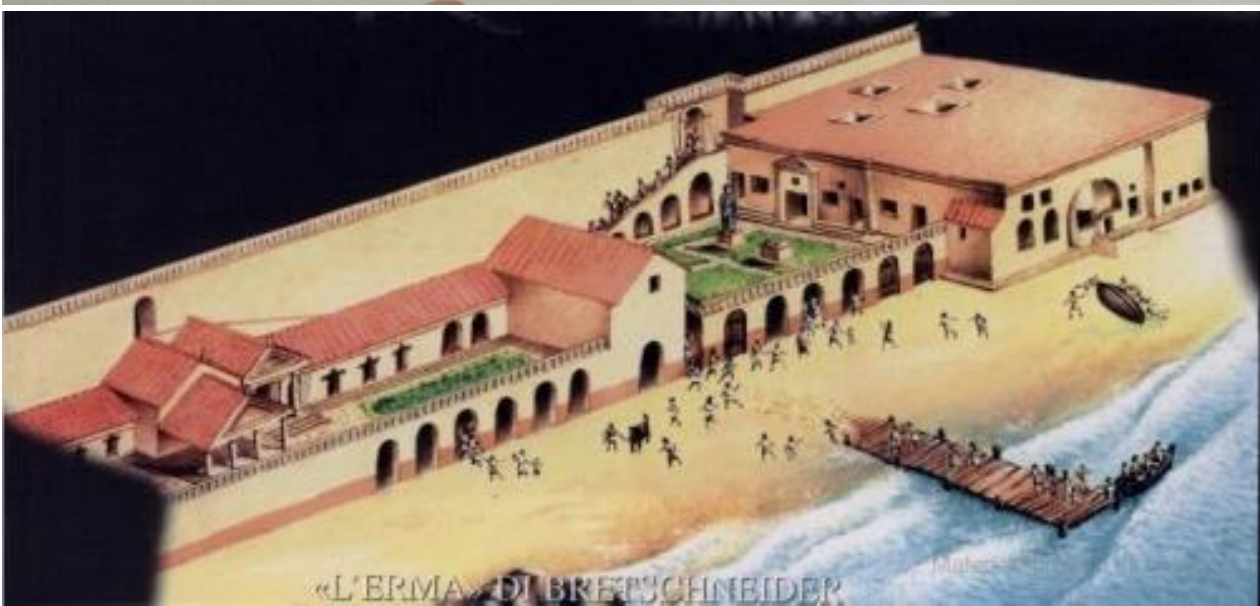
«L'ERMA» DI BRETSCHNEIDER

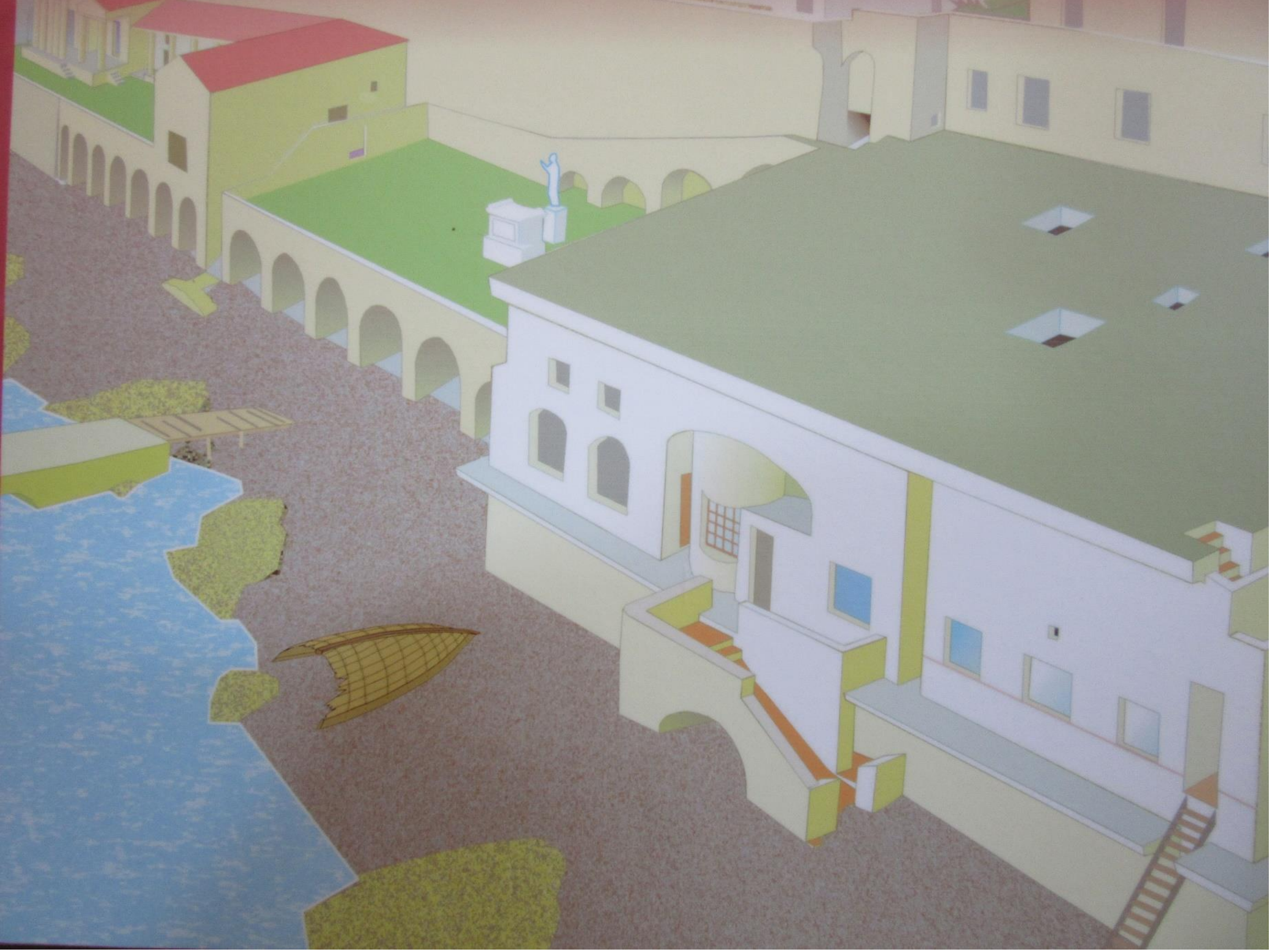


«L'ERMA DI BRETSCHNEIDER


Fig. 29 - Ricostruzione degli effetti dell'impatto del *surge 1* sulla antica spiaggia di Ercolano circa all'1 di notte del 25 agosto del 79 d.C.


Fig. 32 - Ricostruzione della situazione sull'antica spiaggia di Ercolano nella notte fra il 24 ed il 25 agosto 79 d.C. dopo la deposizione del primo flusso piroclastico.

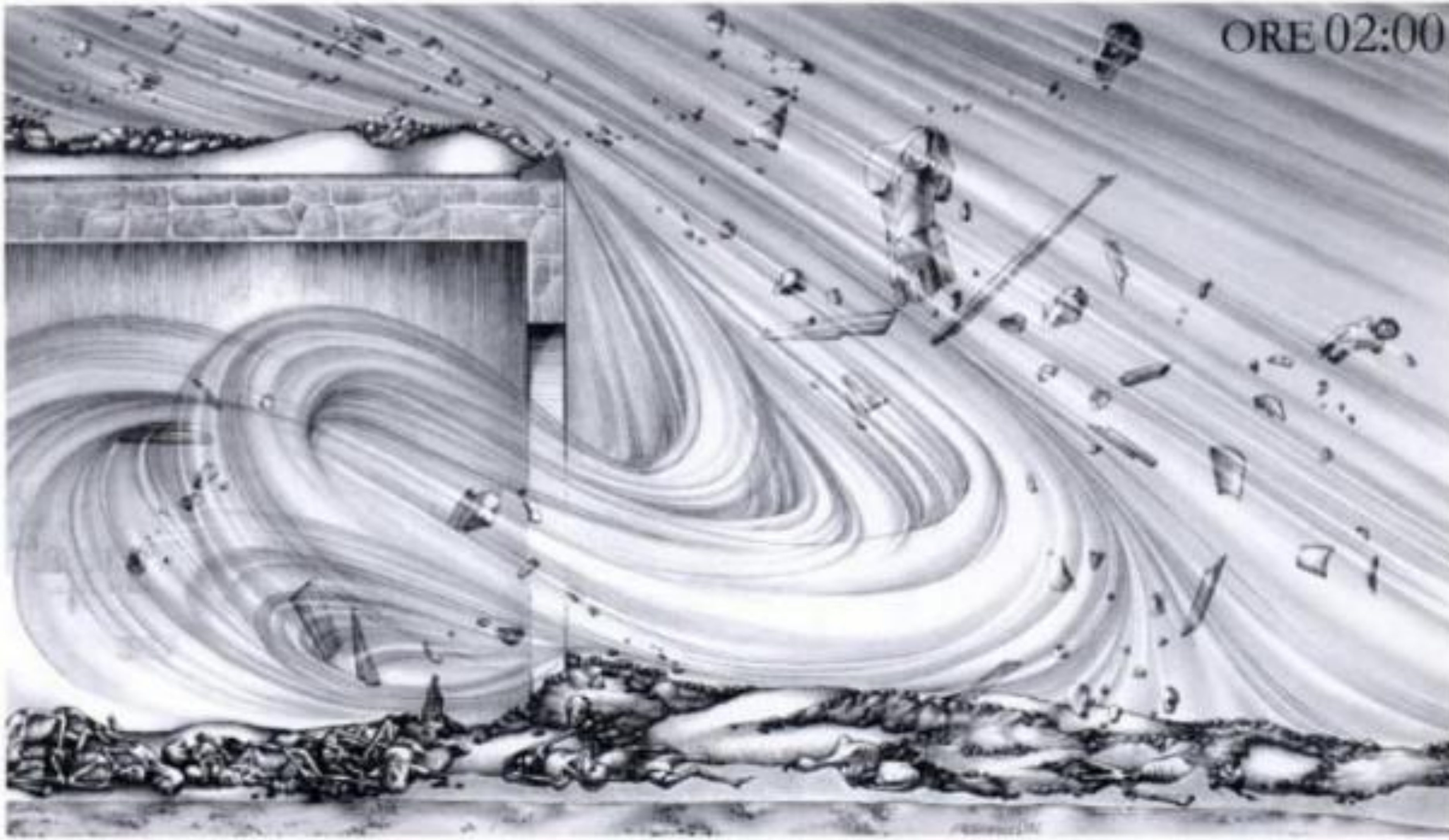


Fig. 33 - Ricostruzione degli effetti dell'impatto del *surge 2* sull'antica spiaggia di Ercolano circa alle ore 2 del 25 agosto 79 d.C.

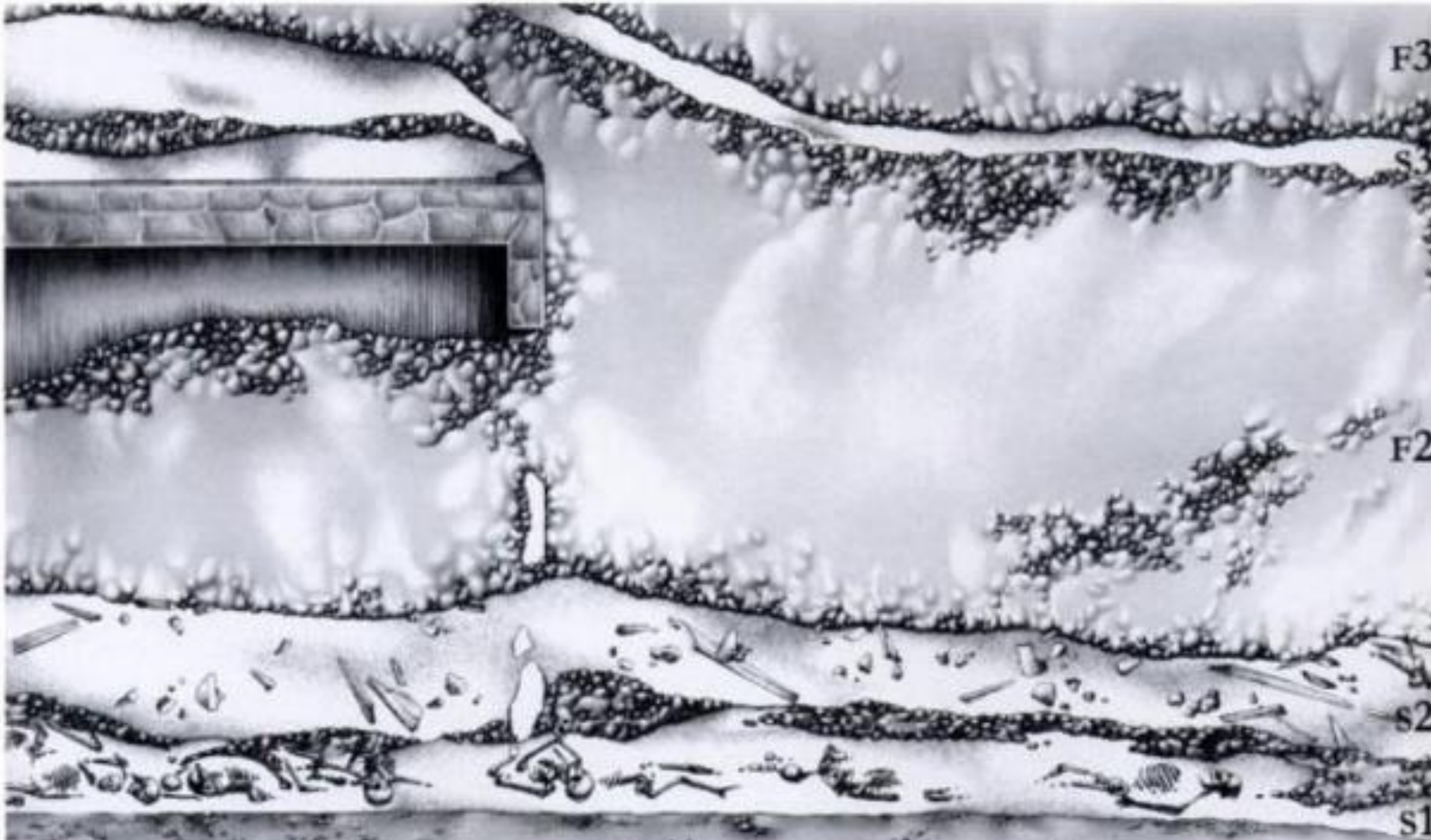


Fig. 34 - Ricostruzione della situazione sull'antica spiaggia di Ercolano dopo la deposizione dei vari flussi piroclastici e *surges* che si susseguirono nel corso della giornata del 25 agosto 79 d.C.

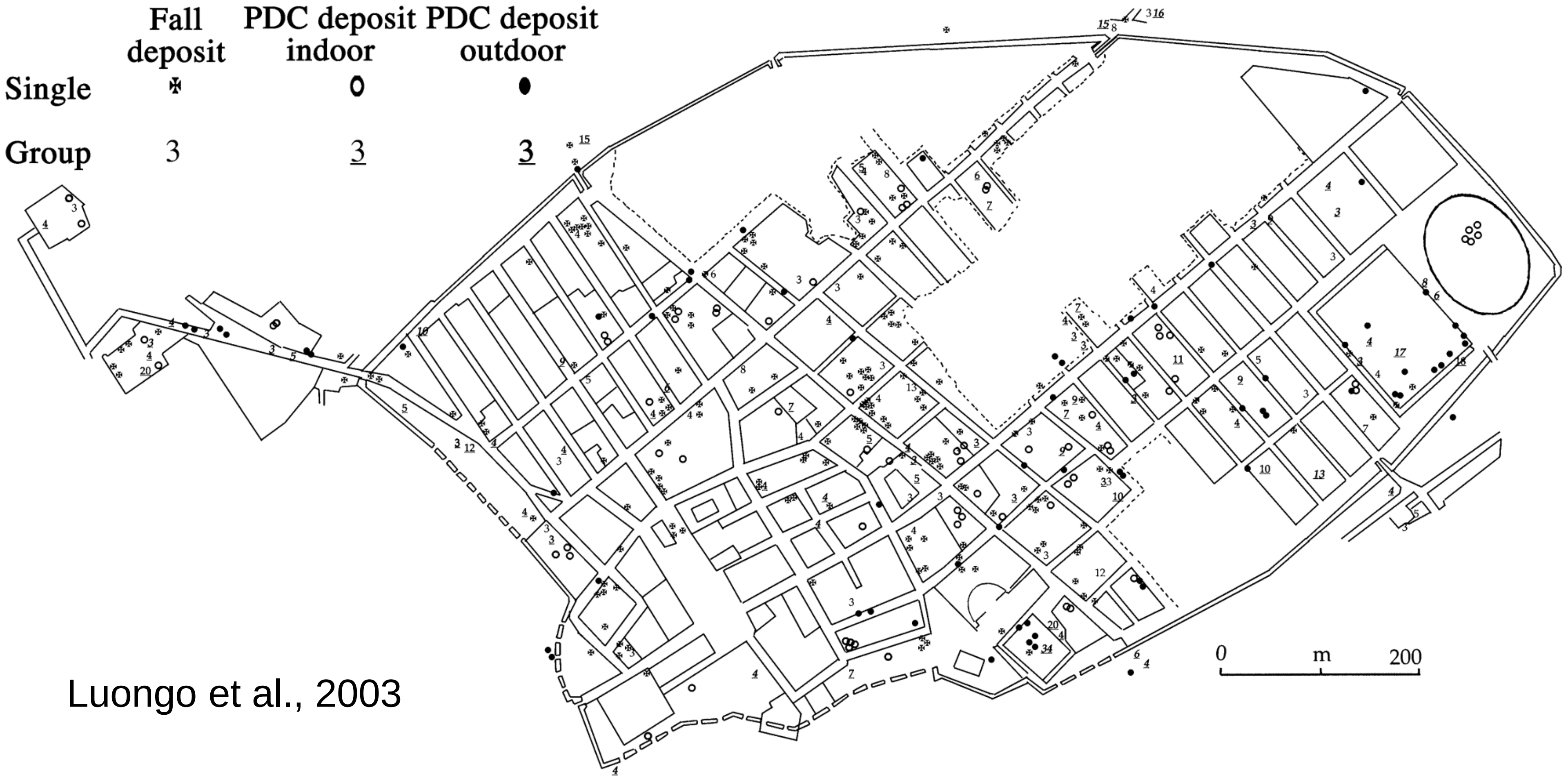


Luongo et al., 2003

Of the 394 intact corpses within the pumice lapilli deposit, 200 were found isolated and 194 in groups; 345 were inside buildings or houses and 49 in outdoor places.
Of the 650 corpses recovered from the PDCs deposit, 152 were isolated and 498 grouped.
334 were found inside buildings, of which 168 were on the upper floors, 166 on the ground floors and 316 outdoors

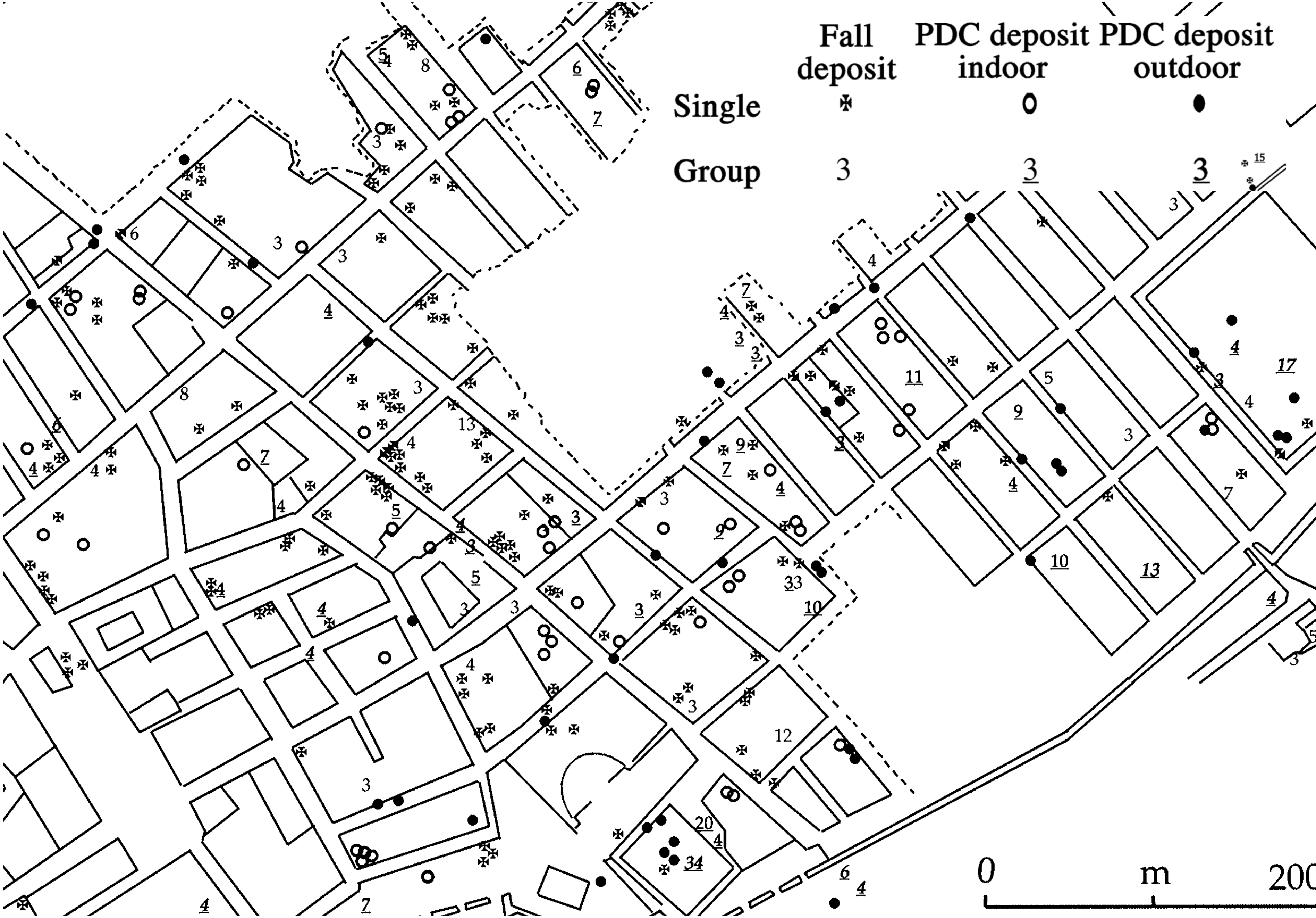
Fall deposit
PDC deposit indoor
PDC deposit outdoor
Single
Group
3
3
3
0
m
200

falling pumice
accumulation rate 15 cm/h (Sigurdsson et al., 1985)
average density 650 $kg/m^3$
incremental load of 100 $kg/m^2$ per hour
No data on the yield strength of the Pompeii roofs available in the literature,
the critical thickness causing the collapse?
Studies carried out on several recent eruptive events (Blong, 1984) report roof collapses to occur with thicknesses ranging 0.1-1 m,
40 cm calculated by Sigurdsson et al. (1985).
roof collapses in Polibius' house might have taken place 1-6 h after the beginning of the eruption.

A significant number of victims has been found in the fall deposit: 38% of the total of Pompeii victims. They probably died as a consequence of the building's collapse.
Accumulation rate in outdoor areas about 15 cm/h.
In the zones of the buildings where material sloughed from roofs, the accumulation rate reached values as high as 25-30 cm/h. Within 6 h the roofs and part of the walls of the buildings had collapsed under the pumice load.
On the morning of August 25, many buildings had been destroyed almost completely and only some edifices were still standing.
1-5 m of pumice lapilli, had filled the impluvia and the rooms the roofs of which had collapsed. Also, the peristyles and the alleys had been filled to these depths.
The lapilli pumice fall deposit, about 3 m thick, buried the lower part of the buildings, partly protecting them from the impact of the later pyroclastic currents.

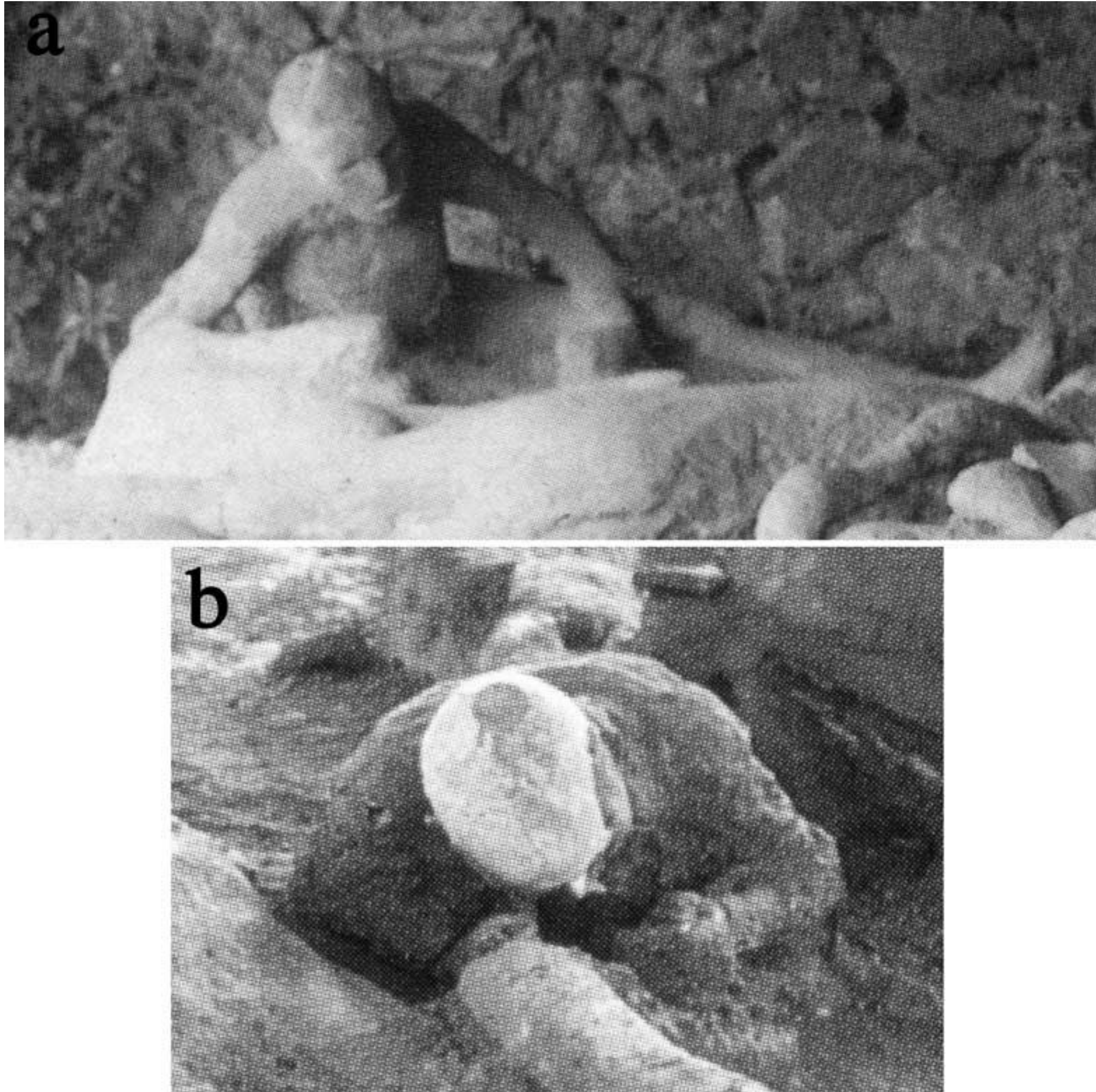


Human casts frozen in the attempt to support their heads from the aggrading deposit. (a) Human cast in the Garden of Fugitives. (b) Human cast in the Casa di Stabianus.

Luongo et al., 2003

Lethal Thermal Impact at Periphery of Pyroclastic Surges: Evidences at Pompeii
Giuseppe Mastrolorenzo, Pierpaolo Petrone, Lucia Pappalardo, Fabio M. Guarino, Plos One 2010

Examination of the corpses' posture suggests the complete absence of any mechanical effect and an instantaneous death followed by sudden muscles contraction (cadaveric spam) due to the heat-shock induced by the PDC, as also testified by hyperflexion of hands and feet toes (flexor reflex)

The primary postures include:
a) ''life-like'' stance: victims that appear in suspended action
b) ''sleep-like'' stance: victims laying on their back, on their right or left side in an apparent relaxed posture
c) ''impact-like'' stance: victims showing corpse displacement and/or rupture of body elements

The secondary postures include:
d) ''limb contraction'' stance: iperflexion of hands and feet
e) ''pugilistic attitude'' stance: limb flexures that result from dehydration and shortening of tendons and muscles.

Postures types e. and f. are generally observed as secondary effects in victims exposed to extreme heat (at least 200–300°C).
The pugilistic attitude was erroneously thought to be the victim's attempt for self-defence by previous authors

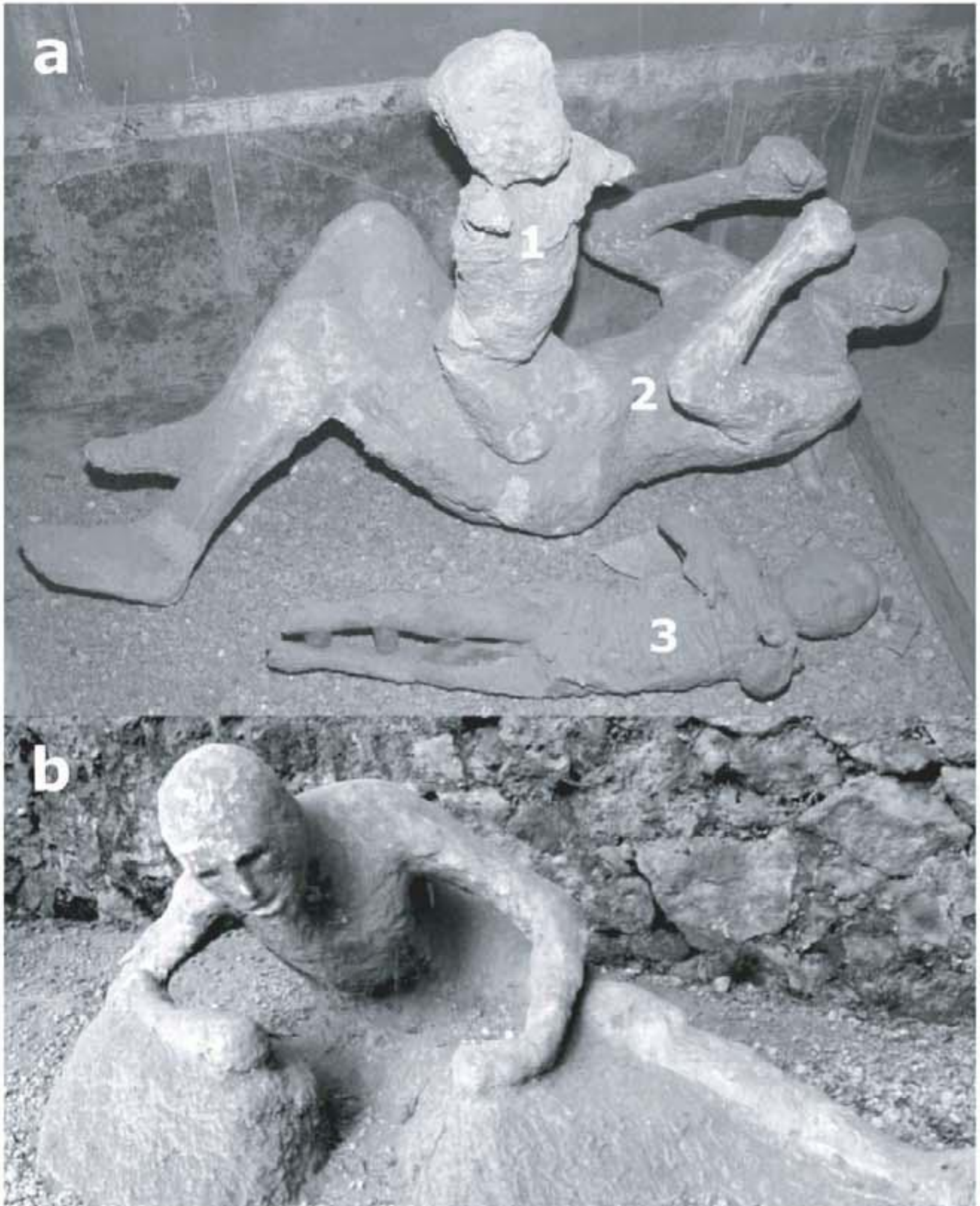


Typical body postures assumed by human victims in PDCs at Pompeii.
“Life-like” stance:
$a_1$. infant and $a_2$. adult female
“pugilistic attitude” stance: $a_3$. child (House of the gold bracelet, Regio VI, Insula 17 [Insula Occidentalis], 42),

b. adult male (The garden of the fugitives, Regio I, Insula 21),

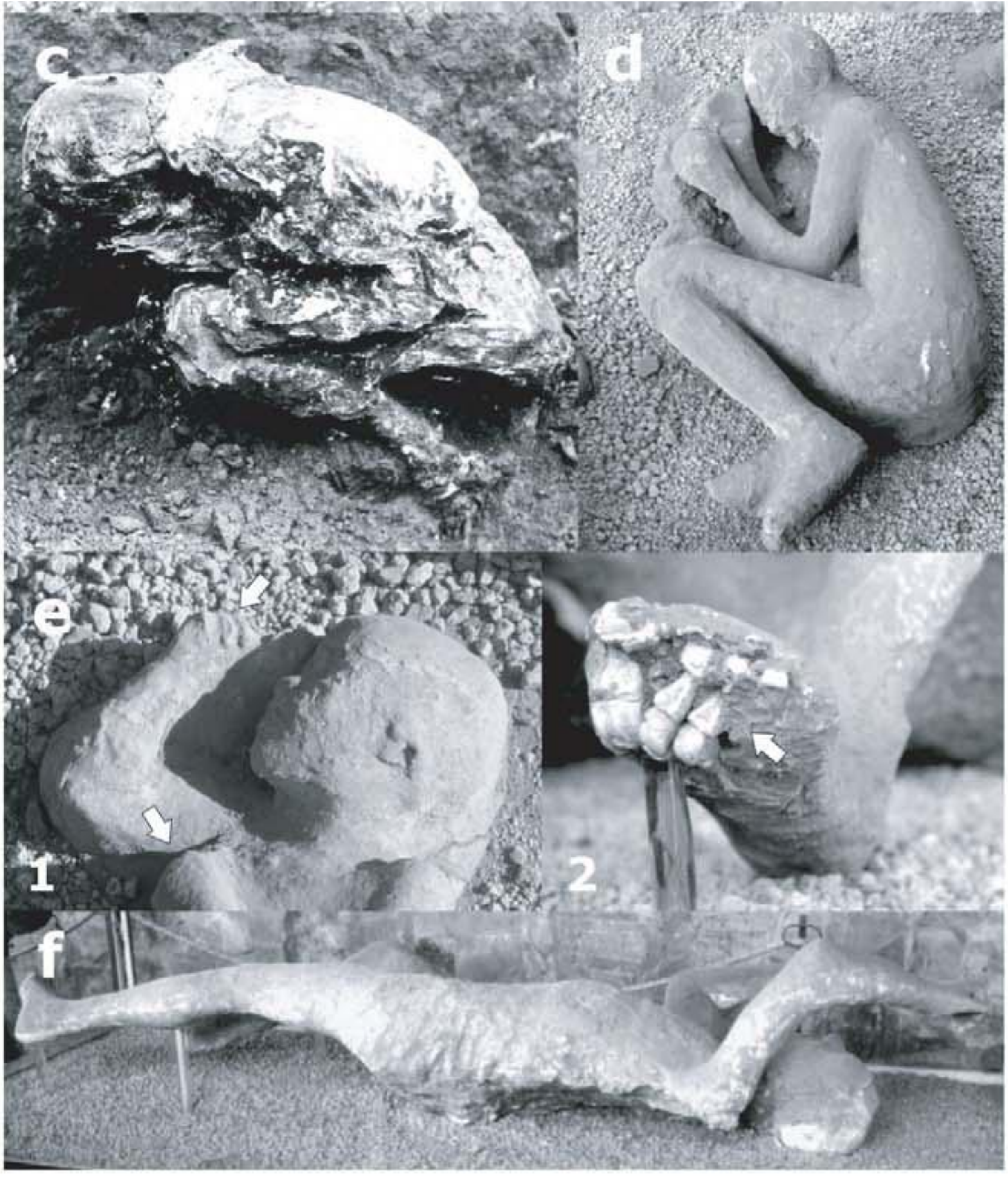


“Life-like” stance: c. Adult male (The Great Palaestra, Regio II, Insula 7);
“sleep-like” stance: d. adult male (The garden of the fugitives, Regio I, Insula 21);
“limb contraction” stance: $e_1$. child (The garden of the fugitives, Regio I, Insula 21) and $e_2$. left foot adult male (outdoor victim, XIX sec. findings);
“pugilistic attitude” stance: f. adult male (outdoor victim, XIX sec. findings).

Pompeii and surroundings
most of the victims are typically frozen in suspended actions (73% life-like stance, 27% sleep-like stance), showing as well as limb contraction (76%) and a large number of corpses presenting the pugilistic attitude (64%).
Different postures often coexist in the same victims group, but the prevalence of people frozen in suspended actions (life-like stance) is univocally indicative of a condition known as cadaveric spasm.

In contrast, postures indicative of mechanical impact effects on victims both inside and outside buildings are extremely rare (2.1%). These evidence confirm that dynamic overpressure was generally below the human lethal threshold as well as their partial or total entrapment into the current (about 2000 Pa), according with the results of our numerical modeling of PDC.

Cadaveric spasm is a rare but diagnostic form of instantaneous muscular stiffening associated with instant violent death, which crystallizes the last activity one did prior to death. Such instant rigor prevents the ordinary onset of muscular relaxation immediately after death, thus avoiding any further substantial body posture modification.
The presence of this stance is indicative that people was alive at the time of posture arrest and its widespread occurrence is a key evidence that all victims groups were exposed to the same lethal conditions.
Cadaveric spasm commonly involves groups of muscles and only exceptionally the entire body. This last condition is described in battle situations, due to the exposure of victims to extreme heat. The predominance of this rare feature in Pompeii victims points

Numerical simulation of S4 PDC

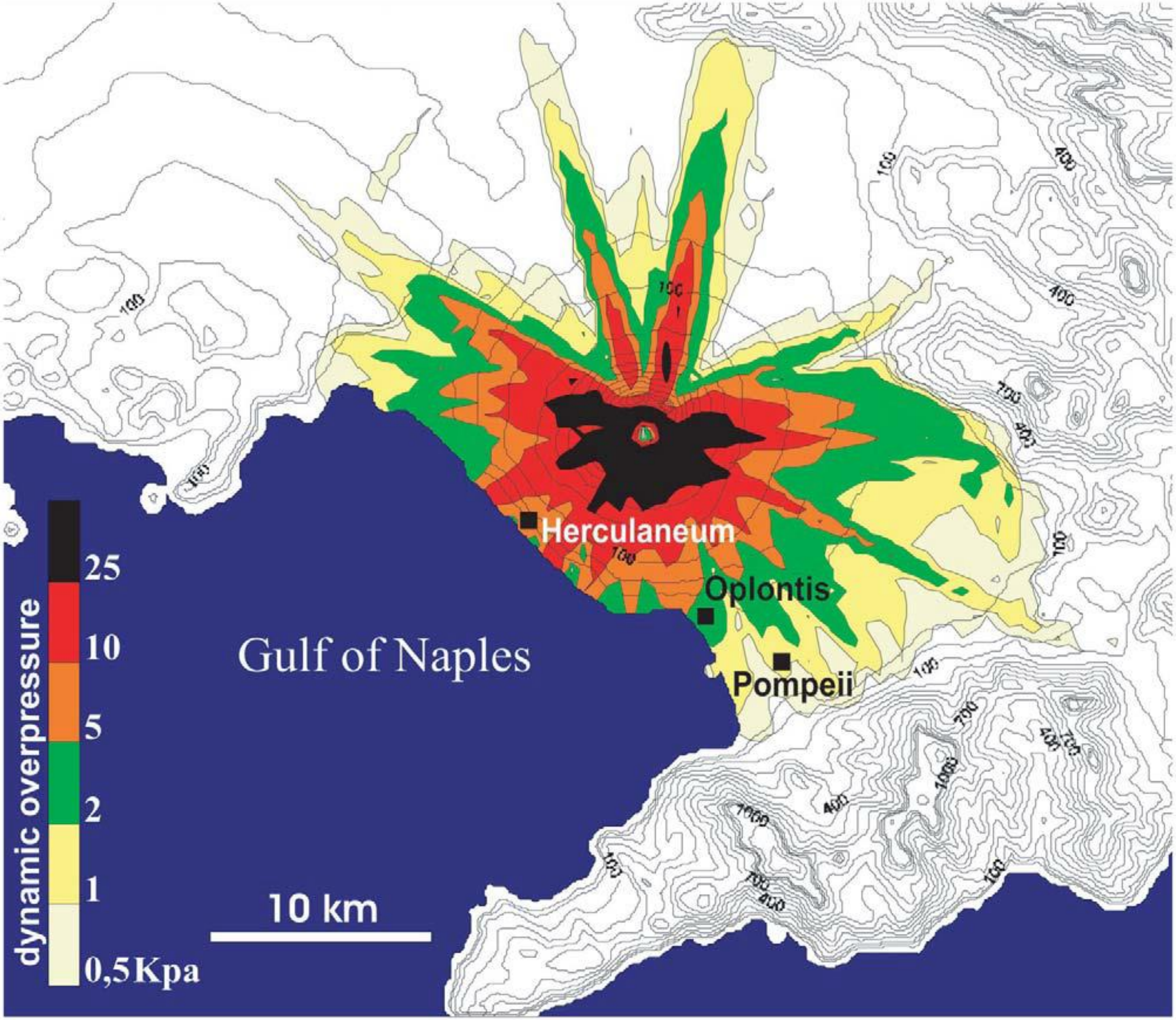


The pyroclastic surge advanced as a dilute turbulent poorly-energetic deflating cloud and emplaced suddenly, also lead by town buildings and walls and trench barrier effect. Such behavior accounts for the lack of evidence of mechanical impact on structures and of engulfment and transport in the S4 deposit of tiles and bricks.

velocity at the vent of 50-100 m/s, front thickness of 30-130 m, density of 1.5450 kg/$m_3$ and average run-out within 10 km passage time of PDC cloud between 30 and 1.5-$10^2$ seconds.


Human victims of the 79 AD eruption at Pompeii and Oplontis.
a. Cast of adult woman, part of 13 human victims died outdoor (Pompeii, Garden of Fugitives), possibly showing some evidence of minor mechanical impact;
b. cast of adult male, part of a group of 21 victims found outdoor (Pompeii, Porta Nola), with evidence of exposure to high temperature typical of fire victims or lethality in PDCs;
c. the group of human victims found in the Villa B at Oplontis, partially just skeletons and to some extent casts.

at high velocities the body is constantly in contact with the heated air. The other reason is that the PDC contains solids with a higher heat capacity than air. For these reasons, while it is possible to tolerate exposure to hot dry air at temperature up to temperatures of 200°C and above for several minutes, even a brief exposure to a surge cloud in the 200–300°C range, or even as low as 100–150°C, is capable of causing severe burns to unprotected skin

In fires it is considered that exposure to hot smoke at temperatures in excess of 200°C (a total heat flux of more than approximately 12kW) is likely to be fatal within a few minutes.

Survival in the open without protection from the intense heat is virtually impossible. The heat flux is so great that the burns may extend below the dermis into the subcutaneous tissues and the muscles (“fourth degree burns”), giving rise to contractions of the limbs and spine to produce the pugilistic attitude, a post mortem finding normally seen in victims of building or other common fires, but which is also in evidence in many of the numerous plaster casts of victims at Pompeii. The body is fixed in its position, which is not due to the rigor mortis found in deaths from other causes and which will typically pass off in 36h. In contrast, the body in the pugilistic attitude can be straightened only by a pathologist cutting apart the contracted muscle tendons. The most recent volcanic settings in which the pugilistic attitude has been observed, namely in the present study of Merapi in 2010, and Soufrière Hills, Montserrat in 1997, suggest exposure to surge temperatures in excess of 200°C around the time of death.

The time required for thermal radiation to cause deep burns is always shorter than that for auto-ignition of clothing materials, so clothing can be left intact even though a person has died from burns, as evidenced at Pompeii where some of the plaster casts in pugilistic attitudes still retain the forms of togas and sandals worn by the victims when they died. In surges the radiant heat comes from the combined contribution of the individual hot particles in the enveloping hot cloud.

The bones of the Pompeii victims show colour variations ranging from natural bone colour to pale yellow as well as evidence of linear microcracking at the interosteonic level. All these features are indicative of exposure to high temperature

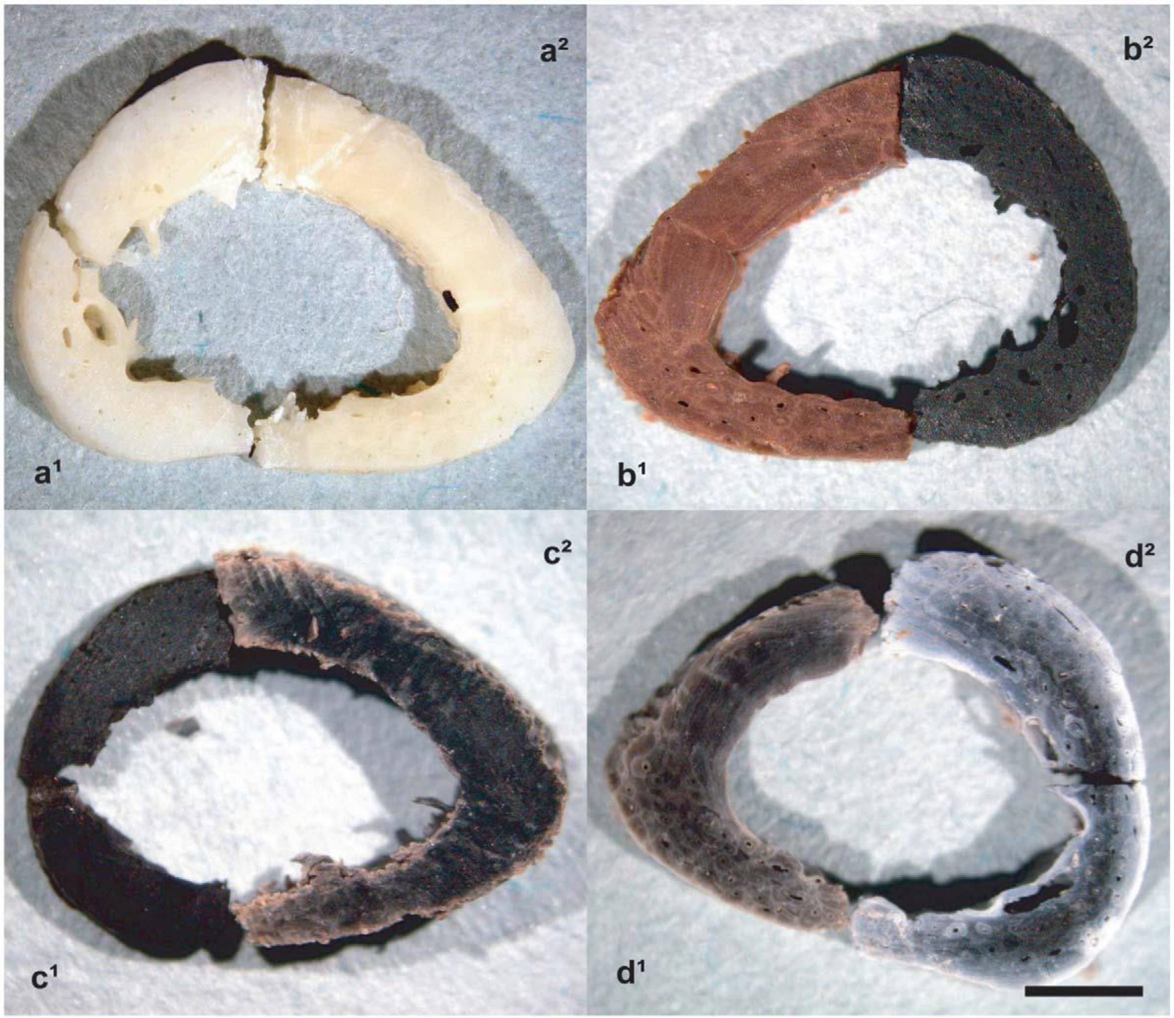


Colour features of recent human bones (adult phalanx) heated in laboratory from 100°C to 800°C. $a_1$. 100uC, natural bone colour, light grey 25YR 8/1; $a_2$. 200°C, pale yellow 25YR 8/3; $b_1$. 300°C, bright brown 2.5YR 5/8; $b_2$. 400°C, reddish black 2.5YR 1.7/1; $c_1$. 500°C, black N 2/0; $c_2$. 600°C, dark grey N 3/0 and pale reddish 2.5YR 7/3; $d_1$. 700°C, brownish grey 7.5Y 4/1 and 5/1; $d_2$. 800°C, grey N 6/0 and greyish white N 8/0 (scale bar, 2.0 mm). Bone colours are based on Munsell (1954) soil colour

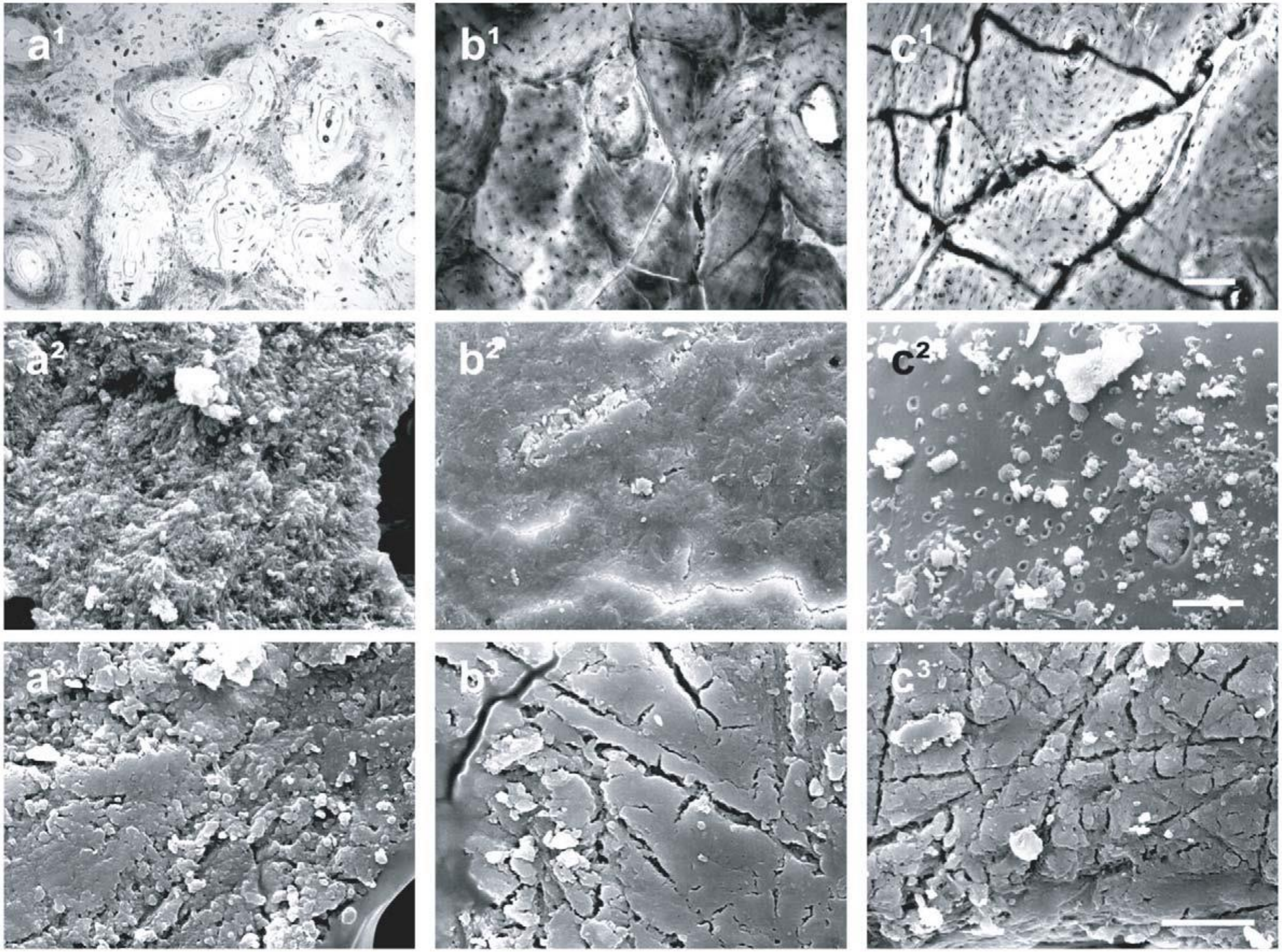


Thermal modifications in human victims bones and in recent human bones heated in laboratory. Adult bone victims analyzed with a light microscope (scale bar 100 mm) and a scanning electron microscope (scale bar 10 µm, 1700x): Femur from Pompeii showing linear cracking ($a_1$) and an intact ultrastructure ($a_2$); radius from Herculaneum showing both linear and polygonal cracking ($b_1$) and incipient recrystallization ($b_2$); fibula from Oplontis characterized by extreme polygonal cracking ($c_1$) and advanced recrystallization ($c_2$). SEM images of recent adult human hand phalanx heated to 200uC ($a_3$), 500uC ($b_3$) and 800uC ($c_3$) (scale bar 5 µm, 2500x).

An independent verification that PDC temperatures in Pompeii exceeded 250°C is the melting of silverware solder. In Roman times this material was made with a lead/tin alloy like Tertiarium (Pb-Sn 2:1), which has a melting point of ca 250°C. A temperature of 250°–300°C was also high enough to char wood objects, vegetal material and food but was unable to affect glass, that is preserved intact in the ash deposits.

The exposure time of the victims to high temperature and dusty gas was very short as resulting from lasting passage of S4 surge in the range of 30-1.5x$10^2$ seconds. This result is crucial being the capability of PDCs to cause death and injury not only depending on their physical conditions but also on the exposure time. The passage time is consistent with the inferred lethal time for temperatures in the range of 250°–600°C evaluated from ca 10 to ca $10^2$ seconds.
Notably, such a time lapse is insufficient to cause asphyxia that would require an exposure time of several minutes, thus indicating that people would be able to survive to suffocation in 0.5 to 2.5 minutes of the S4 surge cloud passage. Nevertheless, the calculated concentration of inhalable ash in the PDC approached the survival condition in the order of ca. 0.1 kg/$m^3$. Consistently, the widespread occurrence ofprim ary life-like postures (cadaveric spasm) in the victims is only compatible with an instantaneous death, while exclude the longer agony and the final floppy posture that characterize suffocation.

while impact force and exposure time to dusty gas dropped below lethal conditions, the pyroclastic cloud retained its high temperature thus being the main cause of instantaneous mortality for the Vesuvius area inhabitants, including people who were sheltered within buildings as far as in Pompeii. Definitely, a group of indoor victims found at Muregine, within the S4 PDC limit about half kilometer south-east of Pompeii walls, suggests that even an extremely short exposure to the pyroclastic surge in the order of seconds to a few tents of seconds was lethal. These facts and the evidence that the late, most powerful 79 AD PDCs reached distance exceeding 20 kilometres from the vent and the findings of several scattered groups of victims in Roman villas even as far as at least 15 kilometres in Stabiae highlight the need to strengthen the emergency plans for Vesuvius and other similar

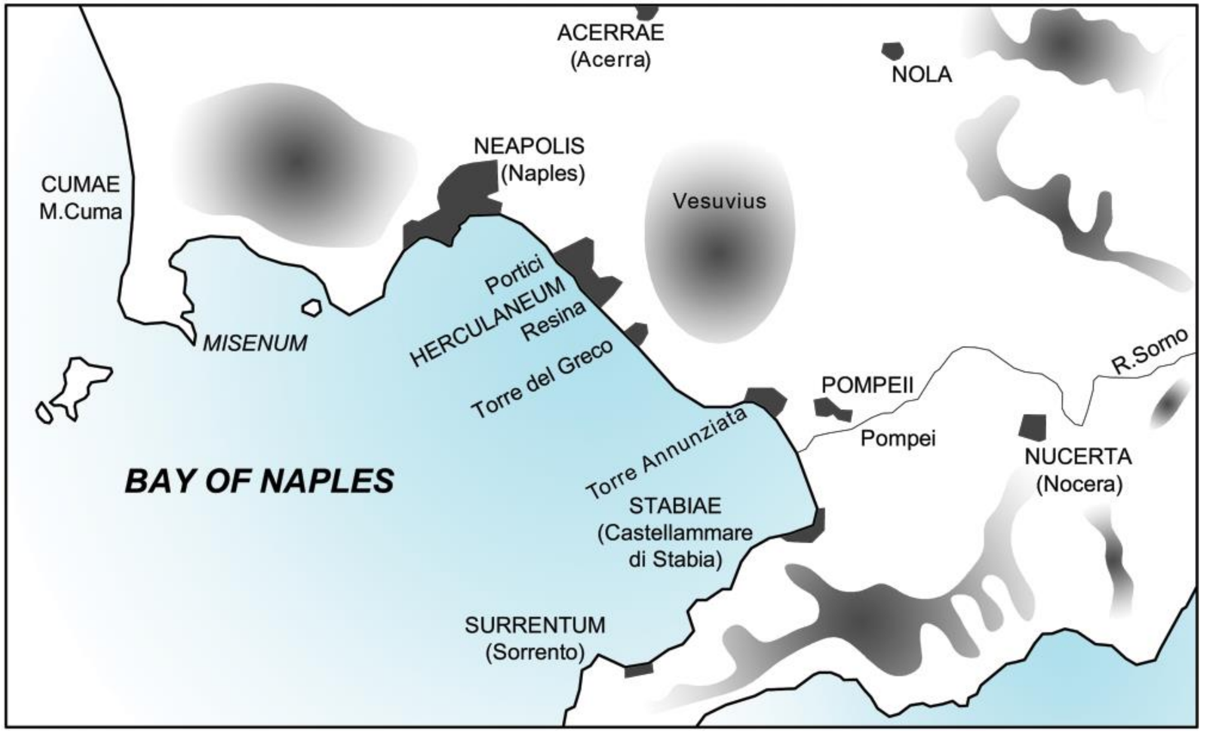

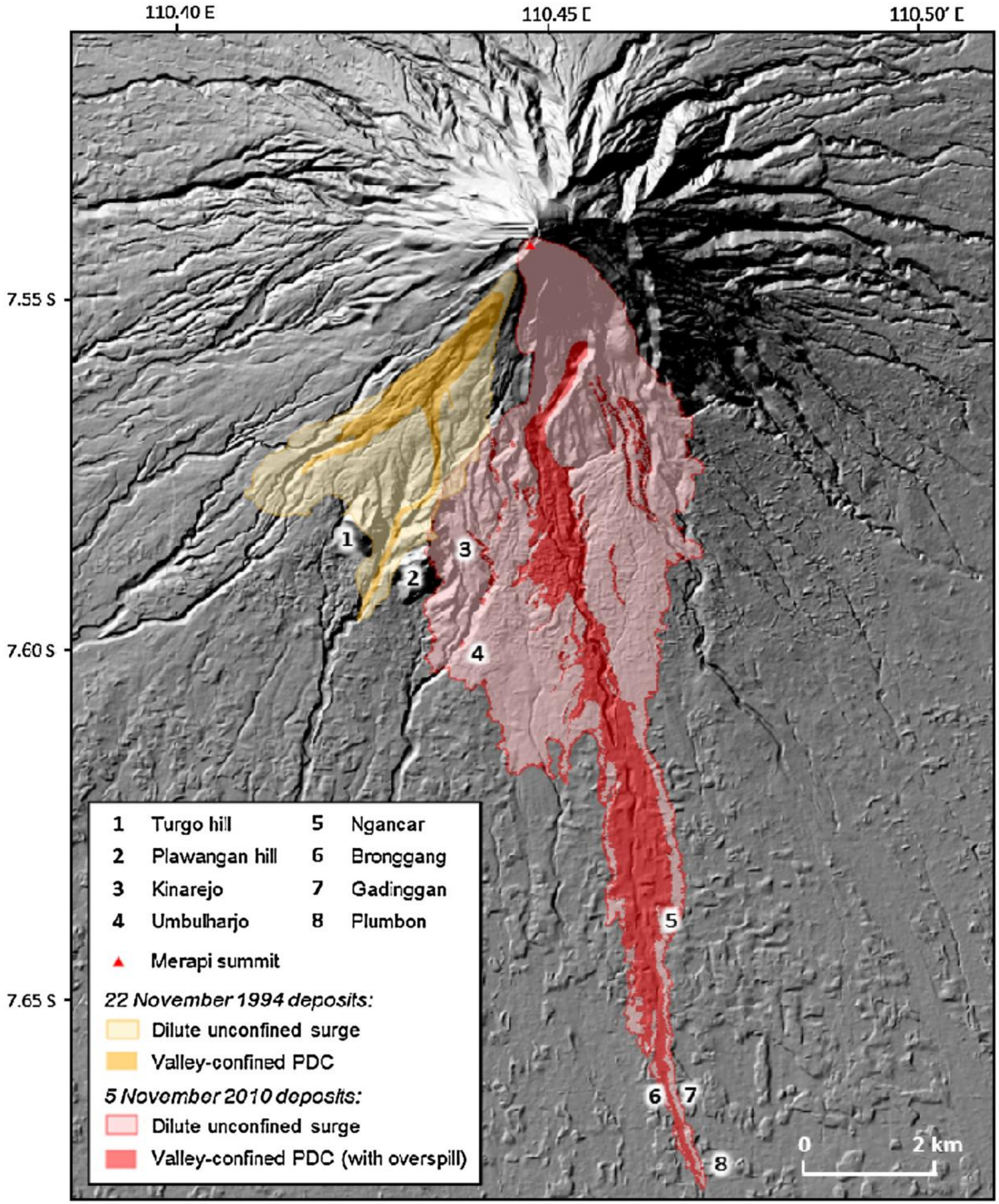


Disaster experience at Merapi volcano: hospital in-patients rescued from pyroclastic surges in 1994 and 2010

P.J. Baxter, et al., Human survival in volcanic eruptions: Thermal injuries in pyroclastic surges, their causes, prognosis and emergency management, Burns (2017),

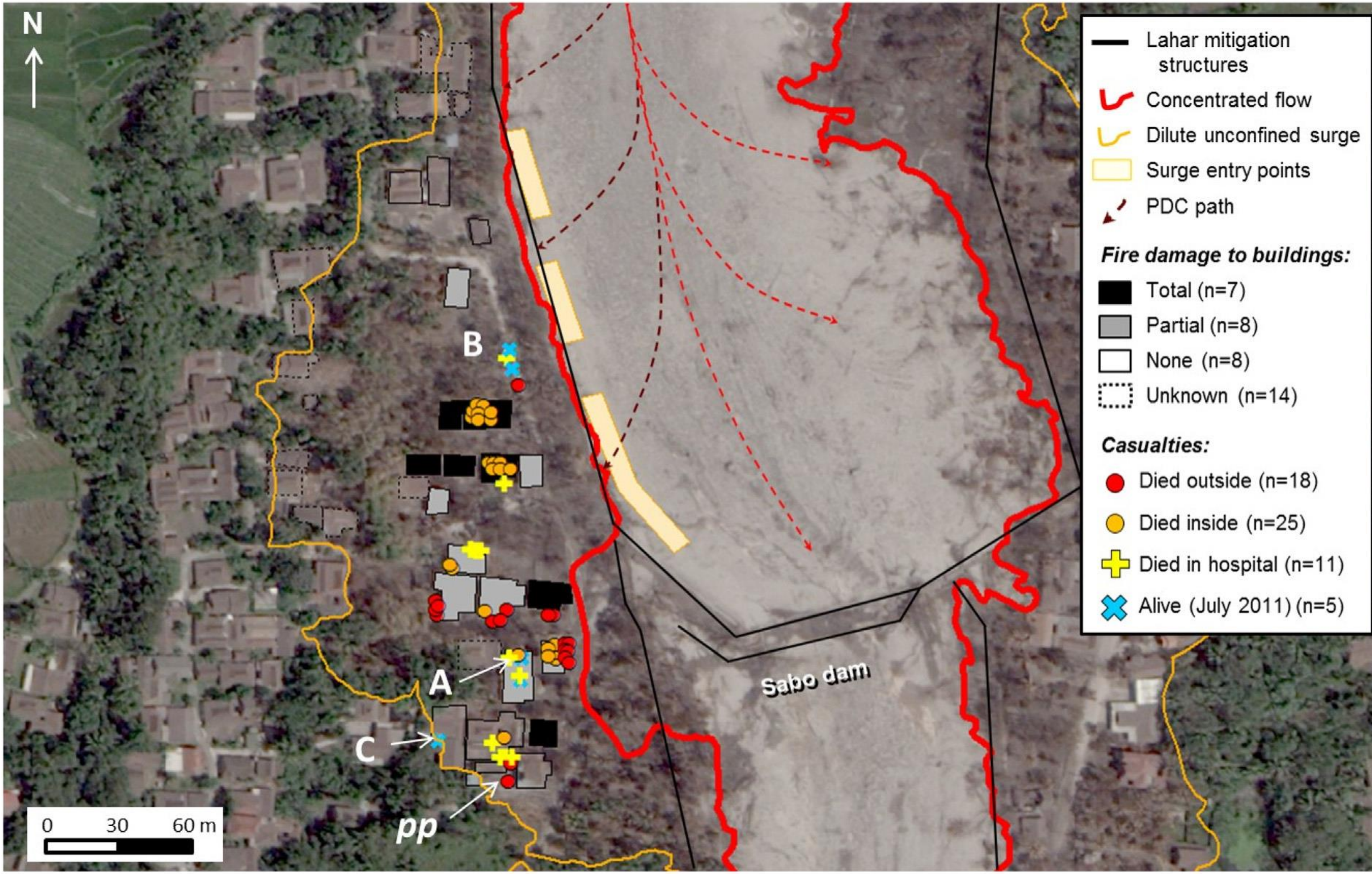


Map of part of Bronggang village along the Gendol valley impacted by the detached surge in 2010 showing reported locations of victims at the time and the damage to buildings due to fires ignited by firebrands carried in the surge cloud. Houses A, B, and C belong to survivors A, B, C (see text), and pp identifies location of deceased in pugilistic attitude seen by survivor C.

3.3.3. Household C Survivor C lived in the village just beyond the limit of where the surge stopped (Fig. 2). He was told by his son at 23.15h that people were getting ready to evacuate but he ignored him. Then his son returned at about 00.00h to say that he heard a rumbling noise growing bigger, so Survivor C got ready to leave in his car with his family. He was waiting in the car outside with the engine running when around 00.20h he heard a sound like an explosion that was later followed by the sound of burning vegetation and people screaming for help. He saw a black cloud illuminated with point flashes of light ("like fireflies") hit the wall of his house and rose upwards, so he went back into the house to lead out his wife and two children, together with his brother and mother. He was wearing sandals only. He drove a few metres when he saw dead bodies, one of whom he recognised as one of his neighbours; he described him as looking dead with his arms in the air (pugilistic attitude—see above: he was Mortuary Victim 1). This made him redirect the car to go around the house to avoid the body and the main surge area as much as possible. About 50m further on a "ball of fire" fell in front of the car (possibly a separate small surge cloud or a fallen burning tree top) and the engine cut out. He unsuccessfully tried to restart it and then got out but stepped onto hot ash that burnt his feet, so he got back inside again. Soon the engine was restarted, but after another 50m a black cloud of ash passed in front (possibly a third small surge cloud) that then engulfed the car and prevented him seeing ahead. He stopped and opened his door to look out but was met by warm ash, so closed the door and drove on while the cloud slowly cleared. No one else got out of the car and none of the rest of the family was burnt. Later, he went to hospital for treatment of his burnt feet.

# Lapis specularis IL VETRO DI PIETRA

# Domus romana

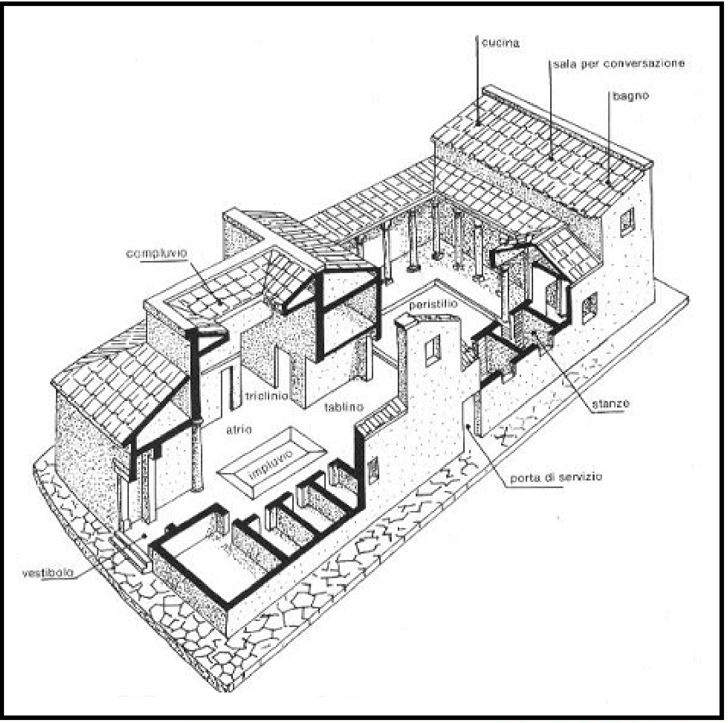



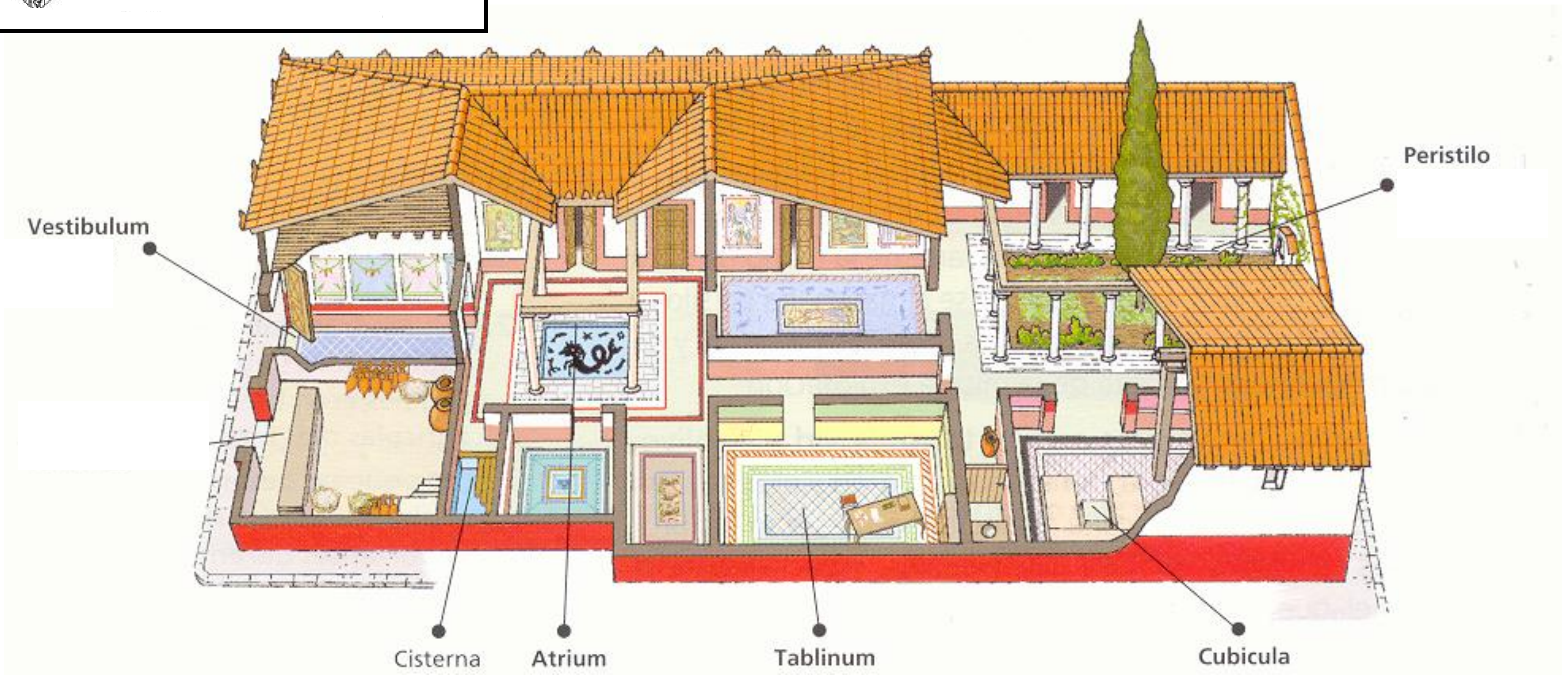

# Editto dei prezzi di Diocleziano, 301 d.C.

1 Una libbra di vetro alessandrino: 24 denarii

2 Una libbra di vetro verde giudeo: 13 denarii

3 una libbra di coppe e di vasellame liscio in vetro alessandrino: 30 denarii

4 una libbra di coppe e di vasellame liscio in vetro giudeo: 20 denarii

5 Una libbra di lapis specularis di prima scelta: 8 denarii

6 Una libbra di lapis specularis di seconda scelta: 6 denarii

1 libbra = circa 327 g

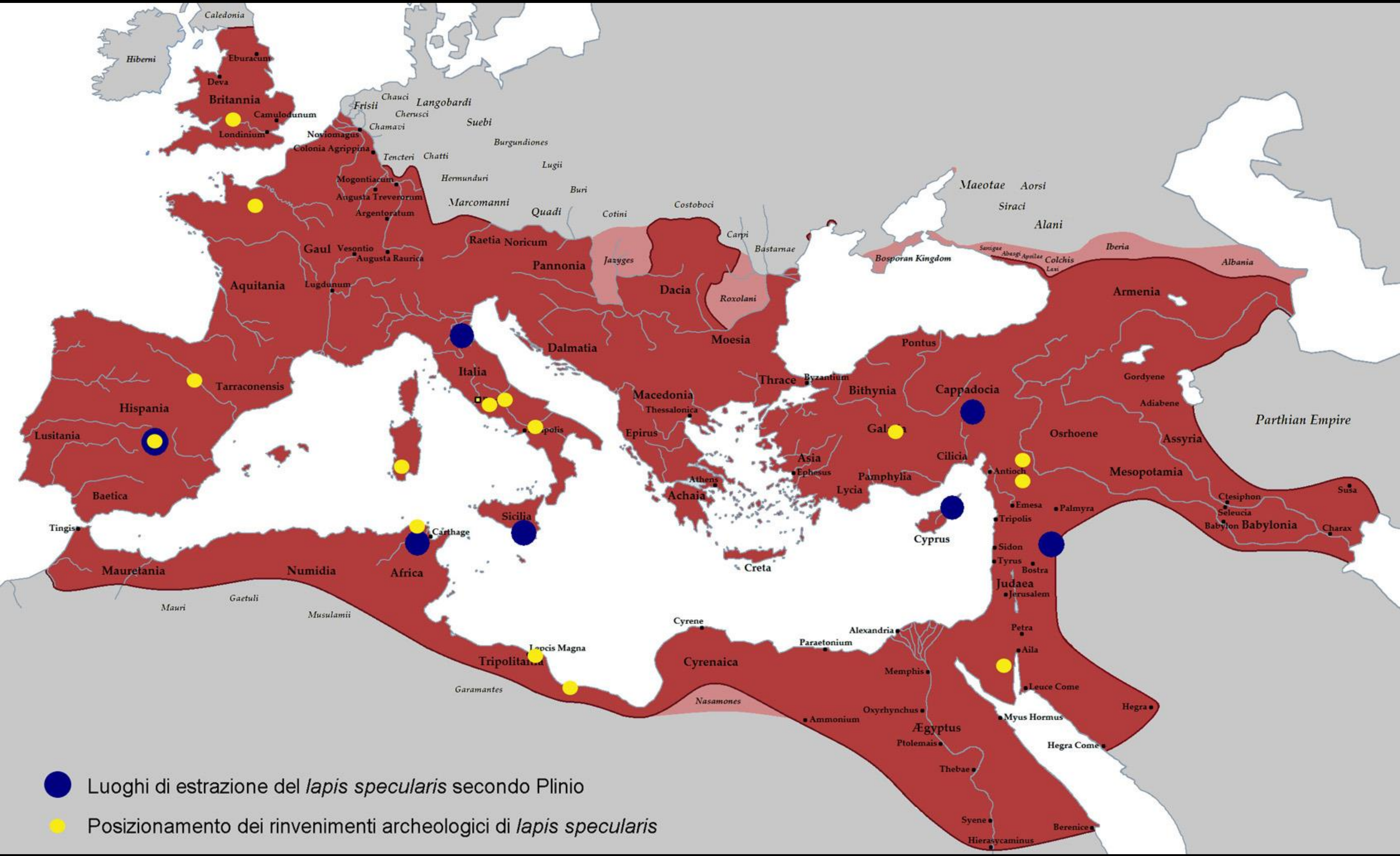
Luoghi di estrazione del *lapis specularis* secondo Plinio
Posizionamento dei rinvenimenti archeologici di *lapis specularis*
Caledonia
Hiberni
Eburacum
Deva
Britannia
Camulodunum
Londinium
Frisii
Chauci
Langobardi
Cherusci
Chamavi
Suebi
Noviomagus
Colonia Agrippina
Burgundiones
Tencteri
Chatti
Lugii
Mogontiacum
Augusta Treverorum
Hermunduri
Buri
Marcomanni
Quadi
Cotini
Costoboci
Argentoratum
Maeotae
Aorsi
Siraci
Alani
Carpi
Bastarnae
Gaul
Vesontio
Augusta Raurica
Raetia
Noricum
Pannonia
Jazyges
Dacia
Roxolani
Bosporan Kingdom
Colchis
Iberia
Albania
Aquitania
Lugdunum
Armenia
Moesia
Dalmatia
Pontus
Italia
Tarraconensis
Hispania
Lusitania
Baetica
Thrace
Byzantium
Macedonia
Thessalonica
Bithynia
Cappadocia
Gordyene
Adiabene
Parthian Empire
Epirus
Galatia
Osrhoene
Assyria
Asia
Ephesus
Cilicia
Mesopotamia
Antioch
Athens
Achaia
Pamphylia
Lycia
Emesa
Palmyra
Ctesiphon
Seleucia
Babylon
Babylonia
Susa
Charax
Tripolis
Sicilia
Tingis
Carthage
Cyprus
Sidon
Tyrus
Bostra
Mauretania
Numidia
Africa
Creta
Judaea
Jerusalem
Mauri
Gaetuli
Musulamii
Cyrene
Alexandria
Petra
Paraetonium
Aila
Leptis Magna
Tripolitania
Cyrenaica
Memphis
Garamantes
Leuce Come
Nasamones
Oxyrhynchus
Hegra
Ammonium
Myus Hormus
Ægyptus
Ptolemais
Hegra Come
Thebae
Syene
Berenice
Hierasycaminus


El Ranal
Cuenca
(Spagna)


El Ranal
Cuenca
(Spagna)

El Ranal
Cuenca
(Spagna)


El Ranal
Cuenca
(Spagna)

El Ranal
Cuenca
(Spagna)

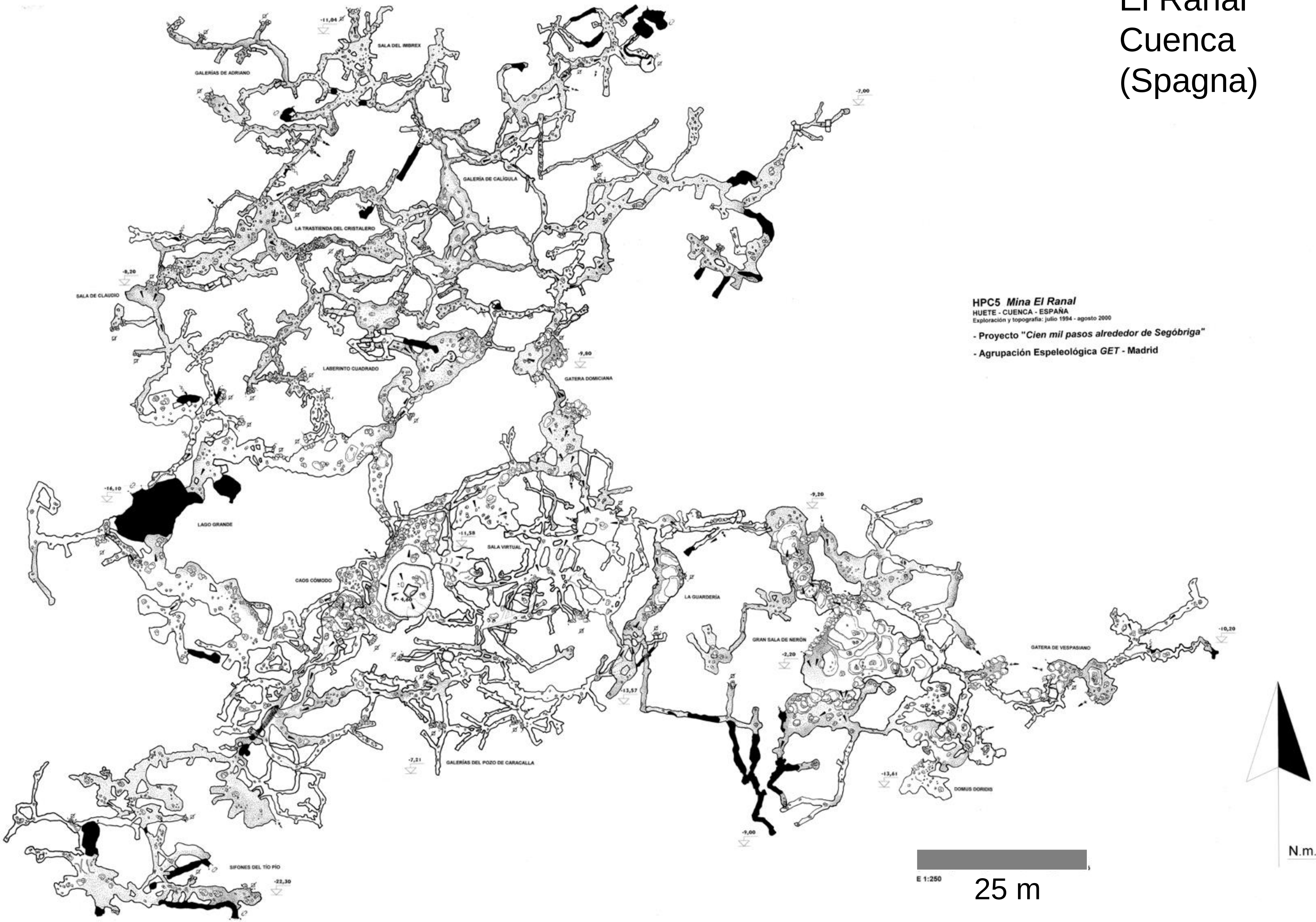


*Bernárdez Gómez & Guisado di Monti, 2012*

El Ranal
Cuenca
(Spagna)

El Ranal
Cuenca
(Spagna)

El Ranal
Cuenca
(Spagna)

La Mudarra
Cuenca
(Spagna)


La Mudarra
Cuenca
(Spagna)

La Mudarra
Cuenca
(Spagna)


Foto P. Lucci



Grotta della Lucerna
Brisighella

Grotta Inferno
Cattolica Eraclea
(Sicilia)

Grotta Inferno
Cattolica Eraclea
(Sicilia)


Pompei


Pompei
3-3-953
REG.T INS.IX
STRATO-SUP

Museo Archeologico Nazionale
Napoli

Museo Archeologico Nazionale
Napoli

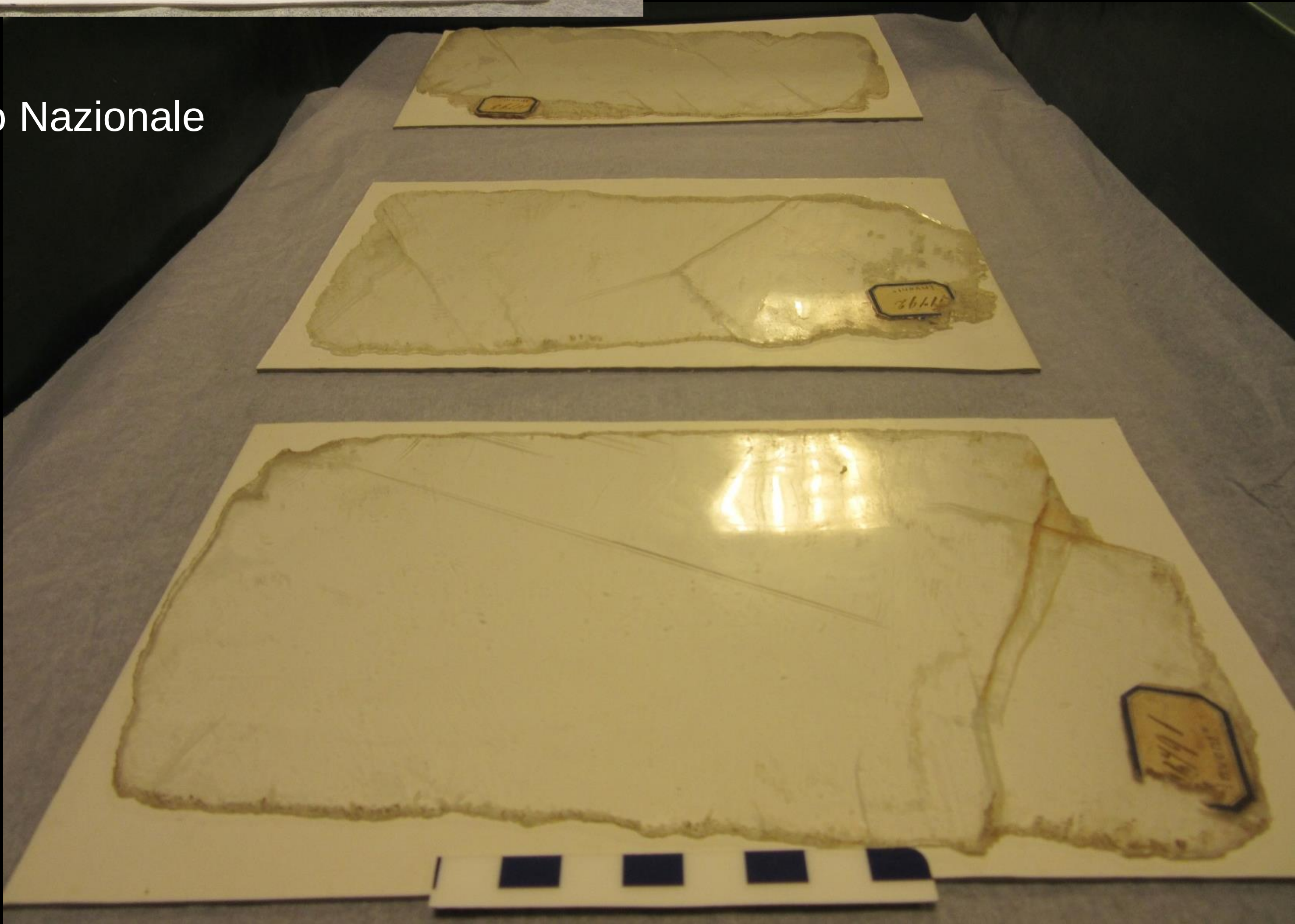

Pompei

Domus Paquius Proculus

Pompei

Domus Paquius Proculus


Pompei Domus Paquius Proculus

Rifugio Ca' Carnè,
Brisighella, (Faenza)
Parco della Vena del Gesso Romagnola